Doctoral Thesis

Photon Surface and Relevant Phenomena

光子曲面とその周辺の理論的現象

Yasutaka Koga

Department of Physics, Graduate School of Science,
Rikkyo University

Abstract

A photon surface is a geometrical structure first introduced by Claudel, Virbhadra and Ellis (2001) as the generalization of a photon sphere. The surface is defined so that it inherits only the local geometrical properties of a photon sphere and does not necessarily have the global symmetries. Because of the definition, it has more applicability to many physical problems in addition to its own interest as a geometrical object. In this thesis, after reviewing the basics of a photon sphere and a photon surface, we see their relevant phenomena; the existence of photon surfaces in asymmetric vacuum spacetimes, which shows the utility of the definition; *sonic point/photon surface (sphere) correspondence*, the coincidence of sonic points of radiation accretion flow and photon surfaces (spheres); the appearance of pure-tensional thin shells on a photon surface, which leads to the uniqueness theorem of pure-tensional thin shell wormholes.

Contents

Chapter 1

Introduction

General relativity predicts formation of black holes in the universe as a consequence of gravitational collapse of massive stars. In the last few years, there have been great developments in the observation of black holes. In 2016, the first detection of gravitational waves from binary black holes had been achieved by the first observing run of Advanced LIGO [1]. Not only does it prove the existence of black holes, but also it is the first step of the gravitational-wave astronomy. From then on, numerous events of gravitational wave detection have been announced by Advanced LIGO and Advanced Virgo. In 2019, the Event Horizon Telescope Collaboration showed the first image of a black hole shadow [2]. A black hole shadow observation is, among several optical observations, the evidence which proves most directly the existence of a black hole. For determination of the parameters characterizing a black hole, further developments of the observation are expected.

A sphere consisting of circular photon orbits around a black hole is called *a photon sphere*. It is the characteristic structure of black hole spacetimes. Photon spheres have attracted much attention due to the variety of their applications to astrophysical problems, black hole shadows [3, 2], quasinormal modes of gravitational waves [4, 5], and nonlinear spacetime instability [6, 7], for example. Since the surface of a black hole, i.e. the event horizon, is invisible by definition, a photon sphere can be only the characteristic structure of a black hole spacetime we can observe.

A photon surface is a geometrical structure first introduced by Claudel, Virbhadra and Ellis [8] as the generalization of a photon sphere. The surface is defined so that it inherits only the local geometrical properties of a photon sphere and does not necessarily have symmetries. Together with the definition, the authors also proved a theorem concerning the equivalent conditions for a surface to be a photon surface as one of the main results. The theorem (Theorem 2.2 in [8]) states that a given timelike hypersurface is a photon surface if and only if it is totally umbilic, i.e. the second fundamental form is pure trace everywhere. Subsequently, Perlick [9] proved that the theorem holds for arbitrary dimensions of the surface and the spacetime. Since a photon surface requires no symmetries, it would have applicability to many physical problems in addition to

its own interest as a geometrical object. For example, there is a photon surface in the uniformly accelerated Schwarzschild spacetime, which is no longer spherically symmetric due to the acceleration [10]. The photon surface corresponds to the photon sphere of the Schwarzschild spacetime in the zero-acceleration limit. Similarly to the black hole uniqueness theorems, uniqueness theorems of spacetimes possessing photon surfaces have been established in Refs. [11, 12, 13, 14].

This thesis presents the basics of photon spheres and photon surfaces and recently found phenomena concerning them.

This thesis is organized as follows:

Chapter 2

We review the photon sphere of the Schwarzschild spacetime. Following Synge's analysis [3], we see that the black hole shadow we will observe is shaped by the photon sphere. The photon sphere of the Reissner-Nordström spacetime is also reviewed.

Chapter 3

We introduce a photon surface and see the equivalent condition for a hypersurface to be a photon surface, which is stated in the theorems in Refs. [8, 9]. We also define and analyze the *stability of photon surface*. It is a notion which generalizes the stability of circular orbits of photons on a photon sphere. The latter part is based on Ref. [15].

Chapter 4

We find explicit examples of photon surfaces appearing in less symmetric, or possibly non-symmetric spacetimes. Remarkably, the spacetimes are solutions to the Einstein equation. This chapter is based on Ref. [16].

Chapter 5

We consider an accretion problem of perfect fluid in a spherically symmetric system. Especially, we focus on the sonic point of the flow, which is known to be crucial in the analysis of accretion problems. As the main result, we establish the theorem of *the sonic point/photon sphere (SP/PS) correspondence*, which states that a sonic point of radiation fluid flow must be located on a photon sphere. The theorem holds in an arbitrary spacetime of arbitrary dimensions as far as it is static and spherically symmetric. This chapter is based on Ref. [17].

Chapter 6

We generalize the SP/PS correspondence to the rotational flow. The fluid is distributed as a rotational thin disk lying on the equatorial plane of a spherically symmetric space-

time. It is revealed that the correspondence exactly holds in this case. This chapter is based on Ref. [18].

Chapter 7

The SP/PS correspondence is generalized to the correspondence between sonic points and photon surfaces in hyperbolically and planar symmetric spacetimes. The result provides a geometrical implication for the correspondence. This chapter is based on Ref. [19].

Chapter 8

The thin-shell formalism allows us to construct a new spacetime by joining two spacetimes and putting thin matter distribution, called a thin shell, along the joint surface. We see that if the equation of state of the shell is *pure tension* and a few conditions are additionally satisfied, the joined boundaries of the two original spacetimes must be photon surfaces. The relation between the stabilities of the joined spacetime and the photon surfaces is also investigated. Applying the photon sphere uniqueness theorem [11], we finally establish the uniqueness theorem of pure-tensional thin shell wormholes. This chapter is based on Ref. [20].

Chapter 9

This chapter is devoted to the conclusion of this thesis.

In this thesis, we use geometrical units $G = c = 1$. We denote vectors and tensors (vector and tensor fields) with or without indices. For the notation with indices, we basically adopt the Wald's convention [21]. The Latin indices $a, b, ...$ of vectors and tensors are the Wald's abstract indices except for Chap. 8, Appendix C.1, and Appendix C.2. The Greek indices $\mu, \nu, ...$ and $\alpha, \beta, ...$ denote indices with respect to a generic or specific coordinate system $\{x^\mu\}$ of a spacetime depending on the context. The Latin indices $i, j, ...$ and $A, B, ...$ denote a part of the coordinate indices. For the notation without indices, we use brackets ( ) to express a tensor acting on vectors. For example, a $(0, 2)$-type tensor T acting on vectors v, u takes the value $T(v, u)$. This is what is expressed as $T_{ab}v^a u^b$ in the abstract index notation. This notation is often adopted in Chap. 8. The other notations concerning geometrical calculations are basically based on Wald's convention [21] throughout this thesis.

Chapter 2

Photon sphere

A photon sphere is a sphere of spacetime on which null geodesics take circular orbits. In astrophysical cases, black holes usually have photon spheres near their horizons. A photon sphere has been widely studied in its various aspects. for optical observations of black holes through background light emission, the photon sphere is related to the size of the black hole shadow. In the case of the Schwarzschild black hole, for example, we can see their relation from the calculation by Synge [3]. Quite recently, the Event Horizon Telescope Collaboration has observed, for the first time, the shadow of the supermassive black hole candidate in the center of the galaxy M87 and derived its mass by comparing the images with the theoretical expectations [2]. properties of gravitational waves from black holes are also closely related to the photon sphere. It is known that the frequencies of quasinormal modes are related to the parameters of null geodesic motions on and near the photon sphere in various situations [4] [5].

Stability of a photon sphere, i.e. stability of the circular orbits on the sphere, plays key roles in the applications of a photon sphere to astrophysics. For instance, a photon sphere that shapes a black hole shadow is unstable. A stable photon sphere, on the other hand, is inferred to cause nonlinear instability of spacetime [22] [23] [6]. When a spacetime is perturbed, gravitational waves propagating nearly along a stable photon sphere would grow nonlinearly while they are being trapped and coupled with each other in the vicinity of the radius. They will probably break the structure near the photon sphere and, finally, the spacetime. In fluid dynamics on a curved spacetime, the stability of a photon sphere also has remarkable importance.

In this chapter, we review the photon spheres of the Schwarzschild spacetime and the Reissner-Nordström spacetime. We see their significance from Synge's analysis [3], which relates photon spheres to black hole shadow observations.

This chapter is organized as follows. In Sec. 2.1, we analyze the photon sphere of the Schwarzschild spacetime and the relation to the black hole shadow. In Sec. 2.2, we also investigate the Reissner-Nordström case. In Sec. 2.3, the other examples of the applications of photon spheres are introduced. In Sec. 2.4, we summarize this chapter.

2.1 Photon sphere in Schwarzschild spacetime

The Schwarzschild spacetime (M, g) is given by the metric,

$$ds^2 = -f(r)dt^2 + \frac{1}{f(r)}dr^2 + r^2(d\theta^2 + \sin^2\theta d\phi^2), \quad f(r) = 1 - \frac{2m}{r}, \tag{2.1}$$

where $m > 0$ is the mass. The spacetime is static, spherically symmetric, and a vacuum solution to the Einstein equation. The radius $r = 2m$ gives $f(r) = 0$ and is called *a Killing horizon*. This is the surface of the Schwarzschild black hole. Note, since the inside is non-stationary, a single patch spanned by the static coordinates $\{t, r, \theta, \phi\}$ can cover only the stationary region $r > 2m$.

Consider a null geodesic $x^\mu = x^\mu(\lambda)$ with the affine parameter λ. We assume the orbit is confined in the equatorial plane, $\theta = \pi/2$, without loss of generality. The null condition leads to the equation

$$\mathcal{H} = \frac{1}{2}g_{\mu\nu}\dot{x}^\mu\dot{x}^\nu = 0 \tag{2.2}$$

for its Hamiltonian $\mathcal{H}$, where $\dot{} = d/d\lambda$. From the two Killing vectors relevant to the motion,

$$\xi_{(t)} = \partial_t, \ \xi_{(\phi)} = \partial_\phi, \tag{2.3}$$

we have the two conserved quantities,

$$E := -g_{\mu\nu}\xi^\mu_{(t)}\dot{x}^\nu = f(r)\dot{t}, \tag{2.4}$$

$$L := g_{\mu\nu}\xi^\mu_{(\phi)}\dot{x}^\nu = r^2\sin^2\theta\dot{\phi} = r^2\dot{\phi}. \tag{2.5}$$

They are the energy and the angular momentum. Then the null geodesic equation reduces to the equation,

$$\frac{1}{2}\dot{r}^2 + V(r) = 0, \quad V(r) := -\frac{1}{2}\left(E^2 - L^2 f(r)r^{-2}\right), \tag{2.6}$$

with its effective potential $V(r)$. The problem reduces to the one-dimensional dynamical system in the r-direction.

With the scaling $\lambda \to \lambda/E$, we have

$$\frac{1}{2}\dot{r}^2 + V(B, r) = 0, \quad V(B, r) := -\frac{1}{2}\left(1 - B^2 f(r)r^{-2}\right) \tag{2.7}$$

where $B := L/E$ is the impact parameter. Synge [3] analyzed the behavior of null geodesics by drawing the curve of $V(B, r) = 0$ in an $r - B^2$ plane as in Fig. 2.1. In the plane, null geodesic motions are described by horizontal lines of $1/B^2 = \text{const}$. The region $r < 2m$ is the inside of the black hole, the solid curve corresponds to $V(B, r) = 0$, and the shaded region below the curve is not allowed for null geodesics since $\frac{1}{2}\dot{r}^2 = -V(r) < 0$ in the region. Thus, null geodesics at a point in the non-shaded region propagate horizontally with finite radial velocity until reflected by the $V(B, r) = 0$ curve. Null

geodesics can asymptote the curve if and only if they approach the maximum. In other words, only the null geodesics starting at the maximum of the potential in the $r - B^2$ plane stay the point. The radius of the maximum is $r = 3m$ and the corresponding critical impact parameter is $B^2 = B_c^2 := 27m^2$. Since the critical null geodesics have non-zero angular momenta, they are the null circular geodesics. In the real space, the set of photons orbiting around the black hole at the radius $r = 3m$ form a sphere. The sphere of $r = 3m$ is called *the photon sphere of the Schwarzschild spacetime*. Note that the circular null geodesics at $r = 3m$ are unstable circular orbits.

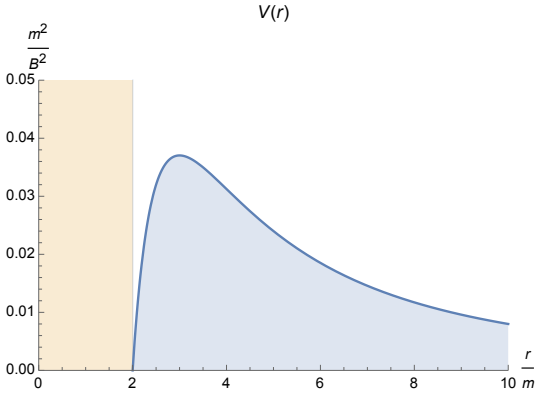

Figure 2.1: The allowed region for null geodesics in the Schwarzschild spaceitme

2.1.1 Black hole shadow

When a black hole in our universe is observed through background light emissions, what we actually see as a black hole shadow is the mapping of the impact parameters of the photons to our sight. Here we see the relation among the black hole shadow, the critical impact parameter of the photons, and the photon sphere.

Suppose that the Schwarzschild black hole and the observer are at rest and the observer observes a photon emitted from a light source. Since the spacetime is spherically symmetric, the free photon orbit and the center of the black hole lie in a common plane. The observer should also lie in the plane to observe the photon. We focus on this plane in the following.

Without loss of generality, we can assume the photon and the observer are on the equatorial plane, i.e. the surface of $\theta = \pi/2$ with respect to the Schwarzschild coordinates in Eq. (2.1). The observer is at a point p_o given by $x^i = (r_o, \pi/2, 0)$ where $x^i = (r, \theta, \phi)$ is the spatial coordinates. The observer's spatial orthonormal basis is defined by

$$\begin{aligned} e_1 &= -f^{1/2}(r_o)\partial_r, \\ e_2 &= r_o^{-1}\partial_\theta, \\ e_3 &= r_o^{-1}\partial_\phi. \end{aligned} \tag{2.8}$$

The vector e_1 is directed to the black hole center. The vector e_3 is orthogonal to e_1 but lies in the equatorial plane. The vector e_2 is orthogonal to the equatorial plane

and therefore to the null geodesic along which the photon propagates. Letting k be the tangent to the null geodesic, the angle of incidence Θ measured from the axis e_1 in the observer's sight is given by

$$\tan\Theta = \frac{g(e_3,-k)}{g(e_1,-k)} = \frac{-r_o k^\phi}{[f(r_o)]^{-1/2}k^r} = -[f(r_o)]^{1/2} r_o^{-1} \frac{B}{[1-B^2 f(r_o) r_o^{-2}]^{1/2}}. \tag{2.9}$$

Since the right-hand side is monotonically decreasing in B, there is a one-to-one mapping between Θ and B in the range $\Theta \in [0, \pi/2)$. Specifically, $B = 0$ for $\Theta = 0$ and $B \to \mp[f(r_o)]^{-1/2} r_o$ as $\Theta \to \pm\pi/2$.

We are interested in light emissions from background sources which shape the black hole shadow. Suppose a photon which is emitted from a source at a point distant to the black hole, passes by the black hole, and finally reaches the distant observer. That is, the orbit decreases its radius initially and increases it finally. From Eq. (2.7) or Fig. 2.1, a photon can change its state from $\dot{r} < 0$ to $\dot{r} > 0$ only if $B^2 > B_c^2$. In other words, a photon with an impact parameter $B^2 \leq B_c^2$, corresponding to the incident angle $-\Theta_c \leq \Theta \leq \Theta_c$, can never reach the observer. From the observer's point of view, there are no photons coming from the angle $-\Theta_c \leq \Theta \leq \Theta_c$ where

$$\Theta_c := \arctan\left[[f(r_o)]^{1/2} r_o^{-1} \frac{|B_c|}{[1-B_c^2 f(r_o) r_o^{-2}]^{1/2}} \right] \tag{2.10}$$

is the critical angle corresponding to the critical impact parameter B_c^2. The outside of the critical angle can be bright depending on the light source distributions around the black hole. The dark region $-\Theta_c \leq \Theta \leq \Theta_c$ is called the black hole shadow. The shadow is said to be shaped by the photon sphere because the photons with the critical impact parameter B_c^2 corresponds to the edge of the shadow and they are the photons reflected by the top of the potential $V(r)$ at $r = 3m$.

2.2 Photon sphere in Reissner-Nordström spacetime

Let (M, g) be the Riessner-Nordström spacetime. The metric is given by

$$ds^2 = -f(r)dt^2 + \frac{1}{f(r)}dr^2 + r^2(d\theta^2 + \sin^2\theta d\phi^2), \quad f(r) = 1 - \frac{2m}{r} + \frac{Q^2}{r^2} \tag{2.11}$$

where Q is the electric charge. The field strength of the electromagnetic field is given by

$$F = \frac{q}{2r^2} dt \wedge dr, \quad q^2 = 2\kappa^{-2}Q^2 \tag{2.12}$$

where $\kappa = 8\pi G/c^4 = 8\pi$. For the parameters $0 < Q^2/m^2 < 1$, there are two Killing horizons,

$$r_\pm = m \pm \sqrt{m^2 - Q^2}. \tag{2.13}$$

The stationary regions are $r < r_-$ and $r > r_+$. This state is called sub-extremal. For $Q^2/m^2 = 1$, the horizons degenerate to $r_\pm = m$. The state is called extremal. For

$Q^2/m^2 > 1$, the spacetime is stationary over $0 < r < \infty$ and the Killing horizons disappear. The state is said to be over-extremal and has the naked singularity at the center. This spacetime is a solution to the Einstein-Maxwell equation and has a photon sphere for the various parameter values.

The null geodesic equation also reduces to Eq. (2.6) with the replacing of $f(r)$ by that of Eq. (2.11). There are photon spheres on the radii given by $V'(r_p) = 0$ in the stationary region. The radii are

$$r_{p\pm} = \frac{3m \pm \sqrt{9m^2 - 8Q^2}}{2}. \tag{2.14}$$

For the sub-extremal case, since $r_- < r_{p-} < r_+ < r_{p+}$, only $r = r_{p+}$ is the photon sphere. Similarly, r_{p+} is the unique photon sphere in the extremal case. The null geodesics staying at $r_\pm = r_{p-}$ are not circular but have fixed angles (θ, ϕ). For the over-extremal case, there are two photon spheres $r_{p\pm}$ as far as $1 < Q^2/m^2 < 9/8$. The outer one corresponds to unstable circular null geodesics like as the photon sphere of the Schwarzschild spacetime. The inner one corresponds to stable circular null geodesics. For the larger $Q^2/m^2 > 9/8$, the spacetime has no photon spheres.

2.2.1 Black hole shadow

For the parameter $Q^2/m^2 \leq 1$, the unique photon sphere $r = r_{p+}$ shapes the black hole shadow. It can be seen from analysis parallel to that in the previous section. Photons with sub-critical impact parameters $B^2 < B_c^2$, where B_c^2 is now given by $B_c^2 = [f(r_{p+})r_{p+}^{-2}]^{-1}$, cannot be reflected by the potential barrier and are absorbed by the black hole. Then the observer observes the shadow of the angle $-\Theta_c < \Theta < \Theta_c$ in the sight where Θ_c is the critical angle corresponding to this B_c^2. However, for $1 < Q^2/m^2 \leq 9/8$, any photon is eventually reflected by the potential and the shadow is not form. Moreover, the inner photon sphere r_{p-} do nothing special for the observer because photons orbiting near the local minimum of $V(r)$ are never observed by the distant observer. In this sense, photon spheres of stable circular null geodesics are irrelevant to black hole shadow observations. Such stable photon spheres are also called anti-photon spheres [10].

As we can see from the above studies, the unstable and stable photon sphere have different physical significance. The other applications of unstable and stable photon spheres are provided in the following.

2.3 Applications to astrophysical problems

Photon spheres play key roles in not only the formation of black hole shadows but also various astrophysical problems. In particular, the stability of corresponding circular null geodesics, namely the stability of the photon sphere, are crucial for the applications.

A black hole has its quasinormal modes (QNMs), which dominate the ringing of the hole. Cardoso *et al.* [4] found surprising coincidence between QNMs of a black hole and the unstable photon sphere surrounding it. That is, the quasinormal frequencies

(QNFs) are determined by the parameters of the photon sphere, Ω_c and λ, where Ω_c is the angular velocity of the unstable circular null geodesics along the photon sphere and λ is their principal Lyapunov exponent representing the instability time scale of the orbits. The relation, being valid in the eikonal limit of a mode $l \to \infty$, is given by

$$\omega_{\rm QNM} = \Omega_c l - i(n + 1/2)|\lambda|, \tag{2.15}$$

where n is the overtone number and l is the angular momentum of the mode. In the mathematical aspect, the equation enables us to calculate QNFs more easily without solving the eigen value problem of the Regge-Wheeler equation for the gravitational, scalar, and vector perturbations. In the astrophysical aspect, it implies that not only optical observations but also gravitational wave observations are characterized by the photon sphere rather than the black hole horizon. The coincidence is also known to appear in another case [5].

A stable photon sphere, on the other hand, is considered to cause nonlinear instability of spacetime [22, 7, 6]. In general, if a spherical star is compactified so that its areal radius is less than $3m$, there must be a stable photon sphere inside the star in addition to the unstable photon sphere of $r = 3m$. Such a compact star is called a ultra compact object (UCO). The emergence of a stable photon sphere inside a UCO causes long-lived modes for the gravitational perturbation in linear order because of the trapping of gravitational waves along the sphere. The long-lived modes imply the growth of the perturbation amplitude in nonlinear order due to the mode-mode coupling and may lead to the generic instability of a UCO. The nonlinear instability of UCOs is also crucial from the observational view point. Suppose the surface of a UCO neither emits nor reflects lights. In that case, the UCO can have the shadow as a black hole does. Thus, the observation of a shadow might not prove the existence of the black hole in the shadow. We need not take into account this possibility if the nonlinear instability of UCOs is concluded.

In the analysis of accretion problems, photon spheres play key roles. In Refs. [17, 18], the correspondence between sonic points of radiation accretion flow and photon spheres was found. The works had shown the one-to-one correspondence between the radii of *critical points*, which is defined in the analysis of accretion problems by Chaverra and Sarbach [24], and photon spheres for accretion problems of radiation fluid. In more detail, saddle-type critical points and extremum-type critical points correspond to unstable and stable photon spheres, respectively. Since the sonic point of the physical accretion flow coincides with one of the saddle points, the one-to-one correspondence implies that any radiation flow has its sonic point on an unstable photon sphere. The coincidence was named *the sonic point/photon sphere (SP/PS) correspondence* and proven for radial [17] and rotational [18] flow in a spherically symmetric spacetime. Subsequently, the result was generalized to the correspondence between the sonic points and photon surfaces in Ref. [19]. We see the works [17, 18, 19] in Chaps. 5–7.

2.4 Summary

In this chapter, we have overviewed the photon spheres of the Schwarzschild spacetime and the Reissner-Nordström spacetime. They are defined as radii where null geodesics take circular orbits. From the symmetry of the spacetimes, the geodesic equations reduce to the potential problems with the effective potentials $V(r)$ and their extrema correspond to the photon spheres.

It is important to recognize that the null geodesics on the photon spheres are unstable circular orbits because the corresponding extrema of the potentials are local maxima. This fact is crucial for the analysis of black hole shadows and we have clarified that the edges of the shadows are shaped by the unstable photon spheres. That is, the critical impact parameters, corresponding to the circular null geodesics on the photon spheres, are the smallest ones for null geodesics we can observe at infinity. The corresponding critical angles of incidence were also derived.

Depending on the stability, photon spheres have many applications to astrophysics. Unstable photon spheres are related to the QNFs for the black holes inside the spheres. On the other hand, stable photon spheres can cause the nonlinear instability of spacetime. We see another physics named SP/PS correspondence in Chaps. 5–7.

Chapter 3

Photon surface

Originally published as:
Y. Koga and T. Harada, *Phys. Rev. D* **100** (2019) 064040.

A photon surface is a geometrical structure first introduced by Claudel, Virbhadra and Ellis [8] as the generalization of a photon sphere. The surface is defined so that it inherits only the local properties of a photon sphere and does not necessarily have global symmetries. Together with the definition, the authors also proved a theorem concerning the equivalent conditions for a surface to be a photon surface as one of the main results. The theorem (Theorem 2.2 in [8]) states that a given timelike hypersurface is a photon surface if and only if it is totally umbilic, i.e. the second fundamental form is pure trace everywhere. Subsequently, Perlick [9] proved that the theorem holds for arbitrary dimensions of the surface and the spacetime. Since a photon surface requires no global symmetries, it would have more applicability to many physical problems in addition to its own interest as a geometrical object.

As with the stability of a photon sphere, the stability of a photon surface should be also important for the applications to various problems of physics. In this paper, we define the stability of null geodesics along a photon surface and derive the stability conditions. Usually, the stability of a photon sphere is easily defined because the null geodesic in static and spherically symmetric spacetime obeys a one-dimensional equation of motion and the problem reduces to the analysis of the effective potential. In particular cases, the stability of photon surface was defined by use of optical metric [10] and by the effective potential method [19]. For a generic photon surface, we define the stability in a covariant manner by considering a geodesic deviation. Since a geodesic deviation is governed by a local geometrical quantity, the Riemann curvature, the stability condition is finally obtained in terms of the curvature.

This chapter is organized as follows. In Sec. 3.1 we introduce *a photon surface* and review the theorems for the equivalent conditions for a hypersurface to be a photon surface. In Sec. 3.2, after reviewing and reformulating the stability of *a photon sphere*, we define the stability of null geodesics along a photon surface based on the arguments for a photon sphere and derive the stability condition in terms of the Riemann curvature. In Sec. 3.3, we derive an alternative expression of the stability condition in terms of the

second fundamental form with an appropriate foliation, and give another interpretation of our definition of stability. The stability conditions in Secs. 3.2 and 3.3 are guaranteed to be equivalent by Raychaudhuri equation for the unit normal vector field of the foliation. The stability conditions indicate that we can a priori identify the stability before finding photon surfaces of spacetime explicitly. For example, any photon surface in conformally flat spacetime is stable if the null energy condition is satisfied. We see the corollaries for such special cases in Sec. 3.4. The summary is given in Sec. 3.5.

3.1 Photon surface

The photon sphere of the Schwarzschild spacetime gives the criterion for trapping of infalling and outgoing light rays. Inside the photon sphere, any null geodesics directed inwardly will fall into the black hole. Outside the sphere, any null geodesics directed outwardly will escape to infinity. Comparing this property with the concept of a closed trapped surface, Claudel, Virbhadra, and Ellis [8] introduced a geometrical definition of a photon surface, which generalizes the photon sphere to a structure of a general spacetime.

The authors first summarized the photon sphere of the Schwarzschild spacetime; the photon sphere is a static and spherically symmetric hypersurface on which every null geodesic initially tangent to it remains tangent. A photon surface is then defined as a hypersurface on which every null geodesic initially tangent to it remains tangent:

Definition 3.1.1 (Photon surface [8])**.** *A photon surface of a spacetime (M, g) is an immersed, nowhere-spacelike hypersurface S of (M, g) such that, for every point $p \in S$ and every null vector $k \in T_pS$, there exists a null geodesic $\gamma : (-\epsilon, \epsilon) \to M$ of (M, g) such that $\dot{\gamma}(0) = k, |\gamma| \subset S$.*

Note that any null hypersurface is trivially a photon surface. Note also that a photon surface is an invariant structure of spacetime under any conformal transformation. That is, a photon surface S of a spacetime (M, g) is a photon surface of $(M, \Omega^2 g)$ for any smooth function $\Omega : M \to (0, \infty)$ [8].

As in the case of photon spheres, we are interested in timelike photon surfaces espeacially. One can find a trivial example of a timelike photon surface in the Minkowski spacetime:

Example 3.1.2 (Plane in Minkowski 3-spacetime)**.** *A timelike plane S in the 3-dimensional Minkowski spacetime $\mathbb{M}^3$ is trivially a photon surface. Let $\{t, x, y\}$ be the Cartesian coordinates such that the metric is given by*

$$\eta = -dt^2 + dx^2 + dy^2 \tag{3.1}$$

and S is given by $y = 0$. Any null vector $k \in T_pS$ tangent to S at a point $p \in S$ is given by $k^\mu = \alpha(1, \pm 1, 0)$ with a constant α. Since a geodesic is a straight line in Minkowski spacetime of any dimensions, the null geodesic γ to which k is tangent at $p \in S$ is given by

$$\gamma^\mu(\lambda) = k^\mu \lambda + x_p^\mu = \alpha(\lambda, \pm\lambda, 0) + x_p^\mu \tag{3.2}$$

with the affine parameter λ where x^μ_p is the coordinates of p. The null geodesic γ is tangent to S for any λ and therefore, the plane S is a timelike photon surface according to Definition 3.1.1.

The example is easily generalized to higher dimensions:

Example 3.1.3 (Hyperplane in Minkowski D-spacetime)**.** *A timelike hyperplane S in the D-dimensional Minkowski spacetime $\mathbb{M}^D$ with $D \geq 3$ is a photon surface. Let $\{t, x_1, ..., x_{D-1}\}$ be the Cartesian coordinates such that the metric is given by*

$$\eta = -dt^2 + dx_1^2 + ... + dx_{D-1}^2 \tag{3.3}$$

and S is given by $x_{D-1} = 0$. Let $k \in T_pS$ be a null vector tangent to S at $p \in S$. The null vector k has the components $k^\mu = \alpha(1, k^1, ..., k^{D-2}, 0)$ with the condition $(k^1)^2 + ... + (k^{D-2})^2 = 1$ where α is a constant. The null geodesic γ to which k is tangent at $p \in S$ is given by the equation,

$$\gamma^\mu(\lambda) = k^\mu\lambda + x^\mu_p = \alpha(\lambda, k^1\lambda, ..., k^{D-2}\lambda, 0) + x^\mu_p, \tag{3.4}$$

with the affine parameter λ where x^μ_p is the coordinates of p. Trivially, γ is tangent to S for any λ and therefore, the hyperplane S is a photon surface of $\mathbb{M}^D$.

Another type of a photon surface in the Minkowski spacetime is a hyperboloid. A single-sheeted hyperboloid of the three-dimensional Minkowski spacetime was proven to be a photon surface in Ref. [8]:

Example 3.1.4 (Hyperboloid in Minkowski 3-spacetime)**.** *A single-sheeted hyperboloid S given by*

$$-t^2 + x^2 + y^2 = a^2 \tag{3.5}$$

for a constant $a > 0$ in the Minkowski 3-spacetime $\mathbb{M}^3$ is a timelike photon surface. One can see that the family of null geodesics given by

$$\gamma^\mu_{\theta,\pm}(\lambda) := a\lambda(1, \mp\sin\theta, \pm\cos\theta) + a(0, \cos\theta, \sin\theta) \tag{3.6}$$

with the parameter $\theta \in [0, 2\pi)$ and the sign $\pm$ are tangent to S for any λ. These are the rulings of S and therefore, at every point $p \in S$, there exist two independent null geodesics tangent to S. Since a two-dimensional timelike hypersurface has only two independent null vectors tangent to it at each point $p \in S$, the two independent null geodesics are the null geodesics to which all the possible null vectors $k_\pm \in T_pS$ are tangent. Hence the single-sheeted hyperboloid S is a photon surface.

The example is also generalized to the D-dimensional case:

Example 3.1.5 (Hyperboloid in Minkowski D-spacetime)**.** *A single-sheeted photon surface S given by*

$$\eta_{\mu\nu}x^\mu x^\nu = -t^2 + x_1^2 + ... + x_{D-1}^2 = a^2 \tag{3.7}$$

for a constant $a > 0$ in the Minkowski D-spacetime $\mathbb{M}^D$ is a timelike photon surface. Defining the function $\Phi := \eta_{\mu\nu}x^\mu x^\nu - a^2$, which gives S by $\Phi = 0$, the normal to S is given by $d\Phi = 2\eta_{\mu\nu}x^\mu dx^\nu$. A null vector $k \in T_pS$ is a vector at $p \in S$ which satisfies $\eta_{\mu\nu}k^\mu k^\nu = 0$ and $d\Phi(k)|_p = 2\eta_{\mu\nu}x_p^\mu k^\nu = 0$. The null geodesic γ to which k is tangent at $p \in S$ is given by

$$\gamma^\mu(\lambda) = k^\mu\lambda + x_p^\mu. \tag{3.8}$$

For any point on γ given by $x_0^\mu = \gamma^\mu(\lambda_0)$ with a parameter value λ_0, it is satisfied that

$$\begin{aligned}
\Phi(x_0) &= \eta_\mu x_0^\mu x_0^\nu - a^2 \\
&= \eta_\mu \gamma^\mu(\lambda_0)\gamma^\nu(\lambda_0) - a^2 \\
&= \eta_{\mu\nu}k^\mu k^\nu\lambda_0^2 + 2\eta_{\mu\nu}x_p^\mu k^\nu + \eta_{\mu\nu}x_p^\mu x_p^\nu - a^2 \\
&= \eta_{\mu\nu}x_p^\mu x_p^\nu - a^2 \\
&= \Phi(x_p) \\
&= 0.
\end{aligned} \tag{3.9}$$

That is, any point on the null geodesic γ is on S, or equivalently, γ is tangent to S for any λ. Therefore, there exists a null geodesic tangent to S for any null vector $k \in T_pS$ such that k is tangent to γ at $p \in S$. Hence the single-sheeted hyperboloid S is a timelike photon surface of $\mathbb{M}^D$.

Since a photon surface is an invariant structure under a conformal transformation, the flat FLRW spacetime also has photon surfaces as many as the Minkowski spacetime does [8]:

Example 3.1.6 (The Robertson-Walker models)**.** *Since all the Robertson-Walker models are conformally flat and therefore locally conformally transformable to the Minkowski spacetime, the photon surfaces of any such model may thus be obtained, at least locally, by conformal transformations of the Minkowski spacetime.*

Gibbons and Warnick [10] found photon surfaces in the uniformly accelerated black hole spacetime, which is less symmetric and less trivial than the examples above:

Example 3.1.7 (Photon surface of the C-metric)**.** *A uniformly accelerated Λ-vacuum black hole spacetime is given by the C-metric,*

$$ds^2 = \frac{1}{A^2(x+y)^2}\left[-F(y)dt^2 + \frac{1}{F(y)}dy^2 + \frac{1}{G(x)}dx^2 + G(x)d\phi^2\right], \tag{3.10}$$

where

$$\begin{aligned}
F(y) &= y^2 + 2mAy^3 - 1 - \frac{\Lambda}{3A^2}, \\
G(x) &= 1 - x^2 - 2mAx^3,
\end{aligned} \tag{3.11}$$

and $A > 0$, $m > 0$, and Λ are the constants representing the acceleration, mass, and the cosmological constant, respectively. The function F is positive on an interval (y_0, y_1)

and vanishes at y_0 and y_1, where $y_0 < y_1 < 0$, if $\Lambda < \Lambda_c := (1 - 27m^2A^2)/(9m^2)$. The region corresponds to the stationary region of the spacetime and the zero-points of F at y_0 and y_1 correspond to the black hole horizon and the acceleration horizon, respectively. For $\Lambda < \Lambda_c$, there is a photon surface given by $y = -(3mA)^{-1} \in (y_0, y_1)$. The photon surface corresponds to the photon sphere $r = 3m$ of the Schwarzschild (anti-)de Sitter spacetime in the zero-acceleration limit $A \to 0$.

See [10] for the details and charged and scalarized cases.

The works by Claudel et al. [8] and Perlick [9] give the equivalent condition for a timelike hypersurface to be a photon surface:

Theorem 3.1.8 (Claudel et al. (2001), Perlick (2005))**.** *Let S be a timelike hypersurface of spacetime (M, g) with $D := \dim M \geq 3$. Let n be the unit normal to S. Let $h_{ab} = g_{ab} - n_a n_b$, $\chi_{ab} = h_a^c \nabla_c n_b$, $\Theta = h^{ab}\chi_{ab}$, and $\sigma_{ab} = \chi_{ab} - \frac{\Theta}{D-1} h_{ab}$ be the induced metric, the second fundamental form, the mean curvature, and the trace-free part of χ_{ab}, respectively. S is a photon surface if and only if it is totally umbilic, i.e.,*

$$\sigma_{ab} = 0 \quad \forall p \in S. \tag{3.12}$$

The theorem enables us to see whether a given hypersurface is a photon surface or not by straight forward geometrical calculations. With this useful technique, we investigate other interesting examples of photon surfaces in Chap. 4.

3.2 Stability of null orbits along Photon Surface

Here, after reviewing the stability of a photon sphere, we define the stability of a photon surface. Then we derive the stability condition in terms of curvature.

3.2.1 Stability of Photon Sphere

Consider static and spherically symmetric spacetime. A hypersurface of constant radius, $S = \mathbb{R} \times S^2$, is called a photon sphere if there exist null circular orbits, i.e. null geodesics whose spatial orbits are circles, on S. The photon sphere is said to be stable if the circular orbits are stable circular orbits and unstable if unstable circular orbits. We can describe the stability in a covariant manner as follows.

For a stable photon sphere, if a null geodesic on the sphere is perturbed from the sphere, the perturbed geodesic is attracted to (accelerated toward) the unperturbed geodesic. On the other hand, the perturbed geodesic is repelled from (accelerated fromward) the unperturbed geodesic if the photon sphere is unstable. Therefore, the stability of a null circular geodesic is given by the relative acceleration between the circular geodesic and its infinitesimally nearby null geodesic.

The above argument is represented in terms of a geodesic deviation. Consider a null circular geodesic γ with its tangent vector k on a photon sphere S and the infinitesimally nearby null geodesic $\tilde{\gamma}$ which is obtained by perturbing γ in the radial direction at a point

$p \in S$. Let X be the deviation vector arising from γ and $\tilde{\gamma}$. It satisfies the condition $X \propto n$ at p for the unit normal vector n of S. Then the relative acceleration between γ and $\tilde{\gamma}$ is given by $a = \nabla_k (\nabla_k X)$ and γ is stable if $g(X,a)|_p < 0$ while unstable if $g(X,a)|_p > 0$. If $g(X,a)|_p = 0$, γ is marginally stable.

Note that because of the symmetry, if there is a null geodesic γ on a photon sphere S that is stable, unstable, and marginally stable at p, γ is stable, unstable, and marginally stable, respectively, everywhere on S and all other null geodesics on S has the same stability as γ. Therefore photon spheres are completely classified into stable, unstable, and marginally stable ones.

3.2.2 Stability of null geodesics on a photon surface

Following the argument in Sec. 3.2.1, we define the stability of a null geodesic γ on a photon surface S in terms of the deviation vector orthogonal to S. The deviation is interpreted as what gives the perturbation of γ from S:

Definition 3.2.1 (Stability of a null geodesic)**.** *Let S be a timelike photon surface of (M,g) and n be the unit normal vector of S. Let γ be a null geodesic on S passing a point $p \in S$ and k be the tangent vector to γ. Let X be the deviation vector of γ satisfying the condition,*

$$X|_p \propto n|_p \,. \tag{3.13}$$

The null geodesic γ is said to be stable, unstable, and marginally stable at p if the acceleration scalar $a := g\left(X, \nabla_k (\nabla_k X)\right)$ satisfies

$$a|_p < 0, \quad > 0, \quad \text{and} \quad = 0, \tag{3.14}$$

respectively.

The spacetime dimension is implicitly assumed to be $\dim M \geq 3$ since a photon surface in spacetime with $\dim M = 2$ is one-dimensional, i.e. a null geodesic itself, and cannot be timelike. The deviation vector X is, usually, physically interpreted as what gives the null geodesic $\tilde{\gamma}$ which is obtained when γ is perturbed at p in the direction orthogonal to S. a represents the relative acceleration of $\tilde{\gamma}$ to γ or S. This is what we need for our description of the stable or unstable behaviors of (perturbed) null geodesics, being attracted to or repelled from S. Note that γ can be either stable or unstable depending on the point p. Furthermore, the stability also depends on the direction $k \in T_p S$ of the null geodesic. If γ is stable, unstable, and marginally stable at $\forall p \in |\gamma|$, we simply call it stable, unstable, and marginally stable, respectively.

From the geodesic deviation equation, the left-hand side of Eq. (3.14) is calculated as

$$\begin{aligned} a|_p &= -\left[R_{acbd} X^a k^c X^b k^d\right]_p \\ &= -\left[X^2 R_{acbd} n^a k^c n^b k^d\right]_p \end{aligned} \tag{3.15}$$

where $X^2 := g_{ab} X^a X^b$ is positive. Then we reach the following stability condition:

Proposition 3.2.2. *Let S be a timelike photon surface and γ be a null geodesic on S with the tangent vector k at $p \in S$. Then γ is stable, unstable, and marginally stable at p if and only if*

$$R_{acbd}k^a n^c k^b n^d > 0, \ < 0, \ \text{and} \ = 0, \tag{3.16}$$

respectively, at p.

It is worth noting that the component $R_{acbd}k^a n^c k^b n^d$, or more generally $R_{ecfd}h^e_a n^c h^f_b n^d$ where h^a_b is the induced metric on S, is the missing component in Gauss-Codazzi equations for the decomposition of the curvature concerning S and n. Therefore it cannot be expressed solely in terms of the intrinsic and extrinsic curvatures [25].

The decomposition of Riemann tensor into Weyl tensor C_{abcd} and Ricci tensor R_{ab} often helps us to understand the physics. We also have the expression alternative to Proposition 3.2.2:

Proposition 3.2.3. *Let S be a timelike photon surface and γ be a null geodesic on S with the tangent vector k at $p \in S$. Then γ is stable, unstable, and marginally stable at p if and only if*

$$C_{acbd}k^a n^c k^b n^d + \frac{1}{D-2}R_{ab}k^a k^b > 0, \ < 0, \ \text{and} \ = 0, \tag{3.17}$$

respectively, at p where $D \geq 3$ is the spacetime dimension.

Although a photon surface S of spacetime (M, g) is invariant submanifold under a conformal transformation $(M, g) \to (M, \Omega^2 g)$ [8], Proposition 3.2.3 tells us that the stability of S is not conformally invariant due to the presence of Ricci tensor in the stability condition.

3.2.3 Stability of a photon surface

There can be both stable and unstable null geodesics on a photon surface S. We define *the stability of a photon surface* in cases where all the null geodesics on S are (un)stable:

Definition 3.2.4 (Stability of a photon surface)**.** *Let S be a timelike photon surface. Let $k_p \in T_pS$ be a null vector on a point $p \in S$. Let γ be the null geodesic on S passing p with the tangent vector k_p. The photon surface S is said to be*

- *stable if $a_{k_p}\big|_p \leq 0 \ \forall k_p \in T_pS, \ \forall p \in S$,*
- *strictly stable if $a_{k_p}\big|_p < 0 \ \forall k_p \in T_pS, \ \forall p \in S$,*
- *unstable if $a_{k_p}\big|_p \geq 0 \ \forall k_p \in T_pS, \ \forall p \in S$,*
- *strictly unstable if $a_{k_p}\big|_p > 0 \ \forall k_p \in T_pS, \ \forall p \in S$, and*
- *marginally stable if $a_{k_p}\big|_p = 0 \ \forall k_p \in T_pS, \ \forall p \in S$,*

where a_{k_p} is the acceleration scalar defined for each γ at each p as in Definition 3.2.1.

The left-hand side of the conditions can be expressed in terms of curvatures from Propositions 3.2.2 and 3.2.3.

3.3 Stability and second fundamental form

With a spacetime foliation, the curvature of spacetime is related to the first derivative of second fundamental forms, which is the tensor constructed from the second derivative of the unit normal vector field. Therefore, the stability condition in Proposition 3.2.2 can be rewritten in terms of the second fundamental form instead of the curvature. We here derive the stability condition in terms of the second fundamental form and give another interpretation of the stability, defined in Definition 3.2.1, with a particular spacetime foliation.

3.3.1 Stability condition in Gaussian normal foliation

Consider a timelike photon surface S of (M, g) and a spacetime foliation $\{S_r\}$ in the vicinity of S which includes S as

$$S_0 = S \tag{3.18}$$

for the parameter $r = 0$. For any foliation, the unit normal vector field n^a of the surfaces generates curves and the congruence consisting of them. Then the trace-free part of the second fundamental form, σ_{ab}, of each surface coincides with the shear of the congruence, while the vorticity $\omega_{ab} = 0$ by construction. We identify the shear of the congruence with σ_{ab}. Raychaudhuri equation for the congruence gives the relation between the shear evolution and the curvature,

$$\begin{aligned}\nabla_n \sigma_{ab} + \sigma_{ac}\sigma^c{}_b + 2\frac{\Theta}{D-1}\sigma_{ab} + \dot{n}_a\dot{n}_b + \nabla_{(a}\dot{n}_{b)} - \frac{1}{D-1}h_{ab}\left[\sigma^{cd}\sigma_{cd} + \dot{n}_c\dot{n}^c + \nabla_c\dot{n}^c\right] \\ = -R_{acbd}n^c n^d + \frac{1}{D-1}R_{cd}n^c n^d h_{ab}\end{aligned} \tag{3.19}$$

where $\dot{n}^a := \nabla_n n^a$. On the photon surface $S_{r_p} = S$, the equation reduces to

$$\nabla_n \sigma_{ab} + \dot{n}_a\dot{n}_b + \nabla_{(a}\dot{n}_{b)} - \frac{1}{D-1}h_{ab}\left[\dot{n}_c\dot{n}^c + \nabla_c\dot{n}^c\right] = -R_{acbd}n^c n^d + \frac{1}{D-1}R_{cd}n^c n^d h_{ab} \tag{3.20}$$

from the fact $\sigma_{ab} = 0\ \forall p \in S$. The left-hand side of the stability condition in Proposition 3.2.2 is therefore rewritten as

$$R_{acbd}k^a n^c k^b n^d = -k^a k^b \nabla_n \sigma_{ab} - k^a k^b \dot{n}_a \dot{n}_b - k^a k^b \nabla_a \dot{n}_b \tag{3.21}$$

for any foliation satisfying Eq. (3.18). Thus a null geodesic on a photon surface in the direction k at p is stable, unstable, and marginally stable if and only if the right-hand side of Eq. (3.21) is negative, positive, and zero, respectively.

Suppose the foliation in the vicinity of S satisfies the condition,

$$dn = 0, \tag{3.22}$$

for the unit normal n in addition to Eq. (3.18). The condition implies

$$n^b \nabla_b n^a = 0 \tag{3.23}$$

and therefore the parameter r is the one of Gaussian normal coordinates which parametrizes each hypersurface S_r. We refer to the foliation $\{S_r\}$ satisfying the conditions Eqs. (3.18) and (3.22) as *Gaussian normal foliation*. (One can rescale $r \to r' = r'(r)$ so that $n = dr$, however, here we only assume that the unit normal n points in the same direction as the normal dr.) From Eq. (3.22), Eq. (3.21) reduces to

$$R_{acbd}k^a n^c k^b n^d = -k^a k^b \nabla_n \sigma_{ab} \tag{3.24}$$

for the Gaussian normal foliation. Then we obtain the alternative expression of stability condition in Proposition 3.2.2 in terms of the second fundamental form:

Proposition 3.3.1. *Let S be a timelike photon surface and γ be a null geodesic on S with the tangent vector $k \in T_pS$ at $p \in S$. Let $\{S_r\}$, χ_{ab}, and σ_{ab} be Gaussian normal foliation, defined by the conditions in Eqs. (3.18) and (3.22), second fundamental form of each S_r, and its trace-free part, respectively. Then γ is stable, unstable, and marginally stable at p if and only if*

$$k^a k^b \left.\nabla_n \sigma_{ab}\right|_p < 0, \ > 0, \ \textit{and} \ = 0, \tag{3.25}$$

respectively.

A timelike photon surface is a hypersurface characterized by the vanishing of σ_{ab}. Similarly, stability of null geodesics on a photon surface is determined by $\nabla_n \sigma_{ab}$. To identify the stability of a photon surface, it would be easier to calculate the left-hand side of Eq. (3.25) in Proposition 3.3.1 rather than the curvature, Eq. (3.16), in Proposition 3.3.1 in many cases. In the analysis of the photon surfaces in Chap. 4, we derive the stability by using Proposition 3.3.1.

We give the interpretation of Proposition 3.3.1 by considering *acceleration of a geodesic with respect to a surface* in the following.

3.3.2 Acceleration with respect to a hypersurface

Consider a non-null hypersurface $\mathcal{S}$ of spacetime (M, g) and a (null or non-null) geodesic γ which is tangent to $\mathcal{S}$ at a point $p \in \mathcal{S}$ with the tangent vector $v \in T_p\mathcal{S}$. The tangent vector v to γ at p also generates the geodesic $\tilde{\gamma}$ of the subspace $(\mathcal{S}, h)$ where h is the induced metric on $\mathcal{S}$. For the tangent vector $\tilde{v}$ to $\tilde{\gamma}$, it holds that $\tilde{\nabla}_{\tilde{v}}\tilde{v} = 0$ along $\tilde{\gamma}$ where $\tilde{v} = v$ at p and $\tilde{\nabla}$ is the covariant derivative associated with h. The geodesic $\tilde{\gamma}$ of $(\mathcal{S}, h)$, as the curve of (M, g), has the acceleration $\nabla_{\tilde{v}}\tilde{v}$,

$$\begin{aligned} \tilde{v}^b \nabla_b \tilde{v}^a &= \tilde{v}^b \tilde{\nabla}_b \tilde{v}^a - \epsilon \chi_{bc} \tilde{v}^b \tilde{v}^c n^a \\ &= -\epsilon \chi_{bc} \tilde{v}^b \tilde{v}^c n^a \\ &= -\epsilon \chi_{bc} v^b v^c n^a \end{aligned} \tag{3.26}$$

at p. Here, n^a is the unit normal vector of $\mathcal{S}$ and $\epsilon := n^2$. This can be interpreted as the acceleration of $\tilde{\gamma}$ with respect to γ at p. Therefore, conversely, the geodesic γ of (M, g) has the relative acceleration,

$$a^a_{\mathcal{S}} := \epsilon \chi_{bc} v^b v^c n^a, \tag{3.27}$$

with respect to $\tilde{\gamma}$, or the hypersurface $\mathcal{S}$, at p.

The relative acceleration takes the form,

$$a^a_{\mathcal{S}} = \sigma_{bc} k^b k^c n^a, \tag{3.28}$$

for null vectors k in the case $\mathcal{S}$ is timelike. From the viewpoint of the relative acceleration $a^a_{\mathcal{S}}$, a photon surface is a hypersurface on which every (temporally) tangent null geodesics has no relative accelerations with respect to the surface due to the vanishing of σ_{ab} at all the point; $a^a_{\mathcal{S}} = 0 \ \forall \ null \ k \in T_p\mathcal{S} \ \forall p \in \mathcal{S}$.

3.3.3 Reinterpretation of the stability

The stability of null geodesics on a photon surface, defined in Definition 3.2.1, can be reinterpreted in terms of the relative acceleration a^a_S with the Gaussian normal foliation. That is, for a photon surface S and the Gaussian normal foliation $\{S_r\}$, the relative acceleration a^a_S of a perturbed null geodesic $\tilde{\gamma}$ with respect to a nearby hypersurface $\tilde{S} \in \{S_r\}$ determines whether $\tilde{\gamma}$ is attracted to or repelled from S.

Consider a null geodesic γ with its tangent vector $k \in T_pS$ at a point $p \in S$. Let $S_{\delta r} \in \{S_r\}$ be a hypersurface close to S with a small parameter δr and $q \in S_{\delta r}$ be the intersection of $S_{\delta r}$ and the geodesic generated by n^a from p. We generate k from p to q by parallel transport along n^a, $\nabla_n k^a = 0$. Then we obtain the nearby null geodesic $\tilde{\gamma}$ with the initial condition $\dot{\tilde{\gamma}}(0) = k \in T_qS_{\delta r}$ at q. The fact $k \in T_qS_{\delta r}$ is guaranteed by the conditions, $n_a k^a = 0$ at p and Eq. (3.23). If γ is stable, i.e. $\tilde{\gamma}$ is attracted to S, $\tilde{\gamma}$ has the relative acceleration, $a^a_{S_{\delta r}}$, with respect to $S_{\delta r}$ which is directed toward S. The condition is

$$\begin{aligned} a_{S_{\delta r}} &< 0 \quad for \quad \delta r > 0, \\ a_{S_{\delta r}} &> 0 \quad for \quad \delta r < 0 \end{aligned} \tag{3.29}$$

where $a_{S_{\delta r}} := n_a a^a_{S_{\delta r}}$. Taking the limit $\delta r \to 0$, i.e. the limit where S_r and $\tilde{\gamma}$ are infinitesimally close to S, the two inequalities reduce to the condition,

$$\nabla_n a_{S_{\delta r}}|_{\delta r=0} < 0. \tag{3.30}$$

In the same way, if γ is unstable, the condition is

$$\nabla_n a_{S_{\delta r}}|_{\delta r=0} > 0. \tag{3.31}$$

From Eq. (3.28), the left-hand sides of the conditions further reduce to

$$\begin{aligned} \nabla_n a_{S_{\delta r}} &= \nabla_n \left(k^b k^c \sigma_{bc} \right) \\ &= k^b k^c \nabla_n \sigma_{bc} \end{aligned} \tag{3.32}$$

where the last equality is verified by the fact $\nabla_n k^a = 0$. Therefore the normal derivative of the second fundamental form, $\nabla_n \sigma_{ab}$, determines the stability of the photon surface and we indeed reproduce Proposition 3.3.1.

3.4 Corollaries

From the propositions in the previous sections, we can identify the stability of null geodesics on photon surfaces or photon surfaces themselves without specifying the photon surfaces explicitly if the spacetime satisfies some geometrical conditions.

From Proposition 3.2.2:

Corollary 3.4.1. *A photon surface of spacetime of constant curvature is marginally stable. Specifically, this applies for the Minkowski spacetime, the de Sitter spacetime, and the anti-de Sitter spacetime.*

Corollary 3.4.2. *The symmetry of spacetime (M, g) and a photon surface S restricts the variation of stability for null geodesics on S. For example, if S is spatially maximally symmetric and also symmetric in a time direction, then all the null geodesics on S has the same stability. Therefore S is stable, unstable or marginally stable. Photon spheres of spherically symmetric spacetimes are in this case.*

From Proposition 3.2.3:

Corollary 3.4.3. *Let (M, g) be a conformally flat spacetime satisfying the null energy condition. Then a photon surface of (M, g) is stable. For example, photon surfaces of the FLRW spacetime with matter satisfying null energy condition must be stable.*

Corollary 3.4.4. *Let (M, g) be a spacetime with $\dim M = 3$ satisfying the null energy condition. Then a photon surface of (M, g) is stable. Therefore, unstable null geodesics are allowed to exist only in spacetime with $\dim M \geq 4$ if the null energy condition is satisfied. For example, the charged BTZ spacetime, which is the electrovacuum solution of Einstein-Maxwell equation [26], has a photon surface (sphere) if the mass is negative, the spin is zero, and the negative cosmological constant is sufficiently small. Since the spacetime satisfies the null energy condition, the photon surface is stable.*

Corollary 3.4.5. *Let (M, g) and S be a spacetime satisfying the null energy condition and a photon surface of S. Then a null geodesic γ in a principal null direction is stable or marginally stable.*

This is because the principal null condition, $k^b k^c k_{[e} C_{a]bc[d} k_{f]} = 0$, implies that only the components corresponding to bases of the form $k^* \otimes \omega$ or $\omega \otimes k^*$ of the second-rank tensor $k^b k^c C_{abcd}$ can be nonzero, where ω is some one-form and $k^* := g(\cdot, k)$ is the one-form dual to the vector k [21]. Therefore, the first term in Eq. (3.17) vanishes from the fact $n^a k_a = 0$ if k^a is in a principal null direction.

3.5 Summary

In the beginning of this chapter, we have reviewed the definition and the equivalent condition of a photon surface, Definition 3.1.1 and Theorem 3.1.8, respectively. The examples of timelike photon surfaces in the known spacetimes have been also given.

After the introduction, we have defined the stability of null geodesics on a photon surface by reformulating the stability of a photon sphere in a covariant manner. The stability represents whether a null geodesic $\tilde{\gamma}$ perturbed from a null geodesic γ on a photon surface is attracted to or repelled from the surface. Since such a behavior is subject to the geodesic deviation equation, the stability condition of null geodesics on a photon surface is given in terms of the Riemann curvature, as in Proposition 3.2.2, or the Weyl and Ricci curvature, as in Proposition 3.2.3. We have named a photon surface on which all the null geodesics are (un)stable *a (un)stable photon surface*. If there exist no marginally stable null geodesics, the surface is called *a strictly (un)stable photon surface*. As we have defined the stability only in terms of a local geometrical quantity, the definition is applicable to any photon surfaces even if the photon surfaces and the spacetime have no symmetries.

Although the stability of null geodesics is interpreted as what represents the behavior of perturbed orbits, Proposition 3.2.2 implies that it depends only on the values of the curvature on the photon surface. This fact can also be seen from our definition, Definition 3.2.1, which requires only the null geodesic and its deviation vector defined just on the surface.

Proposition 3.2.3 tells us that we can a priori identify the stability before finding photon surfaces of spacetime explicitly. For example, any photon surface in conformally flat spacetime is stable if the null energy condition is satisfied. Several corollaries concerning this fact were shown in Sec. 3.4.

We have also found that the stability of null geodesics can be expressed by the normal derivative of the second fundamental form of the surface under an appropriate spacetime foliation, named Gaussian normal foliation, as stated in Proposition 3.3.1. As we see in Chap. 4 and 7, the stability condition of Proposition 3.3.1 is easier to calculate than Proposition 3.2.2.

Chapter 4

Photon surfaces of asymmetric vacuum spacetimes

For spherically symmetric black hole spacetimes which are solutions to the Einstein equation, many photon surfaces, i.e., photon spheres, have been found. Similarly, photon surfaces exist in the hyperbolically and planar symmetric counterparts of the spherical spacetime solutions [19]. However, a photon surface does not exist for rotating vacuum black hole spacetimes such as the Kerr spacetime. One may expect that photon surfaces can exist only in highly symmetric spacetimes although the symmetry of the surfaces and the spacetimes are not assumed in the definition. More specifically, the maximal symmetry of the submanifolds of codimension-two might be necessary for a spacetime to have photon surfaces.

In this chapter, we see that spatially less symmetric, or possibly nonsymmetric spacetimes which are solutions to the Einstein equation have photon surfaces. We consider a spacetime given by the metric ansatz,

$$ds^2 = -f(r)dt^2 + g(r)dr^2 + r^2\gamma_{ij}\left(x\right)dx^i dx^j, \tag{4.1}$$

where the spacetime dimension is $D \geq 3$ and the metric $\gamma_{ij}(x) = \gamma_{ij}(x^1, x^2, ..., x^{D-2})$ of the Riemannian $(D-2)$-submanifold are arbitrary. The spacetime is static but there are no spacelike Killing vectors in general. The spacetime metric can be regarded as the generic form of some class of warped products. See Appendix A for the derivation of Eq. (4.1). If $\gamma_{ij}(x)$ is the metric of the unit $(D-2)$-sphere, the ansatz is the well-known generic form of a static spherically symmetric spacetime.

In Sec. 4.1, we define *an r-photon surface* and derive the pseudopotential V, which allows us to find the photon surface and analyze its stability easily. In Sec. 4.2, we specifically consider the Λ-electrovacuum solutions to the Einstein equation with the ansatz (4.1) and find the parameters for which the r-photon surfaces exist. We summarize the results in Sec. 4.3.

4.1 r-photon surface

Here we define an r-photon surface and derive its stability condition.

4.1.1 Definition

An r-photon surface is a photon surface of a hypersurface of constant r in our spacetime:

Definition 4.1.1 (r-photon surface)**.** *A hypersurface*

$$S_r := \{p \in M | r = \text{const.}\} \tag{4.2}$$

of a spacetime with the metric (4.1) is called an r-photon surface if it is a photon surface.

4.1.2 Condition for an r-photon surface

For general S_r, its unit normal is given by

$$n = \sqrt{g} dr \tag{4.3}$$

provided that it is timelike, i.e., $g(r) > 0$. The trace-free part of the second fundamental form, σ_{ab}, is then given by

$$\sigma_{\mu\nu} = -\frac{1}{2(D-1)} \frac{(fr^{-2})'}{(fr^{-2})} \sqrt{g}^{-1} \left[(D-1) f_{\mu\nu} + h_{\mu\nu}\right] \tag{4.4}$$

where $h_{\mu\nu} = g_{\mu\nu} - n_\mu n_\nu$ is the induced metric of S_r and $f_{\mu\nu} := f(r)\delta^t_\mu \delta^t_\nu$. Theorem 3.1.8 gives the condition for S_r to be an r-photon surface:

Proposition 4.1.2. *A timelike hypersurface S_r is an r-photon surface if and only if*

$$(fr^{-2})' = 0 \tag{4.5}$$

at the radius.

Note that S_r is timelike for r such that $g(r) > 0$. The condition is equivalent to $f(r) > 0$ because otherwise the spacetime (4.1) violates its Lorentz signature.

4.1.3 Stability condition

Let $\{S_r\}$ be a foliation of the spacetime, Eq. (4.1), consisting of S_r. As one can see from Eq. (3.22), it is a Gaussian normal foliation. With σ_{ab} defined on each S_r, we calculate $\nabla_n \sigma_{ab}$. For a radius $r = r_{\rm p}$ such that $S_{r=r_{\rm p}}$ is an r-photon surface, we have

$$\nabla_n \sigma_{\mu\nu} = -\frac{1}{2(D-1)} \frac{(fr^{-2})''}{(fr^{-2})} g^{-1} \left[(D-1) f_{\mu\nu} + h_{\mu\nu}\right] \tag{4.6}$$

by using Eq. (4.5). For any null vector $k \in T_p S_{r_{\rm p}}$, we have

$$k^a k^b \nabla_n \sigma_{ab} = -\frac{1}{2} \frac{(fr^{-2})''}{(fr^{-2})} g^{-1} f (k^t)^2 \tag{4.7}$$

at $r = r_{\rm p}$ Then from Proposition 3.3.1, we obtain the stability condition of an r-photon surface:

Proposition 4.1.3. *A timelike r-photon surface S_{r_p} is strictly stable, strictly unstable, and marginally stable if and only if*

$$(fr^{-2})''\big|_{r=r_\mathrm{p}} > 0 \ , < 0 \ , and \ \ = 0, \tag{4.8}$$

respectively.

r-photon surfaces are classified into only the three types, strictly stable, strictly unstable, and marginally stable ones, which are not overlapped each other. We simply call them stable, unstable, marginally stable r-photon surfaces in the following.

4.1.4 Pseudopotential

Here we define *the pseudopotential*,

$$V(r) := f(r)r^{-2}, \tag{4.9}$$

which is useful for investigating r-photon surfaces. From Proposition 4.1.2 and 4.1.3, the conditions for an r-photon surface are given by this proposition:

Proposition 4.1.4. *Suppose $f(r_\mathrm{p}) > 0$, or equivalently, $V(r_\mathrm{p}) > 0$ at a radius r_p. Then S_{r_p} is an r-photon surface if and only if*

$$V'(r_\mathrm{p}) = 0. \tag{4.10}$$

It is stable, unstable, and marginally stable if and only if

$$V''(r_\mathrm{p}) > 0 \ , < 0 \ , and \ \ = 0, \tag{4.11}$$

respectively.

r-photon surfaces appear as the extrema of $V(r)$.

4.2 r-photon surface in vacuum spacetimes

We see that timelike r-photon surfaces exist in spacetimes of solutions to the Einstein equation.

4.2.1 Electrovacuum spacetime with cosmological constant

Ansatz (4.1) gives the solution to the electrovacuum Einstein equation with a cosmological constant [27],

$$f(r) = g^{-1}(r) = k - \frac{2\Lambda}{(D-2)(D-1)}r^2 - \frac{2m}{r^{D-3}} + \frac{Q^2}{r^{2(D-3)}}, \tag{4.12}$$

where the $(D-2)$-dimensional space given by the metric $\gamma_{ij}dx^i dx^j$ is an arbitrary Einstein manifold with the constant curvature k, that is, it is an arbitrary $(D-2)$-dimensional Rieamannian space with the Ricci curvature given by $\mathcal{R}_{ij} = (D-3)k\gamma_{ij}$. The parameters m and Λ are the mass and the cosmological constant, respectively. The parameter Q is related to the electric charge $\bar{Q}$ by

$$Q^2 := \frac{\kappa^2 \bar{Q}^2}{(D-2)(D-3)} \tag{4.13}$$

where κ is the gravitational constant. The electromagnetic field is given by

$$F = \frac{1}{2}\frac{\bar{Q}}{r^{D-2}} dt \wedge dr. \tag{4.14}$$

The spacetime is invariant under an appropriate simultaneous scaling of the coordinates t, r and the parameters k, m, Q, Λ. For nonzero k, we can scale it so that $k = \pm 1$.

Einstein manifolds have been extensively investigated and there are many examples for them. A constant curvature space of any dimension d is an Einstein manifold. For a space of the dimension $d = 1$, although the Ricci curvature is not defined, the metric can always be written in the form analogous to a flat space, $\gamma_{ij}(x)dx^i dx^j = dl^2$. For $d = 2$, all the Riemaniann spaces are Einstein manifolds. For $d = 3$, all the Einstein manifolds are constant curvature spaces. For $d \geq 4$, various nontrivial Einstein manifolds have been found. The variety of Einstein manifolds in higher d should be due to the degrees of freedom of Weyl curvature. See [28, 29, 30, 31, 32] for more examples of Einstein manifolds.

The solution Eq. (4.12) would be less symmetric spacetime in the sense that the $(D-2)$-space $\gamma_{ij}dx^i dx^j$ can be less symmetric than the maximal. If there exist Einstein manifolds without any Killing vectors, the spacetime can be a static vacuum spacetime with only the timelike Killing vector, ∂_t.

4.2.2 Existence and stability

Let us focus on a timelike hypersurface S_{r_p}. The timelike condition of S_{r_p} is given by

$$f(r_\mathrm{p}) > 0. \tag{4.15}$$

For S_{r_p} to be an r_p-photon surface, the radius r_p must be a real positive solution to Eq. (4.10). Using the explicit form of $V(r)$,

$$V(r) = -\frac{2\Lambda}{(D-2)(D-1)} + \frac{k}{r^2} - \frac{2m}{r^{D-1}} + \frac{Q^2}{r^{2(D-2)}}, \tag{4.16}$$

the equation is rewritten as

$$k r_\mathrm{p}^{2(D-3)} - (D-1) m r_\mathrm{p}^{D-3} + (D-2)Q^2 = 0. \tag{4.17}$$

Once find an $r_{\rm p}$-photon surface, we can determine the stability of $S_{r_{\rm p}}$ by the sign of

$$V''(r_{\rm p}) = \frac{4(D-3)}{r_{\rm p}^4}\left[\frac{(D-1)m}{2r_{\rm p}^{D-3}} - k\right]. \tag{4.18}$$

Let us focus the case $D = 3$. Then Eqs. (4.15), (4.17), and (4.18) reduce to $f(r_{\rm p}) = -\Lambda r_{\rm p}^2 > 0$, $k - 2m + Q^2 = 0$, and $V''(r_{\rm p}) = 0$, respectively. Therefore, we conclude that only for $Q^2 = 2m - k \geq 0$ and $\Lambda < 0$ (i.e., 3D anti-de Sitter spacetime), a hypersurface $S_{r_{\rm p}}$ is a timelike $r_{\rm p}$-photon surface at any $r_{\rm p}$ and is marginally stable.

We focus on the case $D \geq 4$ in the what follows. In each case, $k = 0$ in Sec. 4.2.2, $k \neq 0$ & $m = 0$ in Sec. 4.2.2, and $k \neq 0$ & $m \neq 0$ in Sec. 4.2.2, we apply the following procedure to show the existence of a timelike $r_{\rm p}$-photon surface: First, we find a solution to Eq. (4.17) and restrict parameters to the range where the solution is real and positive. The timelike condition (4.15) further restricts the allowed range of a dimensionless cosmological constant,

$$\lambda := \Lambda |m|^{2/(D-3)}. \tag{4.19}$$

Evaluating the sign of Eq. (4.18), we determine the stability of $S_{r_{\rm p}}$ by Eq. (4.11). Here for later convenience, we introduce a dimensionless charge for $m \neq 0$,

$$q := \frac{|Q|}{|m|}. \tag{4.20}$$

The results are summarized in Table 4.1 for $k = 0$, Table 4.2 for $k = 1$, and Table 4.3 for $k = -1$.

Case $k = 0$

Suppose that $k = 0$. Then Eqs. (4.17) and (4.18) reduce to

$$(D-1)mr_{\rm p}^{D-3} - (D-2)Q^2 = 0, \tag{4.21}$$

$$V''(r_{\rm p}) = (D-3)(D-1)\frac{2m}{r_{\rm p}^{D+1}}. \tag{4.22}$$

Note that if $S_{r_{\rm p}}$ is a timelike $r_{\rm p}$-photon surface, then it is stable for $m > 0$, unstable for $m < 0$, and marginally stable for $m = 0$ because the sign of m coincides with that of $V''(r_{\rm p})$. In the followings, we consider each case, $m = 0$ and $m \neq 0$, separately.

($k = 0$ & $m = 0$) Suppose that $k = 0$ and $m = 0$. Then Eq. (4.21) leads to $Q = 0$. Hence, V becomes constant, $V = -2\Lambda/[(D-2)(D-1)]$, and satisfies $V'(r_{\rm p}) = 0$ and $V''(r_{\rm p}) = 0$ for any value of $r_{\rm p}$. The timelike condition of $S_{r_{\rm p}}$ in Eq. (4.15) reduces to $f(r_{\rm p}) = -2\Lambda r_{\rm p}^2/[(D-2)(D-1)] > 0$, and therefore,

$$\Lambda < 0. \tag{4.23}$$

Finally we conclude that only for $k = 0$, $m = 0$, $Q = 0$ and $\Lambda < 0$, a timelike $r_{\rm p}$-photon surface exists at any $r_{\rm p} > 0$ and is marginally stable.

($k = 0$ & $m \neq 0$) Suppose that $k = 0$ and $m \neq 0$. Then we obtain the solution to Eq. (4.21) in the form

$$r_{\rm p}^{D-3} = \frac{D-2}{D-1}\frac{Q^2}{m}. \tag{4.24}$$

The positivity of $r_{\rm p}$ requires $Q \neq 0$ and $m > 0$, and thus, $V''(r_{\rm p}) > 0$. The timelike condition of $S_{r_{\rm p}}$ in Eq. (4.15) leads to a negative upper bound for λ,

$$\lambda < -\frac{(D-3)(D-1)^2}{2(D-2)}\left(\frac{D-1}{D-2}\right)^{2/(D-3)} q^{-2(D-1)/(D-3)} < 0. \tag{4.25}$$

Finally we conclude that only for $k = 0$, $m > 0$, $Q \neq 0$, and Eq. (4.25), a timelike $r_{\rm p}$-photon surface exists at the radius (4.24) and is stable.

Case $k \neq 0$ & $m = 0$

Suppose that $k \neq 0$ and $m = 0$. Then Eq. (4.17) reduces to

$$k r_{\rm p}^{2(D-3)} + (D-2)Q^2 = 0. \tag{4.26}$$

The positivity of $r_{\rm p}$ requires $Q \neq 0$ and $k = -1$. The positive branch takes the form

$$r_{\rm p+}^{D-3} = \sqrt{D-2}|Q| \tag{4.27}$$

and leads to $V''(r_{\rm p+}) = 4(D-3)/r_{\rm p+}^4 > 0$ from Eq. (4.18). The timelike condition (4.15) gives a negative upper bound for Λ,

$$\Lambda < -\frac{(D-3)(D-1)}{2(D-2)^{1/(D-3)}}|Q|^{-2/(D-3)} < 0. \tag{4.28}$$

Finally we conclude that only for $k = -1$, $m = 0$, $Q \neq 0$, and Eq. (4.28), a timelike $r_{\rm p}$-photon surface exists at the radius (4.27) and is stable.

Case $k \neq 0$ & $m \neq 0$

Suppose that $k \neq 0$ and $m \neq 0$. Then Eq. (4.17) has roots

$$r_{\rm p\pm}^{D-3} = \frac{D-1}{2k} m(1 \pm \gamma), \tag{4.29}$$

where

$$\gamma := \sqrt{1 - k\frac{q^2}{q_{\rm c}^2}}, \tag{4.30}$$

$$q_{\rm c} := \frac{D-1}{2\sqrt{D-2}}. \tag{4.31}$$

Using these roots, $V''(r_{\rm p})$ in Eq. (4.18) is formally written as

$$V''(r_{\rm p\pm}) = \mp(D-3)(D-1)\frac{2m\gamma}{r_{\rm p\pm}^{D+1}}, \tag{4.32}$$

where $V''(r_{\rm p+})$ corresponds to the upper sign in the right-hand side and vice versa. In the followings, we consider each case, $k = 1$ and $k = -1$, separately.

($k=1$) Suppose that $k=1$. Then γ is restricted to the range $0 \leq \gamma = (1-q^2/q_{\rm c}^2)^{1/2} \leq 1$ (i.e., $0 \leq q \leq q_{\rm c}$). First, let us focus on the case $\gamma = 1$ (i.e., uncharged case, $q=0$). The branch $r_{\rm p-}$ of the roots (4.29) vanishes, and therefore, here is no photon surface. On the other hand, if $m > 0$, then the branch

$$r_{\rm p+}^{D-3} = (D-1)m \tag{4.33}$$

is positive definite, and $V''(r_{\rm p+}) < 0$ holds. The timelike condition (4.15) provides a positive upper bound of λ,

$$\lambda < \frac{(D-3)(D-2)}{2(D-1)^{2/(D-3)}}. \tag{4.34}$$

Finally we conclude that only for $k=1$, $m>0$, $q=0$, and Eq. (4.34), a timelike $r_{\rm p+}$-photon surface exists at the radius (4.33) and is unstable.

Next, we focus on the case $\gamma = 0$ (i.e., $q = q_{\rm c}$). The roots (4.29) are degenerate as

$$r_{\rm p}^{D-3} = \frac{D-1}{2}m. \tag{4.35}$$

The positivity of $r_{\rm p}$ requires $m > 0$. Since $\gamma = 0$, we have $V''(r_{\rm p}) = 0$ from Eq. (4.32). The timelike condition (4.15) provides a positive upper bound of λ,

$$\lambda < \frac{(D-3)^2}{2}\left(\frac{2}{D-1}\right)^{2/(D-3)}. \tag{4.36}$$

Finally we conclude that only for $k=1$, $m>0$, $q=q_{\rm c}$, and Eq. (4.36), a timelike $r_{\rm p}$-photon surface exists at the radius (4.35) and is marginally stable.

Next, we focus on the case $0 < \gamma < 1$ (i.e., $0 < q < q_{\rm c}$). If $m < 0$, both roots (4.29) are negative and hence unsuitable. Suppose that $m > 0$. Then the roots satisfy $r_{\rm p+} > r_{\rm p-} > 0$. For each branch, $V''(r_{\rm p+}) < 0$ and $V''(r_{\rm p-}) > 0$. The timelike condition (4.15) reduces to upper bounds of λ,

$$\lambda < \lambda_{\pm}(D,q) := \frac{D-3}{2}\left[\frac{2}{(D-1)(1\pm\gamma)}\right]^{2/(D-3)}\left(D-1-\frac{2}{1\pm\gamma}\right). \tag{4.37}$$

Note that $\lambda_+ > 0$, and on the other hand, $\lambda_- \geq 0$ for $1 \leq q < q_{\rm c}$ and $\lambda_- < 0$ for $0 < q < 1$. Finally we conclude that only for $k=1$, $m>0$, $0<q<q_{\rm c}$, and Eq. (4.37), a timelike $r_{\rm p+}$-photon surface exists at the radius $r_{\rm p+} = (D-1)(1+\gamma)m/2$ and is unstable, and a timelike $r_{\rm p-}$-photon surface exists at the radius $r_{\rm p-} = (D-1)(1-\gamma)m/2$ and is stable.

($k=-1$) For $k=-1$, γ is restricted to the range $\gamma = (1+q^2/q_{\rm c}^2)^{1/2} \geq 1$. We consider each case, $m>0$ and $m<0$, separately.

Suppose that $k = -1$ and $m > 0$. For $\gamma = 1$ (i.e., uncharged case, $q = 0$), the roots (4.29) satisfy $r_{\mathrm{p}-}^{D-3} = 0 > r_{\mathrm{p}+}^{D-3}$, and hence, here are no photon surfaces. Now, we focus on the case $\gamma > 1$ (i.e., $q \neq 0$). The branch $r_{\mathrm{p}-}$ of the roots (4.29) becomes

$$r_{\mathrm{p}-}^{D-3} = \frac{D-1}{2} m(\gamma - 1) > 0, \tag{4.38}$$

while the other branch is unsuitable because $r_{\mathrm{p}+}^{D-3} < 0$. We find that $V''(r_{\mathrm{p}-}) > 0$ from Eq. (4.32). The timelike condition (4.15) provides a negative upper bound of λ,

$$\lambda < -\frac{D-3}{2} \left[\frac{2}{(D-1)(\gamma-1)} \right]^{2/(D-3)} \left(D - 1 + \frac{2}{\gamma - 1} \right) < 0. \tag{4.39}$$

Finally we conclude that only for $k = -1$, $m > 0$, $q \neq 0$, and Eq. (4.39), a timelike $r_{\mathrm{p}-}$-photon surface exists at the radius (4.38) and is stable.

Suppose that $k = -1$ and $m < 0$. The branch $r_{\mathrm{p}+}$ of the roots (4.29) becomes

$$r_{\mathrm{p}+}^{D-3} = \frac{D-1}{2} |m| (1 + \gamma), \tag{4.40}$$

while the other branch is unsuitable because $r_{\mathrm{p}-}^{D-3} < 0$. We find that $V''(r_{\mathrm{p}+}) > 0$ from Eq. (4.32). The timelike condition (4.15) provides a negative upper bound of λ,

$$\lambda < -\frac{D-3}{2} \left[\frac{2}{(D-1)(1+\gamma)} \right]^{2/(D-3)} \left(D - 1 - \frac{2}{1 + \gamma} \right) < 0. \tag{4.41}$$

Finally we conclude that only for $k = -1$, $m < 0$, and Eq. (4.41), a timelike $r_{\mathrm{p}+}$-photon surface exists at the radius (4.40) and is stable.

4.3 Summary

In this chapter, we have investigated r-photon surfaces in the spacetime given by the metric ansatz (4.1). The ansatz is a general form of a warped spacetime of some class as shown in Appendix A.

First, we have found that the pseudopotential $V(r)$ gives the radius and stability of an r-photon surface. The local maxima correspond to unstable r-photon surfaces while the local minima correspond to stable ones. It is remarkable that the stabilities of null geodesics along the photon surfaces do not depend on the directions of the null geodesics even if the spacetime is not spatially symmetric. That is, if $V''(r_{\mathrm{p}}) > 0$ (< 0) for an r-photon surface $S_{r_{\mathrm{p}}}$, it is a strictly stable (unstable) photon surface, and therefore, all the null geodesics on it are everywhere stable (unstable).

Next, we have seen that r-photon surfaces indeed exist in the case where the spacetime is the electrovacuum solution to the Einstein equation with the cosmological constant. Since the spacetime is a solution as far as the $(D-2)$-space $\gamma_{ij} dx^i dx^j$ is an Einstein manifold, it provides the examples of static photon surfaces existing in less or non-symmetric electrovacuum spacetimes. For the discussion about the structure that enables the spacetime to have a photon surface regardless of the spatial Killing symmetry, see Ref. [16].

	$m > 0$	$m = 0$	$m < 0$
$Q = 0$	$\nexists$	$\forall r$, Eq. (4.23), marginally stable,	$\nexists$
$Q \neq 0$	Eqs. (4.24) and (4.25), stable	$\nexists$	$\nexists$

Table 4.1: $k = 0$

	$m > 0$	$m = 0$	$m < 0$
$q = 0$	Eqs. (4.33) & (4.34), unstable	$\nexists$	$\nexists$
$0 < q < q_c$	Eqs. (4.29) & (4.37) (upper branch), unstable Eqs. (4.29) & (4.37) (lower branch), stable	$\nexists$	$\nexists$
$q = q_c$	Eqs. (4.35) & (4.36), marginally stable	$\nexists$	$\nexists$

Table 4.2: $k = 1$

	$m > 0$	$m = 0$	$m < 0$
$Q = 0$	$\nexists$	$\nexists$	Eqs. (4.40) & (4.41), stable
$Q \neq 0$	Eqs. (4.38) & (4.39), stable	Eqs. (4.27) & (4.28), stable	Eqs. (4.40) & (4.41), stable

Table 4.3: $k = -1$

Chapter 5

Sonic point/photon sphere correspondence: spherical flow

Originally published as:
Y. Koga and T. Harada, *Phys. Rev. D* **94** (2016) 044053.

The accretion of fluid onto objects is a basic problem in astrophysics and the most important issue concerning growth of stars and black holes. From an observational view point, the accretion is considered to be responsible for the X-ray emission due to the compression of the fluid. This is also connected to the observations of strong gravity fields in a general relativistic context.

The first study of the accretion onto stars was established by Bondi [33]. He investigated stationary spherically symmetric flow of polytropic fluid in Newtonian gravity. One of the interesting features is the existence of a critical point (or sonic point) and transonic flow, that is, flow which experiences transition between subsonic and supersonic states. Michel extended the problem to general relativity on the Schwarzschild spacetime under the assumption that the spacetime is not so strongly modified by the fluid and also estimated several quantities on the critical point [34]. For the (anti-)de Sitter spacetime, Mach, Malec and Karkowski gave not only numerical calculations with a polytropic equation of state (EOS), but also the exact solutions of the accretion of fluid with isothermal EOSs [35]. For other specific cases of spherically symmetric accretion problems in the context of general relativity, see Refs. [36, 37]. For general static spherically symmetric spacetimes and polytropic EOSs, the existence of the unique solution of the accretion problem has been proved by Chaverra and Sarbach [24]. They analyzed the problem by the method of dynamical systems. In the analysis of the outflow of fluid, there exist the same features, i.e., a transonic flow and a sonic point as in the accretion problem. Carter, Gibbons, Lin and Perry discussed the treatment of Hawking radiation from astrophysical black holes as the outflow of perfect fluid [38].

In the study by Mach et. al [35], it was revealed that only for the case of the accretion of radiation fluid, the radius of the sonic point is $3m$ for the black hole mass m. This radius coincides with the photon sphere of the spacetime. This correspondence connects between two independent observations, the observation of lights from sources behind a

black hole and the observation of emission from accreted radiation fluid onto the hole, because the size of the shadow of the hole is determined by the radius of the photon sphere and the accreted fluid can signal the sonic point.

In this chapter, we see there exists the correspondence between the sonic points of photon gas accretion and the photon spheres in a large class by generalizing the analysis [24] to arbitrary dimensions. We consider general static spherically symmetric spacetimes in D dimensions

$$ds^2 = -f(r)dt^2 + g(r)dr^2 + r^2 d\Omega_{D-2}^2, \tag{5.1}$$

where $D \geq 3$ and the condition $0 < f, g < \infty$ are assumed and $d\Omega_{D-2}^2$, given by

$$\begin{aligned} d\Omega_{D-2}^2 = d\theta_1^2 + \quad & \cdots \quad + \sin^2\theta_1 \cdots \sin^2\theta_{D-4} d\theta_{D-3}^2 \\ + \quad & \sin^2\theta_1 \cdots \sin^2\theta_{D-3} d\phi^2, \end{aligned} \tag{5.2}$$

is the unit $(D-2)$-sphere metric. The main result is:

Theorem 5.0.1. *For any physical transonic accretion flow of ideal photon gas in stationary and spherically symmetric state on the fixed background spacetime (5.1), the radius of its sonic point coincides with that of (one of) the unstable photon sphere(s) of the geometry.*

The sonic point is a point at which transition between supersonic and subsonic states occurs. The term unstable photon sphere means the instability of the corresponding circular orbits of null geodesics. The rigorous definitions of "physical flow" and the other terms will be given in the following sections.

In Sec. 5.1, we derive the conditions for the radius of photon sphere of the spacetime and its stability. In Sec. 5.2, we formulate the general accretion problem of stationary and spherically symmetric accretion on the D-dimensional spacetime. The critical point and the sonic point are also defined. In Sec. 5.3, we introduce the EOS of ideal photon gas in d dimensional space. Then the critical point of the ideal photon gas accretion in D dimensions of spacetime is obtained. In Sec. 5.4, the main theorem is proved and the summary is given in Sec. 5.5.

5.1 Photon sphere

A photon sphere is defined as a sphere on which circular null geodesics exist [39]. A photon sphere is said to be stable and unstable, if it has stable and unstable circular orbits, respectively. We present the following lemma for the photon sphere of the spacetime (5.1).

Lemma 5.1.1. *Let the metric be Eq. (5.1). The photon sphere of the spacetime is specified by the equation*

$$(fr^{-2})' = 0. \tag{5.3}$$

The stability condition of the photon sphere is given by

$$\textit{stable (unstable)} \Leftrightarrow (fr^{-2})'' > 0 \ (< 0) \tag{5.4}$$

at the radius of the photon sphere.

Proof. Consider a null geodesic $x^\mu = x^\mu(\lambda)$ confined in $\theta = \frac{\pi}{2}$ surface where λ is the affine parameter. The null condition leads to the equation

$$\mathcal{H} = \frac{1}{2} g_{\mu\nu} \dot{x}^\mu \dot{x}^\nu = 0 \tag{5.5}$$

for its Hamiltonian $\mathcal{H}$, where $\dot{} = d/d\lambda$. From two Killing vectors relevant to the motion,

$$\xi_{(t)} = \partial_t, \ \xi_{(\phi)} = \partial_\phi, \tag{5.6}$$

we have two conserved quantities,

$$E : = -g_{\mu\nu} \xi^\mu_{(t)} \dot{x}^\nu, \tag{5.7}$$

$$L : = g_{\mu\nu} \xi^\mu_{(\phi)} \dot{x}^\nu, \tag{5.8}$$

and the Hamiltonian reduces to

$$\begin{aligned} \mathcal{H} &= \frac{1}{2} g \dot{r}^2 - \frac{1}{2f} [E^2 - L^2 f r^{-2}] \\ &= g \left[\frac{1}{2} \dot{r}^2 + V(r) \right], \end{aligned} \tag{5.9}$$

where

$$V(r) := -\frac{1}{2fg} [E^2 - L^2 f r^{-2}]. \tag{5.10}$$

Defining $F(r) := E^2 - L^2 f r^{-2}$, the conditions for the circular orbit are

$$\dot{r} = 0, \tag{5.11}$$

$$V'(r) = -\frac{1}{2} \left[\left(\frac{1}{fg} \right)' F + \frac{1}{fg} F' \right] = 0. \tag{5.12}$$

The former gives $V(r) = 0$ from Eq. (5.5) and so $F(r) = 0$ from $1/(fg) \neq 0$. Then the latter implies $F'(r) = 0$ and the radius of the photon spheres is specified by the condition

$$(fr^{-2})' = 0. \tag{5.13}$$

Circular orbits are classified into two kinds, stable and unstable orbits. They correspond to the conditions $V''(r) > 0$ and < 0, respectively, at the radius. Using the fact $F = F' = 0$ at the radius, we have

$$V''(r) = -\frac{1}{2} g f^{-1} F''(r). \tag{5.14}$$

Thus the (in)stability is established by $(fr^{-2})'' > 0$ (< 0) uniquely and we get Eq. (5.4). □

The conditions do not depend on the component $g(r)$ of the metric.

5.2 Accretion problem in D-dimensional spacetime and its critical point and sonic point

Here, assuming three conservation laws and the metric (5.1), the formulation of the accretion problem is given. The definitions of the critical point and the sonic point are also given in the subsequent subsections.

We assume three conservation equations, i.e., the first law, continuity equation and energy-momentum conservation with perfect fluid:

$$\begin{cases} dh = Tds + n^{-1}dp & \text{(5.15a)} \\ \nabla_a J^a = 0 & \text{(5.15b)} \\ \nabla_a T^a_b = 0, & \text{(5.15c)} \end{cases}$$

where $J^a := nu^a$ is the number current and $T^a_b = nhu^a u_b + p\delta^a_b$ is the energy-momentum tensor of the perfect fluid. The quantities h, T, s, n, p and u^a represent the enthalpy per particle, the temperature, the entropy per particle, the number density, the pressure and the 4-velocity of the fluid, respectively. The system of the equations means the adiabatic condition of the fluid through Eqs. (5.15a), (5.15b) and (5.15c) contracted with u^b. Furthermore, the stationary and spherically symmetric state of the flow implies that the entropy is constant over the whole spacetime, allowing us to write $h = h(p)$ or

$$h = h(n). \tag{5.16}$$

Integrating Eq. (5.15b), we have

$$j_n := 4\pi(fg)^{1/2} r^{D-2} n u^r = \text{const}, \tag{5.17}$$

from the symmetry of the fluid and the spacetime metric (5.1). The quantity j_n represents the particle flux of the fluid. The contraction of Eq. (5.15c) with $\xi^b_{(t)} = \partial^b_t$ gives another independent equation. Its integration leads to

$$j_\epsilon := 4\pi(fg)^{1/2} r^{D-2} n h u^r \sqrt{f + fg(u^r)^2} = \text{const}, \tag{5.18}$$

for the energy flux. Combining Eqs. (5.16), (5.17) and (5.18), we get

$$\left(\frac{j_\epsilon}{j_n}\right)^2 = h^2\left[f + fg(u^r)^2\right] \tag{5.19}$$

$$= h^2(n)\left[f(r) + \frac{(j_n/4\pi)^2}{r^{2(D-2)}n^2}\right] = \text{const}. \tag{5.20}$$

Then, defining the constant $\mu := j_n/4\pi$, the problem is formulated into the algebraic equation:

$$F_\mu(r, n) := h^2(n)\left[f(r) + \frac{\mu^2}{r^{2(D-2)}n^2}\right] = \text{const}. \tag{5.21}$$

The physical meaning of μ is an accretion rate. Given μ, the function is specified and the constant on the right-hand side (RHS) of Eq. (5.21) determines an accretion flow. Note that this equation does not depend on the rr-component g_{rr} of the metric.

5.2.1 Critical point

From the system (5.21), the stationary accretion solutions are described as curves on the phase space (r, n). These curves can be obtained by integrating the ordinary differential equation,

$$\frac{d}{d\lambda}\begin{pmatrix} r \\ n \end{pmatrix} = \begin{pmatrix} \partial_n \\ -\partial_r \end{pmatrix} F_\mu(r, n), \tag{5.22}$$

as orbits with a parameter λ. Then a notion of a *critical point* (or stationary point as in dynamical systems) at which the RHS of Eq. (5.22) vanishes arises and its conditions are

$$\begin{cases} \partial_n F_\mu = 0 & \text{(5.23a)} \\ \partial_r F_\mu = 0. & \text{(5.23b)} \end{cases}$$

These are equivalent to

$$\begin{cases} v_s^2 \left(f + \dfrac{\mu^2}{r^{2(D-2)} n^2} \right) - \dfrac{\mu^2}{r^{2(D-2)} n^2} = 0 & \text{(5.24a)} \\ f' - \dfrac{2(D-2)}{r} \dfrac{\mu^2}{r^{2(D-2)} n^2} = 0, & \text{(5.24b)} \end{cases}$$

respectively, where the sound speed $v_s = v_s(n)$ is defined by

$$v_s^2 := \frac{\partial \ln h}{\partial \ln n}. \tag{5.25}$$

In the following, (r_c, n_c) denotes the critical point.

Types of critical points

The linearization of Eq. (5.22) around a critical point allows us to classify the critical point into two types. The one is a saddle point and the other is an extremum point. A saddle point is a point, in this case, through which two solution orbits pass. On the other hand, orbits in vicinity of an extremum point are closed curves around the point.

The linearization matrix M_c is given by

$$M_c := \begin{pmatrix} \partial_r \partial_n & \partial_n^2 \\ -\partial_r^2 & -\partial_r \partial_n \end{pmatrix} F_\mu(r_c, n_c). \tag{5.26}$$

This matrix, being real, 2×2 and traceless, has two eigenvalues with opposite signs. The subscript c denotes the values at (r_c, n_c). If the determinant of the matrix is negative (positive), the eigenvalues are real (pure imaginary). As in dynamical systems, real eigenvalues imply that the critical point is a saddle point. For imaginary eigenvalues, the orbits around the critical point are periodic in linear order. However, because they are the contours of the real function $F_\mu(r, n)$, the orbits must be closed loops. Therefore

the imaginary eigenvalues imply an extremum point. We can write the determinant explicitly,

$$\det M_c = -\frac{2}{D-2} r_c (f_c')^2 \frac{h_c^4}{n_c^2} \mathcal{F}_\mu'(r_c), \tag{5.27}$$

where

$$\begin{aligned} \mathcal{F}_\mu(r) &:= v_s^2(\bar{n}(r))\,[1 + 2(D-2)a(r)] - 1, \\ \bar{n}(r) &:= \sqrt{\frac{D-2}{2}} \frac{2|\mu|}{\sqrt{r^{D+1} f'(r)}}, \\ a(r) &:= \frac{f(r)}{r f'(r)}. \end{aligned}$$

Then we have a simple relation:

$$\textit{saddle (extremum) point} \Leftrightarrow \mathcal{F}_\mu'(r_c) > 0\ (< 0) \tag{5.28}$$

5.2.2 Sonic point

Although a critical point is a mathematical notion defined on the phase space (r, n) of a dynamical system, this also is closely related to a physical entity, a sonic point. We define a sonic point and see its relation with a critical point in the following.

The transonic flow and the sonic point

In an accretion problem, one may expect that the fluid element at infinity, which falls with small 3-velocity, becomes faster and faster as approaching the source of the gravity. If the acceleration is sufficient, the velocity, initially smaller than its local sound speed v_s (subsonic) at infinity, would become greater than v_s (supersonic) at the point near the source. Such a fluid flow is said to be *transonic* and here we call any flow which has both sub- and supersonic regions transonic. Since, in our accretion problem, a fluid accretion flow is a solution orbit of Eq. (5.21), we define a *sonic point* of a transonic flow as follows.

Definition 5.2.1 (Sonic point of a flow)**.** *For a stationary and spherically symmetric accretion flow on the spacetime metric (5.1), let $n = n(r)$ be its corresponding solution orbit on the phase space (r, n). Let $v = v(r)$ be the radial component of the 3-velocity of the fluid measured by static observers. A sonic point (r_s, n_s) of the accretion flow is defined as a point on the phase space satisfying the condition,*

$$\left.\frac{v^2}{v_s^2}\right|_{(r_s, n(r_s))} = 1, \tag{5.29}$$

where $n_s = n(r_s)$.

The sonic point and the critical point

The critical point mentioned above is closely related to the sonic point and we present a lemma.

Lemma 5.2.2. *Assume the EOS of the fluid satisfies the condition*

$$0 < v_s^2(n) < 1, \tag{5.30}$$

$$\partial_n v_s^2(n) \geq 0. \tag{5.31}$$

That is, the sound speed of the fluid is subluminal and monotonically increasing with respect to n. For a physical transonic accretion flow in our accretion problem, its sonic point coincides with a critical point on the phase space, which is a saddle point.

Proof. For the flow, the radial component of its 3-velocity $v(r)$ observed by static observers is given by

$$u^\mu \partial_\mu = \frac{1}{\sqrt{1-v^2}}(e_0 + v e_1), \tag{5.32}$$

where $e_0 := f^{-1/2}\partial_t$ is the observers' 4-velocity and $e_1 := g^{-1/2}\partial_r$ is a unit radial vector orthogonal to it. Then, we have

$$v^2(r) = \frac{\mu^2}{\mu^2 + f(r) r^{2(D-2)} n^2(r)} \tag{5.33}$$

along the orbit $n = n(r)$ using Eq. (5.17), $-1 = u^\mu u_\mu$ and $\mu = j_n/4\pi$. On the other hand, letting $n = \tilde{n}(r)$ be a curve satisfying the condition $\partial_n F_\mu = 0$, or equivalently Eq. (5.24a), we have the relation

$$v_s^2(\tilde{n}(r)) = \frac{\mu^2}{\mu^2 + f(r) r^{2(D-2)} \tilde{n}^2(r)} \tag{5.34}$$

for the sound speed v_s. From the two equations above and the assumption $\partial_n v_s^2 \geq 0$, if $n(r_0) > \tilde{n}(r_0)$ for radius $r = r_0$, $v^2(r_0) < v_s^2(\tilde{n}(r_0)) \leq v_s^2(n(r_0))$, i.e., subsonic. In the same way, the flow is supersonic at the radius if $n(r_0) < \tilde{n}(r_0)$. This means that the curve $n = \tilde{n}(r)$ divides the phase space into subsonic and supersonic region and the sonic point must be the point at which the orbit $n = n(r)$ and the curve $n = \tilde{n}(r)$ cross each other. (Conversely, such a crossing point must be the sonic point of the flow.) However, if $\partial_r F_\mu \neq 0$ at the crossing point, such an orbit typically gets 2-valued (so unphysical) at least locally because $dn/dr = \partial_r F_\mu / \partial_n F_\mu = \pm\infty$ there from Eq. (5.22). In the current paper, we require $|dn/dr| < \infty$ as one of the conditions of a physical flow. Then, it is said that physically acceptable transonic orbits cross the curve of $\partial_n F_\mu = 0$ only at a critical point and so the sonic point coincides with the critical point. Furthermore, according to the discussion in Sec. 5.2.1, the critical point is a saddle point because orbits can pass the point. Finally, we must show that the function $\tilde{n}(r)$ is indeed single-valued. We can separate Eq. (5.34) into a function of $\tilde{n}$ and the rest,

$$\begin{aligned} &\mathcal{N}(\tilde{n}(r)) = \mu^{-2} f(r) r^{2(D-2)}, \\ &\text{where } \mathcal{N}(n) := (v_s^{-2}(n) - 1)\, n^{-2}. \end{aligned} \tag{5.35}$$

The conditions (5.30) and (5.31) imply $\partial_n \mathcal{N}(n) < 0$, $\mathcal{N}(n) \to 0$ $(n \to \infty)$ and $\mathcal{N}(n) \to \infty$ $(n \to 0)$. Therefore, the inverse function $\mathcal{N}^{-1} : (0, \infty) \to (0, \infty)$ exists and $\tilde{n}(r)$ can be expressed as a single-valued function,

$$\tilde{n}(r) = \mathcal{N}^{-1}\left(\mu^{-2} f(r) r^{2(D-2)}\right). \tag{5.36}$$

□

5.3 Photon gas accretion and its critical point

In this section, we will construct the accretion problem of ideal photon gas in D dimensions and find the condition of its critical point based on discussions in the previous section.

5.3.1 The EOS of ideal photon gas in d dimensional space

To formulate the accretion of ideal photon gas in D dimensions, we must know its equation of state at first. Here we construct the EOS.

From the discussion of black body radiation in a d dimensional space, we have a relation

$$pV = \frac{1}{d} U, \tag{5.37}$$

where the thermodynamical variables p, V and U are the pressure, the volume and the energy of a system, respectively. This relation gives

$$\left(\frac{\partial U}{\partial V}\right)_S \equiv -p = -\frac{1}{d}\frac{U}{V}, \tag{5.38}$$

where S denotes the entropy. Integrating the both sides concerning U and V

$$U V^{1/d} = C(S), \tag{5.39}$$

with the function $C(S)$ being an arbitrary function. Then, the enthalpy H of the black body radiation is

$$H = U + pV = \frac{d+1}{d} U \propto V^{-1/d}. \tag{5.40}$$

Note that the proportionality coefficient of the last equality can depend on the entropy S. Comparing this result with the usual convention of a polytrope index in the expression per particle, we conclude that the EOS of ideal photon gas is

$$h = \frac{k\gamma}{\gamma - 1} n^{\gamma - 1} \tag{5.41}$$

with

$$\gamma = \frac{d+1}{d} \tag{5.42}$$

and k is an arbitrary function of the entropy. It can be revealed that the quantity k is a constant constructed by the Planck constant and a numerical factor by the argument about photon gas from statistical mechanics. However, the explicit form of k is not relevant to the proof of the theorem. Since the entropy of the fluid is constant over the spacetime, k is also constant. This is relevant to the proof.

5.3.2 The critical point of photon gas accretion

Lemma 5.3.1. *For the accretion of ideal photon gas in our accretion problem, the radius r_c of a critical point is specified by*

$$(fr^{-2})' = 0 \tag{5.43}$$

and the corresponding critical density n_c is

$$n_c = \sqrt{\frac{D-2}{f(r_c)}} \frac{|\mu|}{r_c^{D-2}}. \tag{5.44}$$

The type of the critical point is classified by the equation

$$\textit{saddle point (extremum point)} \Leftrightarrow (fr^{-2})'' < 0 \ (>0) \tag{5.45}$$

at the radius.

Proof. The condition for a critical point (5.24*a*), (5.24*b*) can be transformed to

$$\begin{cases} v_s^2 \left[2(D-2)f + rf'\right] - rf' = 0 & \text{(5.46a)} \\ f' - \dfrac{2(D-2)}{r} \dfrac{\mu^2}{r^{2(D-2)}n^2} = 0. & \text{(5.46b)} \end{cases}$$

From Eq. (5.41), the sound speed of ideal photon gas is constant,

$$v_s^2 = \frac{\partial \ln h}{\partial \ln n} = \gamma - 1. \tag{5.47}$$

Substituting this, Eq. (5.46*a*) determines the position r of the critical point,

$$0 = (\gamma - 2) r^3 (fr^{-2})', \tag{5.48}$$

where the formula Eq. (5.42) and the fact $d = D - 1$ are used in the last equality. The corresponding number density at the critical point is uniquely obtained from Eq. (5.46*b*) using the relation $f'(r_c) = 2f(r_c)/r_c$. The condition for a saddle or extremum point was given in 5.2.1. In this case, the value of the function $\mathcal{F}_\mu'$ at a critical point is written in the form,

$$\mathcal{F}_\mu' = -2(\gamma - 1)(D-2) r f (f')^{-2} (fr^{-2})'', \tag{5.49}$$

where the fact $(fr^{-2})' = 0$ at a critical point is used. Clearly, the sign of the value $\mathcal{F}_\mu'$ is opposite to $(fr^{-2})''$ and the proof has been done. □

Note that the sound speed v_s satisfies the subluminal condition $0 < v_s^2 < 1$ and the monotonically increasing condition $\partial_n v_s^2 \geq 0$ from $v_s^2 = \gamma - 1 = 1/d$ and $d = D - 1 \geq 2$.

5.4 Proof of Theorem: The correspondence among the points

In this section, we see the correspondence among the three objects; the photon sphere, the critical point and the sonic point of our ideal photon gas accretion problem and complete the proof of the main theorem.

From Lemma 5.1.1 and 5.3.1, we can establish the following corollary about the correspondence between the photon spheres and the critical points of ideal photon gas accretion.

Corollary 5.4.1. *If the spacetime has photon spheres, there exists a critical point of the same radius for each of the spheres. Furthermore, for an unstable photon sphere, the critical point on the same radius is always a saddle point while for a stable one, the corresponding critical point is an extremum point.*

The critical point radius r_c depends on μ in general. However, the photon gas accretion is interesting in the sense that its critical radius does not depend on μ and this fact is responsible for the correspondence.

Ideal photon gas satisfies the condition of the EOS in Lemma 5.2.2 since $v_s^2(n) = \gamma - 1$ and the lemma can be applied. Then we have the corollary about the relation between critical points and sonic points.

Corollary 5.4.2. *For any physical transonic accretion flow of the ideal photon gas accretion, its sonic point is a critical and saddle point.*

Then, the above two corollaries complete the proof of Theorem 5.0.1.

5.5 Summary

In this chapter, first we have derived the conditions for photon spheres, the radius and the stability of the corresponding circular orbit of null geodesics. Next, we have generalized the accretion analysis given by Chaverra and Sarbach [24] to arbitrary dimensions and discussed the relation between sonic points and critical points in general. Then, for ideal photon gas, it has been shown that radius of a sonic point always coincides with (one of) photon spheres for physical solutions of the accretion problem.

We can say that a photon sphere is indeed special even for the radial accretion because the flow can be interpreted as a set of geodesic motions of photons and some of the photons must go round on the sphere. However, the sound speed and the fluid velocity are macroscopic quantities. The reason for the correspondence is not yet so clear. Since the correspondence seems to originate from the microscopic construction of radiation fluid, we conjecture that the correspondence will be seen in more general situations, such as axially symmetric steady-state accretion flows onto stationary rotating black holes.

The correspondence can be broken if the effects of the back reaction is included. However, since photon spheres are usually located near the source of gravity, it would

be justified to neglect the self-gravity of the fluid and the correspondence still holds in that case.

It should be noted that the present discussion applies not only to accretion but also to outflow or stellar wind as long as it is steady-state and spherically symmetric. See Ref. [38] for example.

Chapter 6

Sonic point/photon sphere correspondence: rotational flow

Originally published as:
Y. Koga and T. Harada, *Phys. Rev. D* **98** (2018) 024018.

The accretion problem formulated in Chap. 5 are for spherically symmetric fluid flow in a spherically symmetric spacetime. Although the sonic point/photon sphere (SP/PS) correspondence for radiation fluid flow is a surprising result and is generic in the sense that the spacetime metric and the dimension are arbitrary, accretion flows in real astrophysical situations are rarely spherically symmetric. Even for the nearly spherically symmetric central objects, the accretion flows onto them are usually rotating.

In this chapter, we show there exists the correspondence between sonic points and photon spheres in the case of rotational accretion of ideal photon gas. In the first half, we construct our rotational accretion flow model which forms a disk on an equatorial plane of D-dimensional static spherical symmetric spacetime ($D \geq 3$) and analyze its sonic points for a general equation of state (EOS) of fluid. The metric is given by

$$ds^2 = -f(r)dt^2 + g(r)dr^2 + r^2 d\Omega_{D-2}^2 \qquad (D \geq 3), \tag{6.1}$$

where the condition $0 < f, g < \infty$ is assumed and $d\Omega_{D-2}^2$ is the unit $(D-2)$-sphere metric given by

$$\begin{aligned} d\Omega_{D-2}^2 = d\theta_1^2 + \quad \cdots \quad & + \sin^2\theta_1 \cdots \sin^2\theta_{D-4} d\theta_{D-3}^2 \\ + \quad & \sin^2\theta_1 \cdots \sin^2\theta_{D-3} d\phi^2. \end{aligned} \tag{6.2}$$

The polar and the azimuthal angle coordinates are denoted by $\theta_i\,(i = 1, ..., D-3)$ and ϕ, respectively. In the latter half, applying the analysis to radiation fluid, we show there exists the SP/PS correspondence in the rotational accretion. This is the main theorem:

Theorem 6.0.1. *For a physical transonic accretion flow of ideal photon gas fluid of our accretion problem Eq. (6.20), its sonic point(s) must be on (one of) the unstable photon sphere(s) of the spacetime Eq. (6.1).*

We start with the construction of our accretion disk model and the formulation of the problem and present the definition of critical point and sonic point and their relation in Sec. 6.1. In Sec. 6.2, we explicitly analyze the conditions for the critical point and its classification without specifying the EOS. A fact used in this section is proven in Sec. 6.3. In Sec. 6.4, Applying the EOS of the ideal photon gas (or, radiation fluid) to the analysis, we derive the conditions about the critical point and its classifications in that case. Then, recalling the conditions for the photon spheres in the previous chapter, we see that there also exists the correspondence between the sonic point and the photon sphere in the rotational accretion problem. The summary is given in Sec. 6.5.

6.1 Rotating accretion disk, critical point and sonic point

Here assuming three conservation laws and the metric (6.1), we formulate the accretion problem. The conditions for the critical point and the relation between the critical points and the sonic points are also given in the subsequent subsections.

We assume the following three equations, the first law of thermodynamics, continuity equation and energy-momentum conservation with perfect fluid:

$$\begin{cases} dh = Tds + n^{-1}dp & \text{(6.3a)} \\ \nabla_a J^a = 0 & \text{(6.3b)} \\ \nabla_a T^a_b = 0, & \text{(6.3c)} \end{cases}$$

where $J^a := nu^a$ is the number current and $T^a_b = nhu^a u_b + p\delta^a_b$ is the energy-momentum tensor of the perfect fluid. The quantities h, T, s, n, p and u^a represent the enthalpy per particle, the temperature, the entropy per particle, the number density, the pressure and the 4-velocity of the fluid.

6.1.1 Configuration of the accretion disk

We assume several conditions for the accretion disk. Although there are many other possibilities about disk thickness and the vertical equilibrium, we follow the simplest model used by Abraham, Bilic and Das [40]. Although their model is based on the axial coordinate, z, in rotational spacetime, however, we here choose the polar coordinate, θ_i, in spherical spacetime. In this sense, strictly speaking, our model is not the same as their model.

We assume the following conditions for the accretion disk:

1. The disk lying on the equatorial plane has symmetries which respects the background geometry;
   - Stationarity along the Killing vector $\xi_{(t)} = \partial_t$
   - Rotational symmetry along the Killing vector $\xi_{(\phi)} = \partial_\phi$

- Reflection symmetry respective to the equatorial plane

2. The matter distribution is uniform in the θ_i-direction: The number density n, the pressure p, the entropy and the components of the velocity u^μ are independent of θ_i

3. The disk is sufficiently thin so that we can ignore terms of the second or higher order of $\theta_i - \pi/2$ compared to that of the zero-th order.

4. The equilibrium between the inside and the outside of the disk surface in the polar direction is achieved by pressure of external rarefied gas.

The *equatorial plane* here means the 2-plane (r, ϕ) with all the polar angles $\theta_i = \pi/2$ $(i = 1, 2, ..., D-3)$ and the *disk* consists of the 2-dimensional plane with the $(D-3)$-dimensional (sufficiently small) thickness. Note that the disk surface is a spatial $(D-2)$-space of $\theta_i = $ const. and $u^{\theta_i} = 0$ everywhere in the disk as the consequence of conditions 1 and 2.

In accretion problems, we are interested in the accretion rate and it is also important for analysis of the dynamics. Consider $t = $ const. hypersurface and the disk volume Σ_D on the hypersurface. Let Σ_r be the region inside the radius r in Σ_D. The total particle number $N(t, r)$ in the volume Σ_r at the time t is given by

$$N(t, r) := \int_{\Sigma_r} n u^\mu d\Sigma_\mu. \tag{6.4}$$

Then the accretion rate $\dot{N}(t, r)$ of the particle number into the region Σ_r is given by

$$\dot{N}(t, r) = -\int_{S_r} n u^r \sqrt{fg} r^{D-2} d\Omega_{D-2} \tag{6.5}$$

where S_r is the cross-section of Σ_D with the sphere of radius r and $d\Omega_{D-2}$ is the volume element of $(D-2)$-dimensional unit sphere. From stationarity of the disk, we can prove the constancy of the accretion rate about both time t and radius r. Then we have the following expression for the integration of the continuity equation:

$$j_n(r) := \int_{S_r} n u^r \sqrt{fg} r^{D-2} d\Omega_{D-2} = \text{const.} \tag{6.6}$$

This is the constancy of the particle number flux $j_n(r)$.

6.1.2 Construction of the accretion problem

The system of Eqs. (6.3a), (6.3b) and (6.3c) implies the adiabatic condition of the fluid, or equivalently, $u^\mu \partial_\mu s = 0$. The conditions for the disk, the constancy of the entropy in θ_i-direction and the stationarity and the rotational symmetry of the matter distribution mean $\partial_{\theta_i} s = \partial_t s = \partial_\phi s = 0$ and the adiabatic condition reduces to the condition $\partial_r s = 0$.

Therefore the entropy of the fluid is constant over the disk volume and independent of the time. Then we can write the enthalpy as a function of the number density,

$$h = h(n). \tag{6.7}$$

The projection of the energy-momentum conservation equation $\nabla_\mu T^\mu_\nu = 0$ onto the direction of a Killing vector ξ^ν generally gives conservation of the quantity $hu_\mu\xi^\mu$ along the fluid motion if the matter distribution has the symmetry associated with the Killing vector:

$$u^\mu \nabla_\mu \left(hu_\nu \xi^\nu\right) = 0 \tag{6.8}$$

The disk of our accretion problem has symmetries associated with the two Killing vectors, $\xi_{(t)} = \partial_t$ and $\xi_{(\phi)} = \partial_\phi$. Therefore we immediately get the following two integrals of motion,

$$hu_t = \text{const}, \tag{6.9}$$

$$hu_\phi = \text{const}, \tag{6.10}$$

corresponding to $\xi_{(t)}$ and $\xi_{(\phi)}$, respectively. These are the specific energy and the specific angular momentum per particle and constant over the whole region in the disk due to the assumptions on the disk.

From the assumption that n and u^r are independent of all the polar angle θ_i, the particle number flux j_n is calculated as,

$$j_n(r) \;=\; 2\pi\Theta\sqrt{fg}r^{D-2}nu^r, \tag{6.11}$$

where $2\pi\Theta$ is the $(D-2)$-dimensional solid angle subtended by the disk. Together with Eq. (6.9)-(6.10), we also have constancy of the energy flux and the angular momentum flux,

$$j_\epsilon(r) := -2\pi\Theta\sqrt{fg}r^{D-2}nhu_t u^r = \text{const}, \tag{6.12}$$

$$j_\phi(r) := 2\pi\Theta\sqrt{fg}r^{D-2}nhu_\phi u^r = \text{const}. \tag{6.13}$$

Thus, the integration of the conservation equations leads to the constancy of j_n, j_ϵ and j_ϕ

From the assumption that the disk is sufficiently thin, we estimate the values of the components of the 4-velocity through

$$-1 = g_{\mu\nu}u^\mu u^\nu = -f\left(u^t\right)^2 + g\left(u^r\right)^2 + r^2\left(u^\phi\right)^2, \tag{6.14}$$

where it should be noted that $g_{\phi\phi} \to r^2$ in the limit of geometrically thin disk. Introducing the fluid's angular velocity $\Omega_f := u^\phi/u^t$, we have

$$\left(f - r^2\Omega_f^2\right)\left(u^t\right)^2 = 1 + g\left(u^r\right)^2. \tag{6.15}$$

Using Eq. (6.15), we obtain

$$\left(\frac{j_\epsilon}{j_n}\right)^2 = h^2u_t^2 = h^2\left[f + fg\left(u^r\right)^2\right]\frac{f}{f - r^2\Omega_f^2} = \text{const}. \tag{6.16}$$

The angular velocity Ω_f can be expressed as

$$\Omega_f = \frac{u^\phi}{u^t} = -\frac{f}{r^2}\frac{u_\phi}{u_t} = \omega f r^{-2} \tag{6.17}$$

in the limit of geometrically thin disk. The parameter $\omega := j_\phi/j_\epsilon = -u_\phi/u_t$ is constant due to Eqs. (6.12)-(6.13). We can write $(u^r)^2$ in Eq. (6.16) as

$$(u^r)^2 = \frac{\mu^2}{f g r^{2(D-2)} n^2}, \tag{6.18}$$

where Eq. (6.11) is used and the parameter $\mu := j_n/2\pi\Theta$ is constant from Eq. (6.6). Substituting the above results into Eq. (6.16), we finally get

$$\left(\frac{j_\epsilon}{j_n}\right)^2 = h^2 \left[f + \frac{\mu^2}{r^{2(D-2)}n^2}\right] \frac{1}{1-\omega^2 f r^{-2}} = \text{const.} \tag{6.19}$$

The function can be seen as a function of two variables, r and n, and the conservation equations imply its constancy. As a consequence, we have constructed the master equation of the accretion problem by the following algebraic equation with two parameters, μ and ω:

$$F_{\mu,\omega}(r,n) := h^2(n) \left[f(r) + \frac{\mu^2}{r^{2(D-2)}n^2}\right] \frac{1}{1-\omega^2 f(r) r^{-2}} = \text{const.} \tag{6.20}$$

The level curves satisfying the master equation on the phase space (r, n) are the solution curves.

Given μ and ω, the function $F_{\mu,\omega}(r, n)$ is specified and the constant in the rightmost side of Eq. (6.20) determines the accretion flow, or equivalently, the solution curve on the phase space (r, n). Once the distribution of the number density n is obtained, the equations $j_n = 2\pi\Theta\mu$ and $j_\phi/j_\epsilon = \omega$ give the velocity distribution. It is worth noting that the master equation coincides with that of the spherically symmetric accretion problem in Chap. 5 in the irrotational case $\omega = 0$ and does not depend on the (r, r)-component of the metric $g(r)$.

6.1.3 Critical point

Here we give the definition of the critical point and its classification by reformulating the problem in terms of a dynamical system on the phase space (r, n). The analysis of this kind was introduced in an accretion problem by Chaverra and Sarbach [24]. Generally, the critical point plays an important role in accretion problems and is closely related to the sonic point of the flow.

Definition of critical point

In our accretion problem Eq. (6.20), the solutions are described as the level curves of the function $F_{\mu,\omega}(r, n)$ on the phase space (r, n). These curves can be also obtained by

integrating the ordinary differential equation,

$$\frac{d}{d\lambda}\begin{pmatrix} r \\ n \end{pmatrix} = \begin{pmatrix} \partial_n \\ -\partial_r \end{pmatrix} F_{\mu,\omega}(r,n), \tag{6.21}$$

as orbits with a parameter λ. This is reformulation of the master equation Eq. (6.20) in terms of a dynamical system with the right-hand side (RHS) being the Hamiltonian vector field with respect to the Hamiltonian $F_{\mu,\omega}(r,n)$. Then, the notion of a *critical point* (or stationary point as in a dynamical system) at which the RHS of Eq. (6.21) vanishes arises and its conditions are

$$\begin{cases} \partial_n F_{\mu,\omega} = 0 & \text{(6.22a)} \\ \partial_r F_{\mu,\omega} = 0. & \text{(6.22b)} \end{cases}$$

We define a *critical point* (r_c, n_c) of the accretion problem as a point on the phase space (r,n) at which the conditions Eqs. (6.22a)-(6.22b) are satisfied.

Types of critical points

The linearization of Eq. (6.21) around a critical point allows us to classify the critical point into two types. The one is a saddle point and the another one is an extremum point. A saddle point is a point, in this case, through which two solution orbits pass. On the other hand, orbits in vicinity of an extremum point are closed curves around the point.

The linearization matrix M_c is given by

$$M_c := \begin{pmatrix} \partial_r\partial_n & \partial_n^2 \\ -\partial_r^2 & -\partial_r\partial_n \end{pmatrix} F_{\mu,\omega}(r_c, n_c). \tag{6.23}$$

This matrix, being real, 2×2 and traceless, has two eigenvalues with opposite signs. If the determinant of the matrix,

$$\det M_c = \left(\partial_r^2 F_{\mu,\omega}\right)_c \left(\partial_n^2 F_{\mu,\omega}\right)_c - \left(\partial_r\partial_n F_{\mu,\omega}\right)_c^2, \tag{6.24}$$

where the subscript c denotes the values at (r_c, n_c), is negative (positive), the eigenvalues are real (pure imaginary). As in a dynamical system, the real eigenvalues imply that the critical point is a saddle point. For the imaginary eigenvalues, the orbits around the critical point are periodic in linear order. However, because they are the contours of the real function $F_{\mu,\omega}(r,n)$, the orbits must be closed loops. Therefore the imaginary eigenvalues imply an extremum point.

6.1.4 Sonic point

The sonic point is the point on the phase space (r,n) at which the squared 3-velocity v^2 of the fluid equals to the squared sound speed v_s^2, or in other words, Mach number equals to one (sometimes referred to as *sonic surface* because it forms a surface in the physical space). The sonic point usually coincides with the critical point in accretion problem in a reasonable frame. Here we introduce the fluid co-rotating frame (FCRF) and observe that the 3-velocity v^2 in the FCRF gives the coincidence between the sonic point and the critical point.

Fluid co-rotating frame (FCRF)

We refer to the fluid co-rotating frame as the frame staying at the same radius but rotating with the same angular velocity Ω_f of the fluid. The 4-velocity u_o of an observer at rest in this frame is defined as

$$u_o := \gamma \left(\partial_t + \Omega_f \partial_\phi\right) \tag{6.25}$$

where $\Omega_f := u^\phi/u^t$ is the fluid's angular velocity. We consider the observer on the equatorial plane. The factor γ is determined by the normalization of the 4-velocity, $g_{\mu\nu}u_o^\mu u_o^\nu = -1$, and we have

$$\gamma^{-2} = f - r^2\Omega_f^2. \tag{6.26}$$

The squared 3-velocity v^2 of the fluid in the FCRF is given by

$$\frac{1}{1-v^2} = \left(g_{\mu\nu}u^\mu u_o^\nu\right)^2 = 1 + \frac{\mu^2}{fr^\delta n^2} \tag{6.27}$$

or

$$v^2 = \frac{\mu^2}{\mu^2 + fr^\delta n^2}, \tag{6.28}$$

where $\delta := 2(D-2)$ and we have used the normalization condition of the 4-velocity, $u^\mu u_\mu = -1$.

Sonic point of a transonic flow and critical point

In an accretion problem, the fluid flow can transit from subsonic state (i.e. state where its 3-velocity is smaller than its local sound speed v_s) to supersonic state (i.e. state where the 3-velocity is greater than v_s) and vice versa. Such a fluid flow is said to be *transonic* and here we call any flow which has both subsonic and supersonic regions *transonic flow*. The point at which the transition between subsonic and supersonic states of a transonic flow occurs is called *sonic point*. Since, in our accretion problem, a fluid accretion flow is a solution orbit of Eq. (6.20), we define a *sonic point* of a transonic flow as follows.

Definition 6.1.1 (Sonic point of a flow)**.** *For a transonic accretion flow of our accretion problem Eq. (6.20), let $n = n(r)$ be the solution curve on the phase space (r, n). Let $v = v(r)$ be the 3-velocity of the fluid at radius r measured in the FCRF. A sonic point (r_s, n_s) of the accretion flow is defined as a point on the phase space satisfying the condition,*

$$\left.\frac{v^2}{v_s^2}\right|_{(r_s, n(r_s))} = 1, \tag{6.29}$$

where $n_s = n(r_s)$.

Let us calculate explicitly the one of the conditions for the critical point, $\partial_n F_{\mu,\omega}(r,n) = 0$,

$$\begin{aligned} 0 &= \partial_n F_{\mu,\omega} \\ &= \frac{2h^2}{n}\frac{\mu^2}{r^\delta n^2}\left(v_s^2(n)\left[1+f\frac{r^\delta n^2}{\mu^2}\right]-1\right)\frac{1}{1-\omega^2 f r^{-2}}. \end{aligned} \tag{6.30}$$

Therefore, we can see that the sound speed $v_s^2(n) := \partial \ln h/\partial \ln n$ can be always written as

$$v_s^2(n) = \frac{\mu^2}{\mu^2 + f r^\delta n^2} \tag{6.31}$$

on the point (r,n) satisfying the condition $\partial_n F_{\mu,\omega}(r,n) = 0$ including the critical point. Conversely, if Eq. (6.31) is satisfied on a given point (r,n), the condition $\partial_n F_{\mu,\omega}(r,n) = 0$ holds. From these facts, we can show that a sonic point of a physically acceptable transonic accretion flow is identified with a critical point of saddle type as follows. Consider a physical transonic accretion flow which is specified by the solution curve $n = n(r)$. The squared 3-velocity v^2 of the flow at radius r is given by $v^2(r) = \mu^2/\left(\mu^2 + f r^\delta n^2(r)\right)$ from Eq. (6.28), while the squared sound speed v_s^2 at the radius is $v_s^2\left(n(r)\right)$. Therefore the sonic point (r_s, n_s) of the flow is obtained from the condition $v^2(r_s)/v_s^2\left(n(r_s)\right) = 1$, or equivalently,

$$v_s^2\left(n(r_s)\right) = \frac{\mu^2}{\mu^2 + f r^\delta n^2(r_s)} \tag{6.32}$$

and $n_s = n(r_s)$. Since the point (r_s, n_s) satisfies the condition Eq. (6.31), we have $\partial_n F_{\mu,\omega}(r_s, n_s) = 0$ as mentioned below Eq. (6.31). Then we have the following three cases concerning the sonic point (r_s, n_s):

1. $\partial_r F_{\mu,\omega}(r_s, n_s) \neq 0$.
2. $\partial_r F_{\mu,\omega}(r_s, n_s) = 0$ (i.e., the sonic point is a critical point because of the fact $\partial_n F_{\mu,\omega}(r_s, n_s) = 0$).
   (a) The corresponding critical point is of saddle type.
   (b) The corresponding critical point is of extremum type.

In the case 1, the curve $n = n(r)$ typically gets double-valued (so unphysical) at least locally because $dn/dr = -\partial_r F_{\mu,\omega}(r_s, n_s)/\partial_n F_{\mu,\omega}(r_s, n_s) = \pm\infty$ there from Eq. (6.21). Another possibility with diverging density gradient, which is physically acceptable, is a transonic shock. In the current paper, we require the finite density gradient, $|dn/dr| < \infty$, as one of the conditions of a physical flow, thus excluding a transonic shock. Therefore the case 1 is not allowed for the flow $n = n(r)$ and the sonic point must be a critical point. However, the case 2b is also excluded because any solution curve, being a contour of $F_{\mu,\omega}$ originally, cannot pass the critical point of extremum type. Then we have only the case 2a for the sonic point (r_s, n_s) of the physically acceptable transonic flow $n = n(r)$. As a consequence, we have the following theorem:

Theorem 6.1.2. *For a physical transonic accretion flow in our accretion problem, its sonic point coincides with a critical point on the phase space which is a saddle point.*

6.2 Conditions for critical point and its classification

We explicitly calculate the conditions for the critical point Eqs. (6.22a)-(6.22b) and its classification by the sign of the determinant of the matrix Eq. (6.24) without specifying the EOS of the fluid in the following.

The conditions for the critical point Eqs. (6.22a)-(6.22b) can be explicitly written as

$$\partial_n F_{\mu,\omega} = \frac{2h^2}{n}\frac{\mu^2}{r^\delta n^2}\left(v_s^2\left[1+f\frac{r^\delta n^2}{\mu^2}\right]-1\right)\Omega = 0, \tag{6.33}$$

$$\partial_r F_{\mu,\omega} = h^2 f\Omega\left[\frac{(f\Omega)'}{f\Omega}-\frac{\mu^2}{fr^\delta n^2}\frac{\left(r^\delta\Omega^{-1}\right)'}{r^\delta\Omega^{-1}}\right] = 0, \tag{6.34}$$

where the function $\Omega(r)$ is defined by

$$\Omega(r) := \frac{1}{1-\omega^2 f r^{-2}}. \tag{6.35}$$

It should be noted that $\Omega(r) > 0$ is always satisfied because of Eq. (6.20).

We can prove that $\left(r^\delta\Omega^{-1}\right)' \neq 0$ and $(f\Omega)' \neq 0$ at the critical point (see Sec. 6.3) and therefore Eq. (6.34) is solved for n^2 with the help of $\left(r^\delta\Omega^{-1}\right)' \neq 0$ and $(f\Omega)' \neq 0$. Then we get the condition for the radius r_c of critical point eliminating the number density n from Eqs. (6.33)-(6.34) as follows.

$$\mathcal{F}_{\mu,\omega}(r) := v_s^2\left(\bar{n}(r)\right)\left[1+\frac{\left(r^\delta\Omega^{-1}\right)'}{r^\delta\Omega^{-1}}\frac{f\Omega}{(f\Omega)'}\right]-1 = 0, \tag{6.36}$$

$$\bar{n}(r) := \frac{|\mu|}{r^\delta\Omega^{-1}}\sqrt{\frac{\left(r^\delta\Omega^{-1}\right)'}{(f\Omega)'}} \tag{6.37}$$

Once the radius r_c is obtained, the number density n_c of the critical point is uniquely determined by

$$n_c = \bar{n}(r_c). \tag{6.38}$$

The determinant of the matrix M_c can be expressed in terms of the function $\mathcal{F}_{\mu,\omega}(r)$ defined above:

$$\det M_c = -\frac{\left(r^\delta\Omega^{-1}\right)_c}{\left(r^\delta\Omega^{-1}\right)'_c}\frac{4h_c^4}{n_c^2}\left((f\Omega)'_c\right)^2\mathcal{F}'_{\mu,\omega}(r_c) \tag{6.39}$$

Therefore, using the fact that $(r^\delta\Omega^{-1})'_c$ and $(f\Omega)'_c$ have the same sign, we can uniquely classify the critical point through the sign of the derivative of the function $\mathcal{F}'_{\mu,\omega}$ and the factor $(f\Omega)'$ at the critical radius:

$$\textit{saddle (extremum) point} \Leftrightarrow (f\Omega)'_c\,\mathcal{F}'_{\mu,\omega}(r_c) > 0\ (<0) \tag{6.40}$$

6.3 Nonzero terms on the critical point

Here we show that $\left(r^{\delta}\Omega^{-1}\right)' \neq 0$ and $(f\Omega)' \neq 0$ at the critical point as mentioned in Sec. 6.2. Consider the case in which the two conditions, Eq. (6.34) and

$$\left(r^{\delta}\Omega^{-1}\right)' = 0, \tag{6.41}$$

are satisfied, simultaneously. Clearly, this is equivalent to the conditions,

$$\begin{cases} \left(r^{\delta}\Omega^{-1}\right)' = 0 & \text{(6.42a)} \\ (f\Omega)' = 0. & \text{(6.42b)} \end{cases}$$

Eliminating Ω from the above two equations, we get

$$(fr^{\delta})' = 0. \tag{6.43}$$

This condition solely determines the critical radius r_c. Once the radius r_c is obtained, we can specify the parameter ω^2 from the above equations. From Eq. (6.43), we find the expression,

$$(fr^{-2})' = (fr^{\delta-(2+\delta)})' = fr^{\delta}(r^{-(2+\delta)})' = -(2+\delta)fr^{-3}, \tag{6.44}$$

for $r = r_c$. Substituting the result into Eq. (6.42a), we get, at $r = r_c$,

$$0 = \left(r^{\delta}\Omega^{-1}\right)' = r^{\delta-1}\left(\delta + 2\omega^2 fr^{-2}\right). \tag{6.45}$$

By definition, both the terms in the bracket must be positive and we do not have the parameter ω satisfying the condition. Therefore the conditions for the critical point are always accompanied by the additional conditions $\left(r^{\delta}\Omega^{-1}\right)' \neq 0$ and $(f\Omega)' \neq 0$.

Note that the above proof relies on the only one of the critical conditions Eq. (6.34), $\partial_r F_{\mu,\omega}(r,n) = 0$. This implies that the conditions $\left(r^{\delta}\Omega^{-1}\right)' \neq 0$ and $(f\Omega)' \neq 0$ hold anywhere on the curve Γ defined by the equation $\partial_r F_{\mu,\omega}(r,n) = 0$ and the curve Γ can be expressed by $n = \bar{n}(r)$.

6.4 Correspondence between sonic point and photon sphere for photon gas accretion

In this section, we analyze the critical point in the case of ideal photon gas and prove Theorem 6.0.1.

We derived the EOS of ideal photon gas in arbitrary spatial dimensions d in Eq. (5.41) in Chap. 5. It is given by

$$h(n) = \frac{k\gamma}{\gamma - 1} n^{\gamma - 1} \tag{6.46}$$

where the index γ is related to the dimension by $\gamma = (d+1)/d$. The sound speed $v_s^2(n)$ is then computed as

$$v_s^2(n) := \frac{\partial \ln h}{\partial \ln n} = \gamma - 1 = \frac{1}{d} = \frac{1}{D-1}. \tag{6.47}$$

6.4.1 Critical point

For the conditions for the critical point (r_c, n_c) and its classification for the ideal photon gas accretion, we have the following lemma.

Lemma 6.4.1. *For the accretion of ideal photon gas in our accretion problem, radius r_c of a critical point is specified by*

$$(fr^{-2})' = 0 \tag{6.48}$$

and the corresponding critical density n_c is

$$n_c = |\mu| \sqrt{\frac{\delta}{r_c^{\delta+1} f_c'}}. \tag{6.49}$$

The type of the critical point is classified by the equation

$$\textit{saddle (extremum) point} \Leftrightarrow \left(fr^{-2}\right)''_{r=r_c} < 0 \ (> 0). \tag{6.50}$$

Proof. The critical radius r_c is determined by Eq. (6.36). Substituting the sound speed of radiation fluid into Eq. (6.47), the condition for the critical radius r_c is given by

$$\mathcal{F}_{\mu,\omega} = -\frac{1}{\delta+2} \frac{f\Omega}{(f\Omega)'} \frac{\delta + 2\omega^2 f r^{-2}}{f r^{-2}\left(1 - \omega^2 f r^{-2}\right)} \left(f r^{-2}\right)' = 0. \tag{6.51}$$

As mentioned above Eq. (6.36), $(f\Omega)' \neq 0$ is always satisfied at critical point. Therefore, the critical radius is obtained by solving the equation

$$\left(f r^{-2}\right)' = 0. \tag{6.52}$$

Once the radius r_c is obtained, we get the corresponding number density n_c from Eq. (6.38),

$$n_c = |\mu| \sqrt{\frac{\delta}{r_c^{\delta+1} f_c'}}, \tag{6.53}$$

where we used the facts $\Omega'(r_c) = 0$ and $f_c' = 2f_c/r_c$. This expression is also independent of the parameter ω.

From Eq. (6.40) and $(f\Omega)'_c = (f'\Omega)_c > 0$, the types of the critical point (r_c, n_c) are determined by the sign of $\mathcal{F}'_{\mu,\omega}(r_c)$. Using the fact that $\Omega'(r_c) = 0$ and $f_c' = 2f_c/r_c$, we can explicitly write $\mathcal{F}'_{\mu,\omega}(r_c)$ as

$$\mathcal{F}'_{\mu,\omega}(r_c) = -\frac{1}{\delta+2} \left[\frac{r}{2} \frac{\delta + 2\omega^2 f r^{-2}}{f r^{-2}\left(1 - \omega^2 f r^{-2}\right)} \left(f r^{-2}\right)''\right]_{r=r_c}. \tag{6.54}$$

Then we get the explicit form of Eq. (6.40) for radiation fluid accretion:

$$\textit{saddle (extremum) point} \Leftrightarrow \left(fr^{-2}\right)''_{r=r_c} < 0 \ (> 0) \tag{6.55}$$

□

It should be noted that the conditions do not depend on the parameter of the rotation ω and thereby coincides with the condition in the case of spherical flows.

6.4.2 Proof of Theorem: Correspondence among the points

In the following, we see the correspondence among the three objects; the photon sphere, the critical point and the sonic point of our accretion problem with fluid of ideal photon gas and finally prove Theorem 6.0.1.

In the previous chapter, we derived the following lemma about the conditions for photon spheres of the spacetime Eq. (6.1):

Lemma 6.4.2. *The radius photon sphere is specified by the equation,*

$$(fr^{-2})' = 0. \tag{6.56}$$

The stability condition of the photon sphere is given by

$$stable\ (unstable) \Leftrightarrow (fr^{-2})'' > 0\ (< 0) \tag{6.57}$$

at the radius of the photon sphere.

The conditions of the critical radius Eq. (6.48) and its classification Eq. (6.50) coincide with that of the photon sphere Eqs. (6.56) and (6.57), respectively. Then we immediately obtain the following corollary about the correspondence between photon spheres and critical points of ideal photon gas accretion in our accretion problem from Lemma 6.4.1 and 6.4.2:

Corollary 6.4.3. *If the spacetime has photon spheres, there exists a critical point at the same radius for each of the spheres. Furthermore, for an unstable photon sphere, the critical point at the same radius is always a saddle point while for a stable one, the corresponding critical point is an extremum point.*

Note that if a critical point exists, there must be a photon sphere at the same radius and the extremum(saddle) point corresponds to the stable(unstable) sphere. There is a one-to-one correspondence between critical points and photon spheres. It is worth noting that if the spacetime has more than one photon spheres, the stable and unstable spheres appear alternately as we can see from Eqs. (6.56)-(6.57). The fact also leads to the alternate appearance of the corresponding extremum and saddle points on the phase space (r, n).

As mentioned in Theorem 6.1.2 in Sec. 6.1.4, the sonic point of the physical transonic accretion flow coincides with a critical and saddle point. Then Theorem 6.1.2 and Corollary above immediately prove Theorem 6.0.1.

Even if the accretion fluid flow is rotational, there exists a correspondence between the photon sphere and the sonic point of the radiation fluid accretion as far as the fluid rotates around the center on the equatorial plane and satisfies our disk conditions.

6.5 Summary

We have formulated the rotational accretion problem of the disk lying on the equatorial plane of the D-dimensional static, spherically symmetric spacetime. We have adopted

the simplest accretion disk model similar to the one given by Abraham et al. [40]. After giving the definition of a critical point and observing its relation to the sonic point of a transonic accretion flow, we have shown the explicit form of the conditions of the critical point and its classification for the perfect fluid with an arbitrary EOS.

Applying the EOS of radiation fluid to the analysis, we have proved the existence of the correspondence between the sonic points of rotational ideal photon gas accretion and the photon spheres of the spacetime. We have showed, at first, that a critical point that is a saddle point is always on the unstable photon sphere while a critical point that is an extremum point is always on the stable photon sphere. Then, from the relation between the critical point and the sonic point, we have proved a correspondence between the photon sphere and the sonic point of radiation fluid in the rotational case. Then we have proved that the physical transonic accretion flow must have its sonic point on (one of) the unstable photon sphere(s) of the spacetime. The result holds in arbitrary dimensions of the spacetime as in the case of spherical flows shown in the previous chapter.

We have proved the correspondence in our idealized disk model, where the critical and the sonic points are directly related. However, there are many other possibilities about disk configurations such as disk thickness and vertical equilibrium and it is known that the Mach number can deviate from one on the critical point depending on the disk models [41] [42]. Therefore it is not so clear whether the correspondence exists between the sonic point and photon sphere, or, between the critical point and photon sphere in more realistic models, e.g., in the model by Abramowicz et al. [43].

If we focus on a spherical star in vacuum with general relativity, its exterior geometry is described by the Schwarzschild spacetime. As considered in astrophysical cases, such a star typically has a radius greater than $3m$ for the mass m and does not have a photon sphere. Our result says that the star of radius greater than $3m$ cannot have transonic accretion of radiation fluid as far as it meets the conditions in the current or the previous chapter, that is, rotating geometrically thin accretion disks or spherically symmetric accretion flows.

We have extended the correspondence from spherically symmetric flows in the previous chapter to rotating geometrically thin accretion disks. This result, more and more, motivates us to consider its physical origin, that is to say, the connection between the behavior of free photons on the geometry and behavior of photon gas. This is also attractive as one of problems concerning hydrodynamics on curved spacetime.

It is also interesting to investigate a correspondence in a spacetime with a rotating object. The central object in such a spacetime has angular momentum and there is preferred direction of rotation for the motion of matter. The radius of the circular orbits of particles depends on the direction of rotation and also that of the sonic point does. The physics becomes more complicated but more interesting in that situation.

Chapter 7

Sonic point/photon surface correspondence: planar and hyperbolical flow

Originally published as:
Y. Koga, *Phys. Rev. D* **99** (2019) 064034.

The existence of the sonic point/photon sphere (SP/PS) correspondence in quite wide situations, as we have seen in the previous chapters, strongly suggests that there exists some physical reason for it. To reveal the reason, it is necessary to know what properties of a photon sphere are needed for the correspondence to hold; Circularity of null orbits, positivity and constancy of the intrinsic curvature or else. Claudel *et al.* [8] introduced a geometrical concept, *photon surface*, which inherits only the local geometrical property of photon spheres called *umbilicity* but need not have spherical symmetry. In this chapter, we see there exists the correspondence between sonic points and *photon surfaces* in nonspherical spacetime like as the SP/PS correspondence. The result leads us to the conclusion that the SP/PS correspondence is caused by the umbilicity of a photon sphere.

We consider static spacetime of spherical, planar and hyperbolic symmetry given by the metric,

$$ds^2 = -f(r)dt^2 + g(r)dr^2 + r^2\left(d\chi^2 + s^2(\chi)d\Omega_{D-3}^2\right), \tag{7.1}$$

where $f(r) > 0$, $g(r) > 0$ and the function $s(\chi)$ is given by

$$s(\chi) = \begin{cases} \sin\chi & (spherical) \\ \chi & (planar) \\ \sinh\chi & (hyperbolic) \end{cases} \tag{7.2}$$

in the spherically, planar and hyperbolically symmetric case, respectively. $d\Omega_{D-3}^2$ is a unit $(D-3)$-sphere,

$$d\Omega_{D-3}^2 = d\theta_1^2 + \cdots + \sin^2\theta_1 \cdots \sin^2\theta_{D-5} d\theta_{D-4}^2 + \sin^2\theta_1 \cdots \sin^2\theta_{D-4} d\theta_{D-3}^2. \tag{7.3}$$

We investigate photon surfaces of r = const. hypersurfaces, which we call constant-r photon surfaces, in the spacetime. (The photon surfaces in the spherical case are just photon spheres.) Then, after formulating an accretion problem of radial fluid flows for a general equation of state (EOS), we prove our main theorem, which states that there exists the correspondence between the sonic points of the radiation fluid flows and the photon surfaces:

Theorem 7.0.1. *For any physical transonic flow of radiation fluid which is stationary and spherically, planar or hyperbolically symmetric on the spacetime (7.1), the radius of its sonic point coincides with that of (one of) the unstable constant-r photon surface(s).*

We define photon surfaces of constant radius, named *constant-r photon surface*, in the spacetime (7.1) in Sec. 7.1. The stability condition for a constant-r photon surface is also derived. Then we formulate the accretion problem of radial fluid flow in Sec. 7.2 and finally prove the correspondence between the sonic point of radiation fluid flow and the photon surfaces in Sec. 7.3. The summary is given in Sec. 7.4.

7.1 Photon surface of constant radius

We investigate the explicit condition for a timelike surface to be a photon surface in the spherically, planar and hyperbolically symmetric spacetime of D-dimensions given by the metric Eq. (7.1). Here we focus on a timelike photon surface of constant radius. We consider the $(D-1)$-dimensional timelike hypersurface of constant radius,

$$S_r := \{p \in M | r = \text{const.}\}\,, \tag{7.4}$$

and investigate the condition for S_r to be a photon surface. We name the photon surface *constant-r photon surface*:

Definition 7.1.1 (Constant-r photon surface)**.** *Let (M, g) be spacetime with the metric, Eq. (7.1). A hypersurface S_r is called constant-r photon surface if it is a photon surface.*

Note that constant-r photon surfaces of the spacetime given by Eq. (7.1) coincides with the particular cases of r-photon surfaces of the spacetime given by Eq. (4.1) where the $(D-2)$-subspace $\gamma_{ij}(x)dx^i dx^j$ is the constant curvature space of curvature $k = \pm 1, 0$. For $k = 1$ case, the photon surface is what is called photon sphere in Chap. 5.

7.1.1 Second fundamental form

The hypersurface S_r has the normal,

$$n_a = \sqrt{g} dr_a, \tag{7.5}$$

and the induced metric h_{ab} on it,

$$h_{ab} = g_{ab} - n_a n_b. \tag{7.6}$$

The second fundamental form χ_{ab} is given by

$$\begin{aligned}\chi_{ab} &:= h_a^c \nabla_c n_b \\ &= h_a^c (\partial_c n_b - \Gamma^d{}_{cb} n_d) \\ &= -h_a^c \Gamma^d{}_{cb} n_d \end{aligned} \tag{7.7}$$

where we used the fact that $h_\mu^\nu \partial_\nu = (\partial_t, 0, \partial_\chi, \partial_{\theta_1}, ..., \partial_{\theta_{D-3}})$. The components are obtained from

$$\begin{aligned}\chi_{\mu\nu} &= -h_\mu^\sigma \Gamma^\rho{}_{\sigma\nu} n_\rho \\ &= -\Gamma^r{}_{\mu\nu} \sqrt{g} \end{aligned} \tag{7.8}$$

where $\mu, \nu = t, \chi, \theta_1, ..., \theta_{D-3}$. Hereafter we calculate the components in the tetrad system $\{e_{(\mu)}\}$ defined so that

$$e_{(\mu)} \propto \partial_\mu. \tag{7.9}$$

Because the brackets of the third term in Eq. (7.1) represents constant curvature $(D-2)$-space, it is sufficient to evaluate the components $\chi_{(\mu)(\nu)}$ only for $\mu, \nu = t, \chi, \theta$ where $\theta := \theta_1$ corresponds to one of the coordinate of the $(D-3)$-sphere $d\Omega^2_{D-3}$. The calculations of the Christoffel symbols gives

$$\chi_{(i)(j)} = \sqrt{g}^{-1} diag \left[-\frac{1}{2}\frac{f'}{f}, \frac{1}{r}, \frac{1}{r} \right] \tag{7.10}$$

where $i, j = t, \chi, \theta$.

The trace Θ of the second fundamental form is given by

$$\Theta := h^{ab}\chi_{ab} = \eta^{(\mu)(\nu)}\chi_{(\mu)(\nu)} = \sqrt{g}^{-1} \left[\frac{1}{2}\frac{f'}{f} + (D-2)\frac{1}{r} \right]. \tag{7.11}$$

The trace-free part σ_{ab} of the second fundamental form is then given by

$$\sigma_{ab} = \chi_{ab} - \frac{1}{D-1}\Theta h_{ab}. \tag{7.12}$$

Its components are given by

$$\sigma_{(i)(j)} = -\frac{1}{2(D-1)}\frac{(fr^{-2})'}{(fr^{-2})}\sqrt{g}^{-1} diag\left[D-2, 1, 1\right]. \tag{7.13}$$

Finally, for all the components including $\mu, \nu = r$, we have

$$\sigma_{(\mu)(\nu)} = -\frac{1}{2(D-1)}\frac{(fr^{-2})'}{(fr^{-2})}\sqrt{g}^{-1} M_{(\mu)(\nu)} \tag{7.14}$$

where $M_{(\mu)(\nu)} := \mathrm{diag}[D-2, 0, 1, ..., 1]$.

7.1.2 Radius of constant-r photon surface

From Theorem 3.1.8, the timelike hypersurface S_r is a photon surface if and only if it is totally umbilic, i.e. $\sigma_{ab} = 0\ \forall p \in S$. Then we obtain the following proposition from Eq. (3.12):

Proposition 7.1.2. *A timelike hypersurface S_r of the radius r is a photon surface if and only if*

$$(fr^{-2})' = 0 \tag{7.15}$$

is satisfied at the radius.

7.1.3 Stability of constant-r photon surface

Let $\{S_r\}$ be a foliation of the spacetime, Eq. (7.1), consisting of S_r. From Eq. (3.22), it is a Gaussian normal foliation. With σ_{ab} defined on each S_r, we calculate $\nabla_n \sigma_{ab}$. On a constant-r photon surface given by $S_{r=r_p}$, we have

$$\begin{aligned}
\nabla_n \sigma_{(\mu)(\nu)} &= \nabla_n \sigma_{ab} e^a_{(\mu)} e^b_{(\nu)} \\
&= \nabla_n \left[\sigma_{ab} e^a_{(\mu)} e^b_{(\nu)}\right] - \sigma_{ab} \nabla_n \left[e^a_{(\mu)} e^b_{(\nu)}\right] \\
&= \nabla_n \left[\sigma_{(\mu)(\nu)}\right] \\
&= n^r \partial_r \left[-\frac{1}{2(D-1)} \frac{(fr^{-2})'}{(fr^{-2})} \sqrt{g}^{-1} M_{(\mu)(\nu)}\right] \\
&= -\frac{1}{2(D-1)} \frac{(fr^{-2})''}{(fr^{-2})} g^{-1} M_{(\mu)(\nu)}
\end{aligned} \tag{7.16}$$

by using Eq. (7.15). For any null vector $k = k^\mu \partial_\mu \in T_p S_{r_p}$ tangent to S_{r_p},

$$k^a k^b \nabla_n \sigma_{ab} = -\frac{1}{2} \frac{(fr^{-2})''}{(fr^{-2})} g^{-1} f (k^t)^2. \tag{7.17}$$

From Proposition 3.3.1, the constant-r photon surface S_{r_p} is strictly stable, strictly unstable, or marginally stable depending on the value of $(fr^{-2})''$ at r_p. Since constant-r photon surfaces are classified into only the three types, which are not overlapped each other, we simply call them stable, unstable, marginally stable r-photon surfaces in the following. Then we obtain the following proposition:

Proposition 7.1.3. *The stability condition of the constant-r photon surface S_r is given by*

$$\textit{stable}\,(\textit{unstable}) \Leftrightarrow (fr^{-2})'' > 0\,(< 0) \tag{7.18}$$

at the radius.

7.2 Accretion problem

We consider stationary radial fluid flow on the spacetime (7.1). The flow is spherically, planar or hyperbolically symmetric depending on the spatial symmetry of the spacetime, Eq. (7.2). After formulating the accretion problem, we give a general analysis using dynamical systems method. (We sometimes call the problem "accretion problem" conventionally, however, it would not make sense because the spacetime we consider is not interpreted as spacetime made by some central object in the nonspherical cases.) The method clarifies the difference between a critical point, which is a singular point of the system, and a sonic point, which is a point where Mach number of flow equals to one.

We assume three conservation equations, the first law, continuity equation and energy-momentum conservation with perfect fluid:

$$\begin{cases} dh = Tds + n^{-1}dp & \text{(7.19a)} \\ \nabla_a J^a = 0 & \text{(7.19b)} \\ \nabla_a T^a_b = 0 & \text{(7.19c)} \end{cases}$$

where $J^a := nu^a$ is the number current and $T^a_b = nhu^a u_b + p\delta^a_b$ is the energy-momentum tensor of the perfect fluid. The quantities h, T, s, n, p and u^a are the enthalpy per particle, the temperature, the entropy per particle, the number density, the pressure and the 4-velocity of the fluid, respectively.

Contraction of Eq. (7.19c) with u^b gives the adiabatic condition of the fluid, $u^a\nabla_a s = 0$, in general together with Eqs. (7.19a) and (7.19b). The assumption that the fluid is stationary and spherically, planarly or hyperbolically symmetric implies that the entropy is a function of r only, $s = s(r)$, and that the 4-velocity has only the t- and r- components, $u = u^t\partial_t + u^r\partial_r$. Besides, the spatial symmetry of the fluid distribution implies constancy of the entropy s on a time slice. Therefore the entropy s is constant over the whole spacetime and we can write the enthalpy as a function of the number density,

$$h = h(n). \tag{7.20}$$

Integrating Eq. (7.19b), we have

$$j_n := (fg)^{1/2} r^{D-2} n u^r = \text{const}, \tag{7.21}$$

from the symmetries of the fluid and the spacetime metric. The quantity j_n represents the particle flux of the fluid. Contracting with the static Killing vector $\xi^b_{(t)} = \partial^b_t$, Eq. (7.19c) reduces to the equation of conservation of the energy current $I^a := nhu_b\xi^b_{(t)}u^a$,

$$\nabla_a I^a = 0. \tag{7.22}$$

The integration gives

$$j_\epsilon := (fg)^{1/2} r^{D-2} nhu_t u^r = \text{const}. \tag{7.23}$$

where j_ϵ is the energy flux. Combining Eqs. (7.20), (7.21) and (7.23) and using the normalization condition of the 4-velocity u, we have

$$\left(\frac{j_\epsilon}{j_n}\right)^2 = h^2\left[f + \frac{j_n^2}{r^{2(D-2)}n^2}\right] = \text{const.} \tag{7.24}$$

Then, the problem is formulated into the algebraic master equation:

$$F_\mu(r,n) = h^2(n)\left[f(r) + \frac{\mu^2}{r^{2(D-2)}n^2}\right] = \text{const}, \qquad \mu := j_n \tag{7.25}$$

F_μ is the energy square per particle and μ is the parameter interpreted as the accretion rate of the flow. Our accretion problem is the problem of finding the solution of a fluid flow as a level curve $n = n(r)$ on the phase space (r, n) satisfying $F_\mu(r, n(r)) = \text{const.}$ for a given parameter μ. Once the number density distribution $n(r)$ obtained for the parameter μ, the equation $j_n := (fg)^{1/2} r^{D-2} n u^r = \mu$ gives the corresponding velocity distribution $u^r(r)$.

Note that there is no distinction concerning the spatial geometry $s(\chi)$ of the spacetime in the master equation Eq. (7.25). Thus far the problem completely coincides with the accretion problem of spherical flow in Chap. 5. We analyze our accretion problem in exactly the same procedure as Chap. 5 in the following.

7.2.1 Critical point

Here we give the definition of the critical point and its classification by reformulating the accretion problem in terms of a dynamical system on the phase space (r, n). The analysis of this kind was first introduced into an accretion problem by Chaverra and Sarbach [24]. Generally, the critical point plays an important role in accretion problems and is closely related to the sonic point of the flow.

Definition of critical point

In our accretion problem Eq. (7.25), the solutions are described as level curves of the function $F_\mu(r, n)$ on the phase space (r, n). These curves can be also obtained by integrating the ordinary differential equation,

$$\frac{d}{d\lambda}\begin{pmatrix} r \\ n \end{pmatrix} = \begin{pmatrix} \partial_n \\ -\partial_r \end{pmatrix} F_\mu(r,n), \tag{7.26}$$

as orbits with a parameter λ. This is a reformulation of the master equation Eq. (7.25) in terms of a dynamical system with the right-hand side (RHS) being the Hamiltonian vector field with respect to the Hamiltonian $F_\mu(r, n)$. Then, the notion of a *critical point* (or stationary point as in a dynamical system) at which the RHS of Eq. (7.26) vanishes arises and its conditions are

$$\begin{cases} \partial_n F_\mu(r,n) = 0 & \text{(7.27a)} \\ \partial_r F_\mu(r,n) = 0. & \text{(7.27b)} \end{cases}$$

We define a *critical point* (r_c, n_c) of the accretion problem as a point on the phase space (r, n) at which the conditions Eqs. (7.27a)-(7.27b) are satisfied.

Types of critical points

The linearization of Eq. (7.26) around a critical point allows us to classify the critical point into two types. The one is a saddle point and the another one is an extremum point. A saddle point is a point, in this case, through which two solution orbits pass. On the other hand, orbits in the vicinity of an extremum point are closed curves around the point.

The linearization matrix M_c is given by

$$M_c := \begin{pmatrix} \partial_r\partial_n & \partial_n^2 \\ -\partial_r^2 & -\partial_r\partial_n \end{pmatrix} F_\mu(r_c, n_c). \tag{7.28}$$

This matrix, being real, 2×2 and traceless, has two eigenvalues with opposite signs. If the determinant of the matrix is negative (positive), the eigenvalues are real (pure imaginary). As in a dynamical system, the real eigenvalues imply that the critical point is a saddle point. For the imaginary eigenvalues, the orbits around the critical point are periodic in linear order. However, because they are the level curves of the real function $F_\mu(r, n)$, the orbits must be closed loops in the vicinity of the critical point. Therefore the imaginary eigenvalues imply an extremum point.

We know the explicit form of the determinant $\det M_c$ from Chap. 5:

$$\det M_c = -\frac{2}{D-2} r_c (f_c')^2 \frac{h_c^4}{n_c^2} \mathcal{F}_\mu'(r_c) \tag{7.29}$$

where

$$\begin{aligned} \mathcal{F}_\mu(r) &:= v_s^2(\bar{n}(r))\,[1 + 2(D-2)a(r)] - 1, \\ \bar{n}(r) &:= |\mu| \sqrt{\frac{2(D-2)}{r^{2D-3} f'(r)}}, \\ a(r) &:= \frac{f(r)}{r f'(r)}. \end{aligned}$$

The subscript c means the value at (r_c, n_c). Then classification of a critical point at radius r_c is given by

$$\textit{saddle (extremum) point} \Leftrightarrow \mathcal{F}_\mu'(r_c) > 0 \ (< 0) \tag{7.30}$$

while the critical point (r_c, n_c) itself is also obtained from

$$\mathcal{F}_\mu(r_c) = 0, \ n_c = \bar{n}(r_c). \tag{7.31}$$

7.2.2 Sonic point

In an accretion problem, the fluid flow can transit from subsonic state (i.e. state where its 3-velocity is smaller than its local sound speed v_s) to supersonic state (i.e. state where the 3-velocity is greater than v_s) and vice versa. Such a fluid flow is said to be

transonic and here we call any flow which has both subsonic and supersonic regions *transonic flow*. The point at which transition between subsonic and supersonic states of a transonic flow occurs is called *sonic point*. A sonic point is also related to a critical point mathematically.

Definition of sonic point

Since, in our accretion problem, a fluid accretion flow is a solution orbit of Eq. (7.25), we define a *sonic point* of a transonic flow as a point on the phase space (r, n):

Definition 7.2.1 (Sonic point of a flow)**.** *For a transonic fluid flow of our accretion problem Eq. (7.25), let $n = n(r)$ be the corresponding solution curve on the phase space (r, n). Let $v = v(r)$ be the 3-velocity of the flow at radius r measured by static observers. A sonic point (r_s, n_s) of the flow is a point on the phase space satisfying the condition*

$$\left.\frac{v^2}{v_s^2}\right|_{(r_s, n(r_s))} = 1, \tag{7.32}$$

where $n_s = n(r_s)$.

Sonic point and critical point

The static observer $u_o = f^{-1/2}\partial_t$ measures the squared fluid 3-velocity v^2 by

$$\frac{1}{1-v^2} = \left(g_{ab}u^a u_o^b\right)^2 \tag{7.33}$$

which gives

$$v^2 = \frac{\mu^2}{\mu^2 + f r^{2(D-2)} n^2}. \tag{7.34}$$

Let us calculate explicitly one of the conditions for the critical point Eq. (7.27a):

$$\begin{aligned} 0 &= \partial_n F_\mu \\ &= \frac{2h^2}{n}\frac{\mu^2}{r^{2(D-2)}n^2}\left(v_s^2(n)\left[1 + f\frac{r^{2(D-2)}n^2}{\mu^2}\right] - 1\right) \end{aligned} \tag{7.35}$$

where $v_s^2(n) := \partial \ln h / \partial \ln n$ is the sound speed. We can see that the sound speed can be always written as

$$v_s^2(n) = \frac{\mu^2}{\mu^2 + f r^{2(D-2)} n^2} \tag{7.36}$$

on the points (r, n) satisfying the condition Eq. (7.27a) including the critical point. Conversely, if Eq. (7.36) is satisfied on a given point (r, n), the condition Eq. (7.27a) holds. From this fact and Eqs. (7.34) and (7.36), we can show that a sonic point of a physically acceptable transonic flow is identified with a critical point of saddle type as follows.

Consider a physical transonic fluid flow which is specified by the solution curve $n = n(r)$. From Definition 7.2.1 and Eq. (7.34), the sonic point (r_s, n_s) is determined by

$$v_s^2\left(n(r_s)\right) = \frac{\mu^2}{\mu^2 + fr^{2(D-2)}n^2(r_s)} \tag{7.37}$$

and $n_s = n(r_s)$. Since Eq. (7.37) implies that the point (r_s, n_s) satisfies Eq. (7.36), the condition $\partial_n F_\mu(r_s, n_s) = 0$ also holds as mentioned below Eq. (7.36). Then we have the following three cases concerning the sonic point (r_s, n_s):

1. $\partial_r F_\mu(r_s, n_s) \neq 0$ (i.e., the sonic point is not a critical point).
2. $\partial_r F_\mu(r_s, n_s) = 0$ (i.e., the sonic point is a critical point due to the fact $\partial_n F_\mu(r_s, n_s) = 0$).
   (a) The corresponding critical point is of saddle type.
   (b) The corresponding critical point is of extremum type.

In the case 1, the curve $n = n(r)$ typically gets double-valued (so unphysical) at least around (r_s, n_s) locally because $dn/dr = -\partial_r F_\mu(r_s, n_s)/\partial_n F_\mu(r_s, n_s) = \pm\infty$ there from Eq. (7.26). Another possibility with diverging density gradient, which is physically acceptable, is a transonic shock. In the current paper, we require the finite density gradient, $|dn/dr| < \infty$, as one of the conditions of a physical flow, thus excluding a transonic shock. Therefore the case 1 is not allowed for the physical flow $n = n(r)$ and the sonic point must be a critical point. However, the case 2b is also excluded because any solution curve, being a level curve of $F_\mu(r, n)$ originally, cannot pass the critical point of extremum type. Then we have only the case 2a for the sonic point (r_s, n_s) of the physically acceptable transonic flow $n = n(r)$. As a consequence, we have the following theorem:

Theorem 7.2.2. *For a physical transonic fluid flow which is stationary and spherically, planar or hyperbolically symmetric on the spacetime (7.1), its sonic point coincides with a critical point of saddle type on the phase space.*

We can interpret a critical point of saddle type as a sonic point of some transonic flow which is physically acceptable at least in the vicinity of the point on the phase space (r, n).

7.3 SP/PS correspondence

In this section, we analyze a critical point of radiation fluid flow and, as the main result of the current paper, prove Theorem 7.0.1.

7.3.1 Critical point of radiation fluid flow

We derived the EOS of radiation (ideal photon gas) in arbitrary spatial dimensions d in Eq. (5.41) of Chap. 5. It is given by

$$h(n) = \frac{k\gamma}{\gamma - 1} n^{\gamma - 1}, \tag{7.38}$$

where the index γ is related to the dimension by $\gamma = (d+1)/d$. The sound speed $v_s^2(n)$ is then computed as

$$v_s^2(n) := \frac{\partial \ln h}{\partial \ln n} = \gamma - 1 = \frac{1}{d} = \frac{1}{D-1}. \tag{7.39}$$

For the conditions of the critical point (r_c, n_c) and its classification for radiation flow, we have the following lemma:

Lemma 7.3.1. *For radiation fluid flow in our accretion problem Eq. (7.25), radius r_c of a critical point is specified by*

$$(fr^{-2})' = 0 \tag{7.40}$$

and the corresponding critical density n_c is

$$n_c = |\mu| \sqrt{\frac{2(D-2)}{r_c^{2D-3} f_c'}}. \tag{7.41}$$

The type of the critical point is classified by the inequality,

$$\textit{saddle (extremum) point} \Leftrightarrow \left(fr^{-2}\right)''_{r=r_c} < 0 \ (> 0). \tag{7.42}$$

Proof. Substituting the sound speed of radiation fluid, Eq. (7.39), into Eq. (7.31), the condition for the critical radius r_c is given by

$$\mathcal{F}_\mu = -\frac{D-2}{D-1} \frac{1}{f' r^{-2}} \left(fr^{-2}\right)' = 0. \tag{7.43}$$

Therefore, the critical radius is specified by Eq. (7.40). Once the radius r_c is obtained, we get the corresponding number density n_c from Eq. (7.31) which gives Eq. (7.41). With the use of Eq. (7.40), the left-hand side (LHS) of the classification condition of a critical point, Eq. (7.30), is written as

$$\mathcal{F}_\mu'(r_c) = -\frac{D-2}{D-1} \frac{1}{f' r^{-2}} \left(fr^{-2}\right)'' \tag{7.44}$$

and we immediately obtain Eq. (7.42). Note that $f' = 2f/r > 0$ at $r = r_c$ from Eq. (7.40). □

7.3.2 Proof of theorem: SP/PS correspondence

The conditions of the critical radius r_c and its classification in Lemma coincide with the conditions of the radius of the constant-r photon surface and its stability in Proposition 7.1.2 and 7.1.3, respectively. Then we immediately obtain the following proposition about the correspondence between constant-r photon surfaces and critical points of radiation fluid flow:

Proposition 7.3.2. *A critical point of radiation fluid flow in our accretion problem (7.25) exists at a radius r if and only if the spacetime Eq. (7.1) has a constant-r photon surface S_r at the radius. If the constant-r photon surface S_r is stable, the critical point is of a saddle type while if unstable, it is of an extremum type.*

There is a one-to-one correspondence between critical points of radiation fluid flow and constant-r photon surfaces. It is worth noting that if the spacetime has more than one constant-r photon surfaces, the stable and unstable photon surfaces appear alternately as we can see from Eqs. (7.40) and (7.42). The fact also leads to the alternate appearance of the corresponding extremum and saddle points on the phase space (r, n).

Then Theorem 7.2.2 and Proposition 7.3.2 above immediately prove Theorem 7.0.1.

For a sonic point (r_c, n_c), the surface of the constant radius r_c is sometimes referred to as *sonic surface*. In this view point, Theorem 7.0.1 also states that the sonic surface coincides with (one of) the photon surface(s).

7.4 Summary

We have investigated photon surfaces of constant radius and their stability in the spacetime (7.1). In spite of the different spatial geometries, spherical, planar and hyperbolic symmetry, their conditions in Propositions 7.1.2 and 7.1.3 have been found to be exactly the same. In other words, they are independent of the function $s(\chi)$ which depends on the spatial symmetry of the spacetime according to Eq. (7.2). This fact comes from that a photon surface is a structure of spacetime characterized by its second fundamental form and, in the cases we have investigated, the second fundamental forms of the hypersurfaces take the same form irrelevant to the spatial symmetry in the tetrad frame.

We have formulated the accretion problem of stationary radial fluid flow which is also spatially symmetric depending on the spatial symmetry of the spacetime, Eq. (7.2). It has been revealed that the master equation (7.25) does not depend on the spatial symmetry explicitly. Therefore we have applied the dynamical system analysis to the problem and obtained the same results about the critical points and the sonic points as the spherical case in Chap. 5.

Together with the results of the photon surfaces and the sonic points, we have proved the main theorem of this chapter, Theorem 7.0.1, which states the correspondence between sonic points of radiation fluid flow and *photon surfaces*. This is the extension of the theorem for the SP/PS correspondence in spherically symmetric spacetime in Chap. 5 to non-spherically symmetric spacetime of the same degrees of symmetry.

The main theorem has many implications which answers our questions about the SP/PS correspondence. In Chaps. 5 and 6, we have found that there always exits a correspondence between sonic points and photon spheres in the spherically symmetric spacetime for the radial and rotational flow. However, it has been unclear which the aspects of photon spheres are responsible to the correspondence. In this chapter, from the correspondence between sonic points and *photon surfaces*, we can conclude that the umbilicity of the hypersurfaces plays the most important role, or possibly, is needed in the correspondence. Furthermore, the sphericity of the surface, the positivity of the intrinsic curvature and the closed spatial topology are not necessary for the correspondence. We can also infer that the correspondence will occur caused by the local geometrical structure and the extrinsic structure of the hypersurfaces rather than the global structure and the intrinsic structure. Since the correspondence seems to originate from the microscopic construction of radiation fluid, our new result may suggest that transonic fluid flows generally have their sonic points only at points where the geometry has some special structures and the special structures are characterized by the geodesic motions of the particles which constitute the fluid.

Since sonic points, or sonic surfaces, coincide with photon surfaces rather than photon spheres, it would be better to read "the SP/PS correspondence" as "the sonic point/*photon surface* correspondence."

The further investigation of the correspondence in a general setting is given in Ref. [44]. In the work, it has been concluded that the assumptions of the symmetry is essential for this correspondence to realize. Actually, the degrees of the symmetry of the system in this chapter is exactly the same as those in Chap. 5. Similarly, it has been also proved that the rotational extension of this chapter indeed holds, as the spherical case in Chap. 5 has been extended to the rotational case in Chap. 6. See Ref. [44] for the details.

Chapter 8

Photon surfaces as pure tension shells/branes: uniqueness of thin shell wormholes

Originally published as:
Y. Koga, *Phys. Rev. D* **101** (2020) 104022.

A wormhole spacetime is a spacetime having two different asymptotic regions and a throat connecting them. The structure enables us to travel from our universe to another universe. A hole connecting two regions of our universe as a shortcut is also called wormhole. The wormhole solutions to general relativity (GR) and the modified theories of GR have been provided by the many authors [45, 46, 47] (see also [48] and the citation therein). The uniqueness of wormholes has been proved for Einstein-phantom scalar theory [49, 48, 50]. One of the most important properties of wormholes is that they necessarily violate the energy conditions, which makes it difficult to construct physically reasonable wormhole spacetimes [51, 52].

For the construction of *thin shell wormholes*, Visser proposed a mathematical procedure consisting of truncation and gluing of two spacetimes [53]. By the truncation, inner regions of the two spacetimes are removed and the resulting spacetimes become manifolds with the inner boundaries. By gluing the two spacetimes along the inner boundaries, we obtain a wormhole spacetime with two distinct asymptotic regions divided by the joint hypersurface. Through the junction conditions [54, 25] imposed on the hypersurface, the curvature singularity due to the gluing is interpreted as an infinitesimally thin matter distribution along it. The matter is called *a thin shell* and corresponds to the throat of the thin shell wormhole.

Barcelo and Visser [55] investigated four-dimensional thin shell wormholes consisting of two isometric, static and spherically symmetric spacetimes joined at the same radii and found that the radii of the throats coincide with those of photon spheres. Subsequently, Kokubu and Harada [56] extended the analysis to arbitrary dimensions of spacetime and the field equations with the cosmological constant. From their analysis, we can also find

the coincidence of the throats and photon spheres. The key features of those models are that (1) the wormhole spacetimes are Z_2-symmetric across their throats and (2) the thin shells on the throats have pure tension surface stress energy tensors.

In this chapter, we see that any joined spacetime which is Z_2-symmetric across the shell having pure tension surface stress energy tensor has the coincidence shown in Ref. [55] if it is Λ-vacuum. That is, for any Z_2-symmetric Λ-vacuum spacetime joined by a pure tension shell, the glued inner boundaries of the two original spacetimes must be photon surfaces. We call such a joined spacetime Z_2-symmetric pure-tensional joined spacetime (Z2PTJST). Not only the thin shell wormholes but also the brane world models by Randall and Sundrum [57, 58] and baby universes [53, 55] are in the class of Z2PTJST. The theorem we prove allows us to construct Z2PTJSTs from any Λ-vacuum spacetime having a photon surface.

This chapter is organized as follows. In Sec. 8.1, we define a *joined spacetime* (JST) and review Israel's junction conditions, which are the field equations that joined spacetimes have to satisfy in addition to the Einstein equation. In Sec. 8.2, we define the Z_2-symmetry of a JST and see that it reduces the junction conditions to simple forms. In Sec. 8.3, we define a *pure-tensional joined spacetime* (PTJST) and establish one of our main theorems, the coincidence between a pure-tensional shell and a photon surface of a Z2PTJST. In Sec. 8.4, we analyze the stability of the JST against perturbations of the shell preserving the Z_2-symmetry and find the stability also coincides with the stability of the corresponding photon surfaces. In Sec. 8.5, we establish the uniqueness theorem of Z_2-symmetric pure-tensional wormholes, i.e., the wormhole cases of Z2PTJST, applying the uniqueness theorem of photon spheres by Cederbaum [11] to the JST. Section. 8.6 is devoted to the conclusion. We suppose that manifolds and fields on them are smooth and the spacetimes are $(d+1)$-dimensional with $d \geq 2$ if it is not mentioned particularly.

8.1 Joined spacetime

We consider joining two spacetimes $(M_\pm, g_\pm)$ along their inner boundaries $\Sigma_\pm$. The resulting spacetime $(\mathcal{M}, g, \Sigma)$ with the hypersurface Σ corresponding to the joined boundaries $\Sigma_\pm$ is called a joined spacetime. The procedure for constructing the manifold $\mathcal{M}$ consists of *truncation* and *gluing* of $M_\pm$. We also introduce the field equations interpreted as Einstein equation for $(\mathcal{M}, g, \Sigma)$.

8.1.1 Truncation and gluing of manifolds

Let $M_\pm$ be manifolds with hypersurfaces $\Sigma_\pm$ which partition $M_\pm$ into two regions $M_\pm^{\rm ex}$ and $M_\pm^{\rm in}$ and assume $\Sigma_\pm$ are diffeomorphic. Truncating $M_\pm$ along $\Sigma_\pm$, we obtain the manifolds $\bar{M}_\pm := M_\pm \setminus M_\pm^{\rm in}$ with the inner boundaries $\Sigma_\pm$. Gluing $\bar{M}_\pm$ along $\Sigma_\pm$, i.e. identifying $\Sigma_\pm$ by a diffeomorphism $\psi : \Sigma_+ \to \Sigma_-$, we construct a new manifold $\mathcal{M}$ [53]. $\mathcal{M}$ is a manifold such that a hypersurface Σ partitions it into two regions corresponding to $M_\pm^{\rm ex}$.

The gluing also induces tensor fields on $\mathcal{M}$ from $M_\pm$. As we see below, we are

concerned with *a tensor distribution* and *jump of tensor fields* on $\mathcal{M}$ across Σ. Their values on Σ are given by summations of each the tensor fields of $M_\pm$ on $\Sigma_\pm$. To deal with the summations, we need to specify the diffeomorphism which identifies the tangent bundles $T_{\Sigma_\pm}M_\pm$ of $M_\pm$ on $\Sigma_\pm$. Since ψ induces the diffeomorphism $\psi^* : T\Sigma_+ \to T\Sigma_-$ of the tangent bundles $T\Sigma_\pm$ of $\Sigma_\pm$, it is sufficient to specify the diffeomorphism $\psi_N : N\Sigma_+ \to N\Sigma_-$ of the normal bundles $N\Sigma_\pm = T_{\Sigma_\pm}M_\pm/T\Sigma_\pm$ of $\Sigma_\pm$. Given metrics $g_\pm$ on $M_\pm$, it is natural to require

$$\psi_N : N_+ \mapsto N_- \tag{8.1}$$

for the unit normal vector fields $N_\pm \in N\Sigma_\pm$ of $\Sigma_\pm$ which are given so that $g_\pm(N_\pm, N_\pm) = 1$ and N_+ and N_- points inside $M_+^{\rm ex}$ and $M_-^{\rm in}$, respectively. The requirement is frequently seen in, for example, [25, 55, 56].

Then, in the current paper, we express the gluing by

$$\mathcal{M} = \bar{M}_+ \cup_{\psi,\psi_N} \bar{M}_-, \tag{8.2}$$

which is characterized by the diffeomorphisms ψ and ψ_N above. Note that ψ and ψ_N are dependent. The projections of $N\Sigma_\pm$ to $\Sigma\pm$ give ψ from ψ_N. Note also that we have denoted $M_\pm^{\rm ex}$ as the regions we keep for convenience. We can exchange the roles of the exterior regions $M_\pm^{\rm ex}$ and the interior regions $M_\pm^{\rm in}$ freely. See Fig 8.1 for the picture of the construction of $\mathcal{M}$.

8.1.2 Tensor distribution

Let l be a smooth function in the neighborhood of Σ in $\mathcal{M}$ satisfying $l = 0$ on Σ, $l > 0$ on M_+, and $l < 0$ on M_-. *The tensor distribution* T on $\mathcal{M}$ of tensors $T_\pm$ on $M_\pm$ is defined by

$$T = \Theta(l)T_+ + \Theta(-l)T_- \tag{8.3}$$

where $\Theta(l)$ is Heaviside distribution,

$$\Theta(l) = \begin{cases} 1 & (l > 0) \\ 1/2 & (l = 0) \\ 0 & (l < 0). \end{cases} \tag{8.4}$$

The metric g on $\mathcal{M}$ is defined as the distribution,

$$g = \Theta(l)g_+ + \Theta(-l)g_-. \tag{8.5}$$

8.1.3 Definition

According to the discussion above, we define *the joined spacetime (JST)* constructed from the spacetimes $(M_\pm, g_\pm)$ as follows.

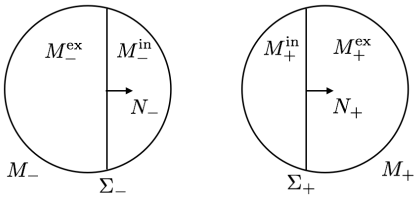

(a) Two manifolds $M_\pm$

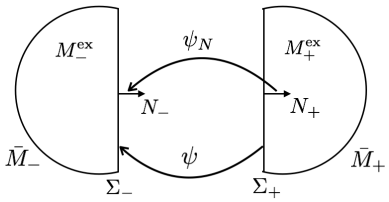

(b) Truncation and gluing along $\Sigma_\pm$

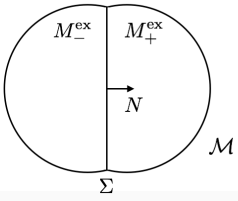

(c) Resulting manifold $\mathcal{M}$

Figure 8.1: (a) Two manifolds $M_\pm$ partitioned by the hypersurfaces $\Sigma_\pm$ are (b) truncated and glued along $\Sigma_\pm$ (identified at $\Sigma_\pm$) by ψ and ψ_N. (c) The resulting manifold $\mathcal{M}$ possesses the regions $M_\pm^{\text{ex}}$ partitioned by Σ.

Definition 8.1.1 (Joined spacetime)**.** *A triple $(\mathcal{M}, g, \Sigma)$ of a manifold $\mathcal{M}$, a metric g, and a hypersurface Σ is called a joined spacetime constructed from $(M_\pm, g_\pm)$ if the hypersurfaces $\Sigma_\pm$ partitioning $(M_\pm, g_\pm)$ into $M_\pm^{\text{in}}$ and $M_\pm^{\text{ex}}$ are timelike and*

$$\mathcal{M} = \bar{M}_+ \cup_{\psi,\psi_N} \bar{M}_-, \tag{8.6}$$
$$\Sigma = \Sigma_+ \equiv \Sigma_-, \tag{8.7}$$
$$g = \Theta(l) g_+ + \Theta(-l) g_-, \tag{8.8}$$

where the diffeomorphisms

$$\psi : \Sigma_+ \to \Sigma_-, \tag{8.9}$$
$$\psi_N : N_+ \mapsto N_- \tag{8.10}$$

are the identifications of $\Sigma_\pm$ and $N\Sigma_\pm$, respectively. Σ is called the shell of the joined spacetime.

8.1.4 Einstein equations

The distribution g of $(\mathcal{M}, g, \Sigma)$ may not be smooth across Σ. Israel's junction conditions [54, 25], which we assume on g on Σ, are motivated from Einstein equation. Here we consider the system consisting of Einstein equation and the junction conditions for joined spacetimes. We call the system *Einstein equations*.

Definition 8.1.2 (Einstein equations)**.** *A joined spacetime $(\mathcal{M}, g, \Sigma)$ is said to satisfy Einstein equations if $(\bar{M}_\pm, g_\pm)$ satisfy Einstein equation and the first junction condition Eq. (8.11), the second junction condition Eq. (8.14), and the equation of motion (EOM) of the shell Eq. (8.16) in the following are satisfied on Σ.*

First junction condition

Israel's first junction condition requires the induced metrics $h_\pm$ of $\Sigma_\pm$ to equal. It is expressed as,

$$[h] = 0 \tag{8.11}$$

where $[A]$ is the jump of tensor fields $A_\pm$ of $M_\pm$ across Σ,

$$[A] := A_+|_{\Sigma_+} - A_-|_{\Sigma_-} . \tag{8.12}$$

Note that the condition together with the gluing condition, Eq. (8.10), implies

$$[g] = 0. \tag{8.13}$$

Thus, the first junction condition for a joined spacetime $(\mathcal{M}, g, \Sigma)$ guarantees the continuity of the metric distribution g across Σ [25].

Second junction condition

The distribution g may not be smooth across Σ and the curvature, the second derivative of g, can be singular there. The second junction condition is what relates such singularity on Σ to the infinitesimally thin matter distribution on the hypersurface. In the presence of the singular terms in Einstein tensor distribution, Einstein equation leads to

$$-\frac{1}{8\pi}\left([\chi] - [\theta]\, h\right) = S \tag{8.14}$$

where $\chi_\pm$ is the second fundamental form of $\Sigma_\pm$ in $M_\pm$ with respect to $N_\pm$, $\theta_\pm$ is the trace of $\chi_\pm$, h is the induced metric on Σ given by $h(X, Y) = g(X, Y)\ \forall X, Y \in T\Sigma$, and S is the surface stress energy tensor of the matter on Σ [25]. This is called *Israel's second junction condition*.

The corresponding stress energy tensor T_Σ of the shell as the matter on $(\mathcal{M}, g, \Sigma)$ is given by,

$$T_\Sigma = \delta(l)\Phi^*(S). \tag{8.15}$$

where $\Phi^* : T_p\Sigma \to T_{\Phi(p)}\mathcal{M}$ is the push forward associated with the embedding $\Phi : \Sigma \to \mathcal{M}$ and $\delta(l)$ is the delta function, or Dirac distribution. As a physical interpretation, Σ

with S is called *a thin shell*. Eq. (8.14) is equivalent to the ordinary Einstein equation with the stress energy tensor T_Σ. Therefore, the brane world models can be regarded as joined spacetimes [57, 58]. See [53] for the details of the interpretation.

If $S = 0$, i.e. $[\chi] = 0$, Christoffel symbols are continuous across Σ and Riemann curvature has no singular terms [25].

EOM of the shell

From Einstein equation, the surface stress energy tensor S of the shell satisfies a conservation law on Σ as ordinary matter does in $\mathcal{M}$. It is given by,

$$\nabla^h \cdot S + [T_N] = 0, \tag{8.16}$$

where ∇^h is the covariant derivative associated with h, $\nabla^h \cdot S$ represents the divergence $\nabla^{h\,b} S_{ab}$, and $T_{N\pm}$ is given by $T_{N\pm a} := T_{\pm\mu\nu} e^\mu_a N^\nu_\pm$. Here the indices $a, b...$ denote those of the coordinate system $\{\xi^a\}$ on Σ and the coordinate basis $\{e^\mu_a\}$ is given by $e^\mu_a = \partial x^\mu / \partial \xi^a$ with respect to the embedding of Σ, $x^\mu(\xi^a)$ [25, 59].

8.2 Z_2-symmetry of a joined spacetime

We focus on a Z_2-symmetric joined spacetime (Z2JST). The Z_2-symmetry is the reflection symmetry across Σ of a joined spacetime $(\mathcal{M}, g, \Sigma)$ across Σ.

8.2.1 Definition

We define the Z_2-symmetry of a joined spacetime as follows.

Definition 8.2.1 (Z_2-symmetric joined spacetime)**.** *A joined spacetime $(\mathcal{M}, g, \Sigma)$ constructed from $(M_\pm, g_\pm)$ is said to be Z_2-symmetric across Σ if there exists an isometry $\phi : (M_+, g_+) \to (M_-, g_-)$ such that*

$$\phi|_{\Sigma_+} : \Sigma_+ \to \Sigma_-, \tag{8.17}$$
$$\phi|_{\Sigma_+} = \psi, \tag{8.18}$$
$$\phi^* : N_+ \mapsto -N_-, \tag{8.19}$$

where $\phi|_{\Sigma_+}$ is the restriction of ϕ to Σ_+, $\psi : \Sigma_+ \to \Sigma_-$ is the diffeomorphism in Eq. (8.9) in Definition 8.1.1, and $\phi^* : TM_+ \to TM_-$ is the map induced from ϕ.

The condition Eq. (8.19) together with Eq. (8.17) implies $\phi : M^{\rm ex}_+ \to M^{\rm ex}_- : M^{\rm in}_+ \to M^{\rm in}_-$. The picture of the definition is shown in Fig 8.2. For the validity of Definition 8.2.1, see Appendix B.

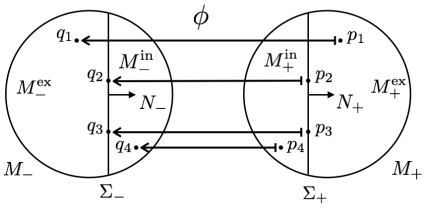

(a) Isometry ϕ

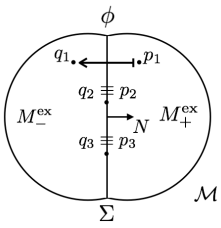

(b) ϕ acting on $\mathcal{M}$

Figure 8.2: (a) Points $p_1, p_2, ... \in M_+$ in the regions $M_+^{\rm in}$, $M_+^{\rm ex}$, and Σ_+ are mapped by the isometry ϕ to $q_1, q_2, ... \in M_-$ in the corresponding regions $M_-^{\rm in}$, $M_-^{\rm ex}$, and Σ_-, respectively. (b) After the truncation and gluing of $M_\pm$, ϕ acts on $\mathcal{M}$ as the reflection across Σ with the fixed points $p_1 \equiv q_1, p_2 \equiv q_2 \in \Sigma$, which have been identified by $\psi = \phi|_{\Sigma_+}$.

8.2.2 Junction conditions under the Z_2-symmetry

The Z_2-symmetry of a joined spacetime simplifies the junction conditions.

Proposition 8.2.2. *Let $(\mathcal{M}, g, \Sigma)$ be a Z2JST. Then, the first junction condition,*

$$[h] = 0, \tag{8.20}$$

is satisfied and the second junction condition reduces to

$$-\frac{1}{4\pi}(\chi - \theta h) = S, \tag{8.21}$$

where $\chi := \chi_+ = -\chi_-$ and θ is the trace of χ.

Proof. Let $X, Y \in T\Sigma_\pm$ be arbitrary vectors which are identical under the isometry ϕ, i.e. the map $\phi^* : TM_+ \to TM_-$ induced from ϕ maps the vectors as $X \mapsto X$, $Y \mapsto Y$. Note that the map ϕ^* is also regarded as the map of any types of tensors [21]. The induced metrics $h_\pm(X, Y) := g_\pm(X, Y)$ are mapped as

$$h_+(X, Y) = g_+(X, Y) \mapsto g_-(X, Y) = h_-(X, Y) \tag{8.22}$$

by ϕ^*. The second fundamental forms $\chi_\pm(X, Y) := (\nabla_\pm n_\pm)(X, Y)$ are mapped as

$$\chi_+(X, Y) = (\nabla_+ n_+)(X, Y) \mapsto (\nabla_- \phi^*(n_+))(X, Y) = -(\nabla_- n_-)(X, Y) = -\chi_-(X, Y). \tag{8.23}$$

by ϕ^*, where $\nabla_\pm$ are the covariant derivatives associated with $g_\pm$ and $n_\pm = g_\pm(N_\pm, \cdot)$ are the normal 1-forms dual to $N_\pm$, which are mapped as $\phi^* : n_+ = g_+(N_+, \cdot) \mapsto g_-(-N_-, \cdot) = -n_-$ from Eq. (8.19). Since $h_\pm$ and $\chi_\pm$ are tensors of $\Sigma_\pm$, i.e. tensors taking the values on the space $T\Sigma_\pm \otimes T\Sigma_\pm$, we can regard Eqs. (8.22) and (8.23) as the mapping induced from $\phi|_{\Sigma_+}$ rather than ϕ due to Eq. (8.17). That is, the map $(\phi|_{\Sigma_+})^* : T\Sigma_+ \to T\Sigma_-$ induced from $\phi|_{\Sigma_+}$ is a map such that

$$(\phi|_{\Sigma_+})^* : h_+ \mapsto h_- \tag{8.24}$$
$$: \chi_+ \mapsto -\chi_-. \tag{8.25}$$

Therefore, from Eq. (8.18), we have

$$\psi^* : h_+ \mapsto h_- \tag{8.26}$$
$$: \chi_+ \mapsto -\chi_- \tag{8.27}$$

for the map $\psi^* : T\Sigma_+ \to T\Sigma_-$ induced from ψ. This means $h_+ = h_-$ and $\chi_+ = -\chi_-$ on Σ since ψ^* is the identification. Then the first junction condition,

$$[h] = h_+ - h_- = 0, \tag{8.28}$$

is satisfied. The second fundamental form and its trace satisfy

$$[\chi] = \chi_+ - \chi_- = 2\chi_+, \tag{8.29}$$
$$[\theta] = \theta_+ - \theta_- = 2\theta_+. \tag{8.30}$$

Defining $\chi := \chi_+$ and $\theta := \mathrm{Tr}(\chi)$, the second junction condition reduces to

$$S = -\frac{1}{8\pi}([\chi] - [\theta]h) = -\frac{1}{4\pi}(\chi - \theta h). \tag{8.31}$$

□

8.3 Pure-tensional joined spacetime

Here, we define *a pure-tensional joined spacetime (PTJST)*. After reviewing photon surfaces, we prove that the shell of the spacetime coincides with a photon surface of the original spacetimes.

8.3.1 Definition

A thin shell having pure-trace stress energy tensor is called *a pure tension shell*. We consider a Λ-vacuum joined spacetime with a pure tension shell in the following.

Definition 8.3.1 (Pure-tensional joined spacetime)**.** *Let $(\mathcal{M}, g, \Sigma)$ be a joined spacetime constructed from $(M_\pm, g_\pm)$. Let S be the surface stress energy tensor of Σ and $T_\pm$ be*

the stress energy tensors of $(M_\pm, g_\pm)$*. The joined spacetime* $(\mathcal{M}, g, \Sigma)$ *is called a pure-tensional joined spacetime if* $(\mathcal{M}, g, \Sigma)$ *satisfies Einstein equations with the conditions,*

$$S = -\epsilon h, \tag{8.32}$$

$$T_\pm = -\frac{\Lambda_\pm}{8\pi} g_\pm \tag{8.33}$$

where $\epsilon : \Sigma \to \mathbb{R}$ *is the tension of the shell* Σ*,* h *is the induced metric on* Σ*, and* $\Lambda_\pm$ *are the cosmological constants of* $(M_\pm, g_\pm)$*.* Σ *is called the pure tension shell of* $(\mathcal{M}, g, \Sigma)$*.*

8.3.2 Photon surface in Λ-vacuum

A photon surface we reviewed in Chap. 3 has a geometrical equivalent condition for a timelike hypersurface to be a photon surface. The theorem proved by Claudel *et al.* [8] and Perlick [9] can also be expressed as follows.

Theorem 8.3.2 (Claudel *et al.* (2001), Perlick (2005))**.** *Let* S *be a timelike hypersurface of spacetime* (M, g) *with* $d + 1 := \dim M \geq 3$*. Let* h*,* χ*, and* θ *be the induced metric, the second fundamental form, the trace of* χ*, respectively. Then* S *is a photon surface if and only if it is totally umbilic, i.e.*

$$\chi = \frac{\theta}{d} h \quad \forall p \in S. \tag{8.34}$$

The following proposition for a photon surface in a Λ-vacuum spacetime is also crucial for our main theorem for PTJSTs.

Proposition 8.3.3 (Photon surfaces in Λ-vacuum)**.** *Let* (M, g) *be a* Λ*-vacuum spacetime with* $\dim M \geq 3$*. Then, a timelike photon surface* S *of* (M, g) *is constant mean curvature (CMC).*

Proof. Let n^μ, $h_{\mu\nu} = g_{\mu\nu} - n_\mu n_\nu$, and $\chi_{\mu\nu}$ be the unit normal vector, the induced metric, and the second fundamental form of S, respectively. From the Codazzi-Mainardi equation, we have

$$\begin{aligned} R_{\mu\alpha\nu\beta} h^\mu_\rho h^\alpha_\gamma h^\nu_\sigma n^\beta &= \nabla^h_\rho \chi_{\gamma\sigma} - \nabla^h_\gamma \chi_{\rho\sigma} \\ &= \frac{1}{d}\left[\left(\nabla^h_\rho \theta\right) h_{\gamma\sigma} - \left(\nabla^h_\gamma \theta\right) h_{\rho\sigma}\right] \end{aligned} \tag{8.35}$$

where d is the dimension of S, $\theta = h^{\rho\gamma}\chi_{\rho\gamma}$ is the mean curvature, and ∇^h_ρ is the covariant derivative on S associated with $h_{\rho\gamma}$. We have used Theorem 8.3.2 in the last equality. Contracting with $h^{\gamma\sigma}$, the equation reduces to

$$h^{\gamma\sigma} R_{\mu\alpha\nu\beta} h^\mu_\rho h^\alpha_\gamma h^\nu_\sigma n^\beta = -R_{\mu\beta} h^\mu_\rho n^\beta = \frac{d-1}{d} \nabla^h_\rho \theta. \tag{8.36}$$

From that (M, g) is Λ-vacuum, i.e. $R_{\mu\nu} = [2/(d-1)]\Lambda g_{\mu\nu}$ for some constant Λ, we have

$$\nabla^h_\rho \theta = 0. \tag{8.37}$$

Therefore, $\theta =$ const. along S and S is CMC. □

See also Proposition 3.3 in [11] for general totally umbilic hypersurfaces.

8.3.3 Photon surfaces as pure tension shells

The following theorem states about the coincidence of pure-tensional shells of joined spacetimes and photon surfaces.

Theorem 8.3.4 (Photon surface as a pure tension shell)**.** *Let* $(\mathcal{M}, g, \Sigma)$ *be a Z2JST constructed from* $(M_\pm, g_\pm)$ *with* $d+1 := \dim \mathcal{M} = \dim M_\pm \geq 3$*. Then* $(\mathcal{M}, g, \Sigma)$ *is a PTJST if and only if* $(\bar{M}_\pm, g_\pm)$ *are* Λ*-vacuum and* $\Sigma_\pm$ *are photon surfaces. The tension* ϵ *and the mean curvature* θ *of the shell* Σ *are constant and given by the relation* $\theta = \pm\theta_\pm = -4\pi[d/(d-1)]\epsilon$*.*

Proof. From the Z_2-symmetry of $(\mathcal{M}, g, \Sigma)$ and Proposition 8.2.2, the first junction condition is automatically satisfied and the second junction condition reduces to Eq. (8.21) where $\chi := \chi_+ = -\chi_-$ and $\theta := \mathrm{Tr}(\chi) = \theta_+ = -\theta_-$. Then the Einstein equations for $(\mathcal{M}, g, \Sigma)$ consist of the reduced second junction condition, Eq. (8.21), the EOM of the shell Σ, Eq. (8.16), and Einstein equation on $(\bar{M}_\pm, g_\pm)$. The induced metric on Σ is given by $h = h_+ = h_-$ due to the fact that the first junction condition is satisfied. In fact, $h(X,Y) := g(X,Y) = \frac{1}{2}(g_+(X,Y) + g_-(X,Y)) = \frac{1}{2}(h_+(X,Y) + h_-(X,Y)) = h_+(X,Y) = h_-(X,Y)\ \forall X, Y \in T\Sigma \equiv T\Sigma_\pm$.

We prove the "if" part. From that $(\bar{M}_\pm, g_\pm)$ are isometric and Λ-vacuum, the energy momentum tensors satisfy $T_\pm = -(\Lambda/8\pi)g_\pm$ for the common cosmological constant Λ and Eq. (8.33) in Definition 8.3.1 is satisfied. From Theorem 8.3.2, the photon surfaces $\Sigma_\pm$ give the conditions

$$\chi = \pm\chi_\pm = \frac{\pm\theta_\pm}{d} h_\pm = \frac{\theta}{d} h. \tag{8.38}$$

From Proposition 8.3.3, we have

$$\theta = \pm\theta_\pm = \text{const.} \tag{8.39}$$

The second junction condition Eq. (8.21) then reduces to

$$\frac{1}{4\pi}\frac{d-1}{d}\theta h = S. \tag{8.40}$$

Letting ϵ be a function on Σ given by

$$\epsilon = -\frac{1}{4\pi}\frac{d-1}{d}\theta, \tag{8.41}$$

the surface stress energy tensor becomes

$$S = -\epsilon h \tag{8.42}$$

and Eq. (8.32) in Definition 8.3.1 is satisfied. From Eqs. (8.39) and (8.41), we have $\nabla^h \epsilon = 0$ implying

$$\nabla^h \cdot S = 0. \tag{8.43}$$

Therefore, from the fact that $T_\pm = -(\Lambda/8\pi)g_\pm$, the EOM of the shell Σ, Eq. (8.16),

$$\nabla^h \cdot S + [T_N] = 0, \tag{8.44}$$

is satisfied. $(\mathcal{M}, g, \Sigma)$ is a joined spacetime satisfying Definition 8.3.1 of PTJST.

We prove the "only if" part. From Definition 8.3.1, the PTJST $(\mathcal{M}, g, \Sigma)$ satisfies $S = -\epsilon h$ and $T_\pm = -(\Lambda/8\pi)g_\pm$. Then $(\bar{M}_\pm, g_\pm)$ are Λ-vacuum and the second junction condition, Eq.(8.21), under Z_2-symmetry requires that

$$\chi = \chi_+ = -\chi_- \propto h, \tag{8.45}$$

i.e. $\Sigma_\pm$ are timelike totally umbilic hypersurfaces. From Theorem 8.3.2, $\Sigma_\pm$ are photon surfaces of $(\bar{M}_\pm, g_\pm)$.

From Eqs. (8.39) and (8.41), we finally obtain

$$\theta = \pm\theta = -4\pi\frac{d}{d-1}\epsilon = \text{const.} \tag{8.46}$$

for the PTJST. □

Theorem 8.3.4 applies to the Λ-vacuum cases of the thin shell wormholes investigated in [55, 56]. That is, the thin shell, or throats, of the wormholes correspond to photon surfaces. From the viewpoint of symmetry, the static throats are $\mathbb{R}\times SO(d)$, $\mathbb{R}\times E(d-1)$, and $\mathbb{R} \times SO(1, d-1)$-invariant photon surfaces depending on the symmetry of the spacetimes. The dynamical throats are $SO(d-1)$, $E(d)$, and $SO(d-2, 1)$-invariant photon surfaces.

The theorem states that two copies of any Λ-vacuum spacetime with a photon surface can be joined to give a Z2PTJST. For example, two copies of the Minkowski D-spacetime can be joined along either the hyperplane or the hyperboloid, which are shown to be photon surfaces in Examples 3.1.3 and 3.1.5. The spacetimes given by C-metrics can be joined along the photon surface shown in Example 3.1.7. If the regions outside the photon surfaces are joined, the resulting spacetime is "a uniformly accelerated wormhole". If the inside regions are joined, it is "a uniformly accelerating baby universe". The Z2PTJSTs constructed from the spacetimes given by Eq. 4.1 in Chap. 4 are the less-symmetric generalizations of the Λ-vacuum cases of the thin shell wormholes investigated in the works [55, 56]. These examples are shown in Sec. 8.3.4.

We can also confirm that the positive and negative branes of the brane world model by Randall and Sundrum [57, 58] are indeed located on the four-dimensional timelike photon surfaces of the five-dimensional bulk spacetime. It follows from the facts that the bulk spacetime is conformally transformed Minkowski spacetime and photon surfaces are invariant manifolds under conformal transformations as mentioned in Chap. 3 or in [8].

8.3.4 Examples

Theorem 8.3.4 states that two copies of any Λ-vacuum spacetime with a photon surface can be joined to give a Z2PTJST by truncating and gluing them along the photon surfaces. Here we show the examples of Z2PTJSTs constructed from the spacetimes investigated in Chaps. 3 and 4.

Example 8.3.5 (Minkowski spacetimes joined along planes)**.** *Example 3.1.3 shows that the hyperplane,*

$$S = \left\{x^{D-1} = 0\right\}, \tag{8.47}$$

is a photon surface of $\mathbb{M}^D$*. By truncating* $\mathbb{M}^D$ *along* S*, we obtain the incomplete Minkowski spacetime,*

$$\bar{\mathbb{M}}^D = \left\{x^{D-1} \geq 0\right\}. \tag{8.48}$$

We denote two copies of $\bar{\mathbb{M}}^D$ *and their coordinates by* $\bar{\mathbb{M}}^D_\pm$ *and* $\left\{x^0_\pm, ..., x^{D-1}_\pm\right\}$*, respectively. Redefining the coordinate of* $\bar{\mathbb{M}}^D_-$ *so that* $x^{D-1}_- \to -x^{D-1}_-$*, we have*

$$\bar{\mathbb{M}}^D_+ = \left\{x^{D-1}_+ \geq 0\right\}, \tag{8.49}$$

$$\bar{\mathbb{M}}^D_- = \left\{x^{D-1}_- \leq 0\right\}. \tag{8.50}$$

The boundaries due to the truncation are given by

$$\partial\bar{\mathbb{M}}^D_\pm = \left\{x^{D-1}_\pm = 0\right\}. \tag{8.51}$$

The unit normal vectors $N_\pm$ *to the boundaries* $\partial\bar{\mathbb{M}}^D_\pm$ *are given by*

$$N_\pm = \partial_{x^{D-1}_\pm}, \tag{8.52}$$

where we have determined the orientations by following the procedure for the truncation of manifolds in Sec. 8.1.1. We glue the two manifolds $\bar{\mathbb{M}}^D_\pm$ *by the indentification* $\psi : \partial\bar{\mathbb{M}}^D_+ \to \partial\bar{\mathbb{M}}^D_-$ *of the boundaries such that* $\partial\bar{\mathbb{M}}^D_+ \ni (x^0_+, ..., x^{D-2}_+, 0) \equiv (x^0_-, ..., x^{D-2}_-, 0) \in \partial\bar{\mathbb{M}}^D_-$ *and the indentification* $\psi_N : N_+ \mapsto N_-$ *of the normal vectors and obtain a new manifold* $\mathcal{M}$*. Then the metric distribution* $g = \Theta(l)\eta_+ + \Theta(-l)\eta_-$ *is induced on* $\mathcal{M}$*, where* $\eta_\pm$ *are the Minkowski metrics on* $\bar{\mathbb{M}}^D_\pm$ *and* l *is the smooth function on* $\mathcal{M}$ *introduced in Sec. 8.1.2, which takes the value* $\pm l \geq 0$ *on each region* $\bar{\mathbb{M}}^D_\pm$ *of* $\mathcal{M}$*. We define the global coordinates* $\left\{x^0, ..., x^{D-1}\right\}$ *of* $\mathcal{M}$ *by the identification* $\left\{x^0, ..., x^{D-1}\right\} = \left\{x^0_\pm, ..., x^{D-1}_\pm\right\}$ *on* $\bar{\mathbb{M}}^D_\pm$*. Then the regions* $\bar{\mathbb{M}}^D_\pm$ *of* $\mathcal{M}$ *correspond to* $\left\{\pm x^{D-1} \geq 0\right\}$ *and the hypersurface corresponding to the glued boundaries, i.e., the shell, is given by* $\Sigma = \left\{x^{D-1} = 0\right\}$*. Since the metrics* $\eta_\pm$ *on* $\bar{\mathbb{M}}^D_\pm$ *are now given by* $\eta_\pm = -(dx^0_\pm)^2 + (dx^1_\pm)^2 + \cdots + (dx^{D-1}_\pm)^2 = -(dx^0)^2 + (dx^1)^2 + \cdots + (dx^{D-1})^2$ *and the function* l *can be identified with* x^{D-1}*, the metric distribution* g *is given by*

$$g = \Theta(l)\eta_+ + \Theta(-l)\eta_- = \Theta(x^{D-1})\eta + \Theta(-x^{D-1})\eta = \eta \tag{8.53}$$

where $\eta = -(dx^0)^2 + (dx^1)^2 + \cdot + (dx^{D-1})^2$*. The resulting joined spacetime* $(\mathcal{M}, g, \Sigma)$ *is a Z2PTJST according to Theorem 8.3.4 and is trivially the Minkowski* D*-spacetime* $\mathbb{M}^D$*. Indeed, the mean curvatures* $\theta_\pm$ *of the photon surfaces* $S_\pm = \partial\bar{\mathbb{M}}^D_\pm$ *vanish and therefore, the energy of the thin shell vanishes,* $\epsilon = 0$*. The pure tension shell* Σ *at* $x^{D-1} = 0$ *is absent in this case.*

Example 8.3.6 (Minkowski spacetimes joined along hyperboloids)**.** *Example 3.1.5 shows that the hyperboloid,*

$$S = \left\{-t^2 + x_1^2 + \cdots + x_{D-1}^2 = a^2\right\}, \tag{8.54}$$

for a constant $a > 0$ is a photon surface of $\mathbb{M}^D$. By transforming the spatial coordinates $\{t, x_1, ..., x_{D-1}\}$ to the spherical coordinates $\{r, \theta_1, ..., \theta_{D-2}\}$, the further transformation given by $T = \text{arctanh}(t/r)$ and $R = \sqrt{r^2 - t^2}$ gives the expressions of the metric and the hyperboloid,

$$\eta = -R^2 dT^2 + dR^2 + R^2 d\Omega_{D-2}^2 \tag{8.55}$$

and

$$S = \{R = a\}, \tag{8.56}$$

respectively. Truncating $\mathbb{M}^D$ along S and removing the inside of S, we obtain the manifold,

$$\bar{\mathbb{M}}^D = \{R \geq a\}. \tag{8.57}$$

Two copies of $\bar{\mathbb{M}}^D$, denoted by $\bar{\mathbb{M}}^D_\pm$ with the coordinates $\left\{T_\pm, R_\pm, \theta_1^\pm, ..., \theta_{D-2}^\pm\right\}$, are given by

$$\bar{\mathbb{M}}^D_\pm = \{R_\pm \geq a\}. \tag{8.58}$$

The boundaries are given by

$$\partial\bar{\mathbb{M}}^D_\pm = \{R_\pm = a\}. \tag{8.59}$$

Before joining the manifolds, we introduce new radial coordinates $l_\pm$ by $R_\pm = \pm l_\pm + a$ so that we can smoothly introduce the global coordinates of the resulting joined spacetime. The new coordinates give

$$\eta_\pm = -(\pm l_\pm + a)^2 dT_\pm^2 + dl_\pm^2 + (\pm l_\pm + a)^2 d\Omega_{D-2,\pm}^2, \tag{8.60}$$

$$\bar{\mathbb{M}}^D_\pm = \{\pm l_\pm \geq 0\}, \tag{8.61}$$

$$\partial\bar{\mathbb{M}}^D_\pm = \{l_\pm = 0\}. \tag{8.62}$$

The unit normal vectors $N_\pm$ to $\partial\bar{\mathbb{M}}^D_\pm$ are given by

$$N_\pm = \partial_{l_\pm}. \tag{8.63}$$

Then the indentification $\psi : \partial\bar{\mathbb{M}}^D_+ \to \partial\bar{\mathbb{M}}^D_-$ of the boundaries given by $\partial\bar{\mathbb{M}}^D_+ \ni (T_+, l_+ = 0, ..., \theta_1^+, ..., \theta_{D-2}^+) \equiv (T_-, l_- = 0, ..., \theta_1^-, ..., \theta_{D-2}^-) \in \partial\bar{\mathbb{M}}^D_-$ and the identification $\psi_N : N_+ \mapsto N_-$ of the normal vectors give a new manifold $\mathcal{M}$. Defining the global coordinates $\{T, l, \theta_1, ..., \theta_{D-2}\}$ of $\mathcal{M}$ by the identification $\{T, l, \theta_1, ..., \theta_{D-2}\} = \left\{T_\pm, l_\pm, \theta_1^\pm, ..., \theta_{D-2}^\pm\right\}$ on $\bar{\mathbb{M}}^D_\pm$, the regions $\bar{\mathbb{M}}_\pm$ of $\mathcal{M}$ are given by $\bar{\mathbb{M}}^D_\pm = \{\pm l \geq 0\}$ and the shell is given by $\Sigma = \{l = 0\}$. Since the metrics of $\bar{\mathbb{M}}^D_\pm$ are now given by $\eta_\pm = -(|l| + a)^2 dT^2 + dl^2 + (|l| + a)^2 d\Omega_{D-2}^2$ for $\pm l \geq 0$, the metric distribution on $\mathcal{M}$ is given by

$$g = -(|l| + a)^2 dT^2 + dl^2 + (|l| + a)^2 d\Omega_{D-2}^2. \tag{8.64}$$

The resulting joined spacetime $(\mathcal{M}, g, \Sigma)$ is a Z2PTJST. The mean curvatures of the photon surfaces $S_\pm = \partial\bar{\mathbb{M}}^D_\pm$ of $\bar{\mathbb{M}}^D_\pm$ are $\theta_\pm = \pm(D-1)a^{-1}$. The tension of the pure tension shell is thus $\epsilon = -[(D-2)/(4\pi)]a^{-1}$.

Remark 8.3.7. *In Example 8.3.6, the timelike infinities has been removed from the original two spacetimes. Thus, the resulting Z2PTJST does not have timelike infinities corresponding to them. Although the Z2PTJST have two different null infinities corresponding to $\mathscr{I}_{\mathbb{M}_\pm}$, from the viewpoint of the causal structures, it should be distinguished from the thin shell wormholes obtained in [55, 56], which have the throats (shells) extended to the timelike infinities.*

Remark 8.3.8. *We have removed the inside of the hyperboloid S from the original spacetime $\mathbb{M}^D$ in Example 8.3.6. We can instead remove the outside and obtain another Z2PTJST by the same procedure with the opposite orientation of the unit normal vectors, $N_\pm$. The opposite orientation gives the flip of the sign of $\theta_\pm$ and hence ϵ. Note that, in that case, the coordinates $\{T, R, \theta_1, ..., \theta_{D-2}\}$ can cover only a part of the inside. Namely, the coordinates are valid in the region between the hyperboloid S, $R^2 = -t^2 + r^2 = a^2$, and the null cone, $R^2 = -t^2 + r^2 = 0$. One needs to introduce other patches or further transform the coordinates to cover the whole of the Z2PTJST.*

Example 8.3.9 (Joined C-metrics)**.** *The photon surface of the uniformly accelerated black hole spacetime, (M, g), with the metric (3.10) is given by*

$$S = \left\{ y = y_{\rm ph} := -\frac{1}{3mA} \right\} \tag{8.65}$$

as shown in Example 3.1.7. Since the spacetime is a Λ-vacuum solution to the Einstein equation, we can construct a Z2PTJST from two copies of it by the truncation and gluing along S. In the truncation, one can remove either the inside region, $y < y_{\rm ph}$, or outside region, $y > y_{\rm ph}$, from the two copies of (M, g). The former case gives "a uniformly accelerated wormhole" while the latter does to "a uniformly accelerated baby universe." In particular, the wormhole case corresponds to, in the zero-acceleration limit, the wormhole constructed from two copies of the Schwarzschild spacetime investigated in Ref. [55] and results in a characteristic causal structure due to the acceleration since the causal structure of the infinity of the spacetime with the C-metric drastically differs from that of the Schwarzschild spacetime. Letting $(M_\pm, g_\pm)$ be the spacetimes with the metrics $g_\pm$ given by Eq. (3.10) and $\{t_\pm, x_\pm, y_\pm, \phi_\pm\}$ be the corresponding coordinates, the truncated manifolds of $M_\pm$ for the wormhole case are given by

$$\bar{M}_\pm = \{ y_\pm \geq y_{\rm ph} \} . \tag{8.66}$$

By identifying the boundaries $\partial\bar{M}_\pm = \{y_\pm = y_{\rm ph}\}$ so that $(t_+, x_+, y_+ = y_{\rm ph}, \phi_+) \equiv (t_-, x_-, y_- = y_{\rm ph}, \phi_-)$, we obtain the Z2PTJST $(\mathcal{M}, g_{\rm dis}, \Sigma)$ where $g_{\rm dis}$ is the metric distribution and Σ is the shell given by $y_+ = y_- = y_{\rm ph}$. Transforming the radial coordinates $y_\pm$ of $\bar{M}_\pm$ to the new coordinates $l_\pm := \pm (y_\pm - y_{\rm ph})$ and identifying the coordinates $\{t, x, l, \phi\}$ of $\mathcal{M}$ with the coordinates $\{t_\pm, x_\pm, l_\pm, \phi_\pm\}$ of each region $\bar{M}_\pm$, we obtain the explicit form of the metric distribution,

$$g_{\rm dis} = \frac{1}{A^2 \left(x + |l| + y_{\rm ph} \right)^2} \left[-F\left(|l| + y_{\rm ph} \right) dt^2 + \frac{1}{F\left(|l| + y_{\rm ph} \right)} dl^2 + \frac{1}{G(x)} dx^2 + G(x) d\phi^2 \right] . \tag{8.67}$$

The shell Σ corresponding to the wormhole throat is given by $l = 0$. The stationary region, $-(y_1 - y_{\rm ph}) < l < y_1 - y_{\rm ph}$, which includes the throat, is surrounded by the two acceleration horizons, $l = \pm(y_1 - y_{\rm ph})$. The mean curvatures of the boundaries $\partial\bar{M}_\pm$ are given by $\theta_\pm = \pm(\sqrt{3}m)^{-1}$ and therefore, the tension of the thin shell is $\epsilon = -(6\sqrt{3}\pi m)^{-1}$. They do not depend on the parameter A of the acceleration.

Remark 8.3.10. *As shown in Refs. [10, 60], the C-metric can be extended beyond the acceleration horizon, $y = y_1$, and there is another acceleration horizon, beyond which there is another stationary region isometric to the stationary region $\{y_0 < y < y_1\}$. Therefore, for the wormhole spacetime $(\mathcal{M}, g_{\rm dis}, \Sigma)$ in Example 8.3.9, there also exist such acceleration horizons and stationary regions beyond each of the acceleration horizons, $l = \pm(y_1 - y_{\rm ph})$. There can be black holes in the stationary regions or, since there also exist other photon surfaces in the regions, thin shell wormhole throats.*

Example 8.3.11 (Junction along r-photon surfaces)**.** *The Λ-vacuum cases of the spacetime investigated in Chap. 4 give other examples of Z2PTJSTs if there exist the r-photon surfaces. Consider a spacetime (M, g) with the metric given by Eqs. (4.1) and (4.12) and $Q^2 = 0$. Suppose there exist an r-photon surface at $r = r_{\rm p}$ in (M, g). We denote two copies of the truncated outside region of the r-photon surface of (M, g), $r \geq r_{\rm p}$, by $(\bar{M}_\pm, g_\pm)$ and the coordinates by $\{t_\pm, r_\pm, x^i_\pm\}$. Identifying the boundaries $\partial\bar{M}_\pm = \{r_\pm = r_{\rm p}\}$ so that $(t_+, r_+ = r_{\rm p}, x^i_+) \equiv (t_-, r_- = r_{\rm p}, x^i_-)$, we obtain a Z2PTJST $(\mathcal{M}, g_{\rm dis}, \Sigma)$ where $g_{\rm dis}$ is the metric distribution and Σ is the shell given by $r_+ = r_- = r_{\rm p}$. Transforming the radial coordinates $r_\pm$ of $\bar{M}_\pm$ to the new coordinates $l_\pm := \pm(r_\pm - r_{\rm p})$ and introducing the coordinates $\{t, l, x^i\}$ of $\mathcal{M}$ by the identification $\{t, l, x^i\} = \{t_\pm, l_\pm, x^i_\pm\}$ on each region $\bar{M}_\pm$, the metric distribution is expressed as*

$$g_{\rm dis} = -f\left(|l| + r_p\right) dt^2 + f^{-1}\left(|l| + r_p\right) dl^2 + \left(|l| + r_p\right)^2 \gamma_{ij}(x) dx^i dx^j. \tag{8.68}$$

The mean curvatures of the boundaries are given by $\theta_\pm = \pm 3\sqrt{f(r_{\rm p})r_{\rm p}^{-2}}$ and the tension of the thin shell is $\epsilon = -[(D-2)/4\pi]\sqrt{f(r_{\rm p})r_{\rm p}^{-2}}$.

Remark 8.3.12. *Example 8.3.11 can be viewed as the topological extension of the Λ-vacuum cases of the thin shell wormholes in Refs. [55, 56]. Barcelo and Visser investigated the spherically symmetric cases of thin shell wormholes in Ref. [55]. Kokubu and Harada extended the work to the hyperbolically and planar symmetric cases with extensions in other directions [56]. If compactified, the hyperbolically and planar symmetric submanifolds of codimension-two become double and single toruses, respectively [61]. The Einstein submanifolds γ_{ij} of the Z2PTJST in Example 8.3.11 can be compact manifolds with various topology [32]. In that sense, the Z2PTJST would be the topological extension of the above works. Note that, although the geometry and the topology of γ_{ij} are non-trivial, the structures in the radial direction of the Z2PTJST is not different from that given in Refs. [55, 56]. This is because the geometry of γ_{ij} contributes to the metric coefficients $f(r)$ and $g(r)$ only by the scalar curvature $k = \pm 1, 0$ as we can see from Eq. (4.12). Although we have extended the geometry of γ_{ij} from a constant curvature space to an Einstein manifold, the difference does not appear in the coefficients $f(r)$ and $g(r)$.*

8.4 Stability of pure-tensional joined spacetime

We consider a shell perturbation of a Z2JST preserving its Z_2-symmetry. That is, perturbing the hypersurfaces $\Sigma_\pm$ of $(M_\pm, g_\pm)$ to $\widetilde{\Sigma}_\pm$, we rejoin the spacetimes along the new boundaries $\widetilde{\Sigma}_\pm$ to give a new perturbed Z2JST $(\widetilde{\mathcal{M}}, g, \widetilde{\Sigma})$ (Fig. 8.3). Since $(M_\pm, g_\pm)$ are isometric to each other including their hypersurfaces $\Sigma_\pm$ and $\widetilde{\Sigma}_\pm$, it is sufficient to focus only on the "plus" ones and we denote them as (M, g), Σ, $\widetilde{\Sigma}$, and so on in the following.

After reviewing the deformation formalism of surfaces given by Capovilla and Guven [59], we apply it to Z2PTJSTs, that is, the case where Σ is a photon surface. We also see that the stability of Σ corresponds to *the stability of null geodesics on* Σ defined in Chap. 3.

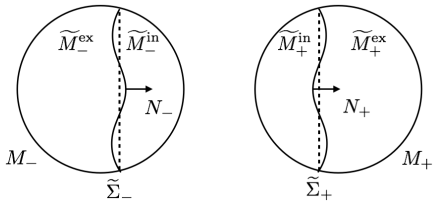

(a) Perturbed inner boundaries $\widetilde{\Sigma}_\pm$

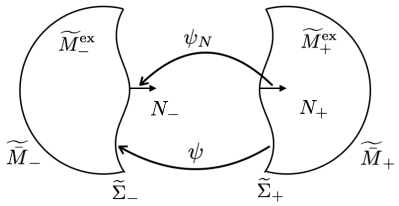

(b) Rejoining along $\widetilde{\Sigma}_\pm$

Figure 8.3: (a) The unperturbed inner boundaries $\Sigma_\pm$ (dashed lines) are perturbed to $\widetilde{\Sigma}_\pm$ (solid lines). (b) The truncation and gluing of $M_\pm$ along $\widetilde{\Sigma}_\pm$ gives the perturbed joined manifold $\widetilde{\mathcal{M}}$ with the perturbed shell $\widetilde{\Sigma} := \widetilde{\Sigma}_+ \equiv \widetilde{\Sigma}_-$.

8.4.1 Deformation of a hypersurface

Let Σ be a timelike hypersurface of a spacetime (M, g). Consider a one-parameter family of the deformation,

$$\mathcal{F}_\varepsilon \ : \ \Sigma \to \Sigma_\varepsilon, \tag{8.69}$$

with the parameter ε where $\Sigma_0 = \Sigma$. Expanding in ε, points on the surfaces are expressed as

$$\Sigma_\varepsilon^\mu = \Sigma^\mu + \varepsilon X^\mu + \mathcal{O}\left(\varepsilon^2\right) \tag{8.70}$$

in a coordinate system $\{x^\mu\}$. The vector field X on Σ is called *the deviation* between Σ and its infinitesimal deformation $\lim_{\varepsilon\to 0}\Sigma_\varepsilon$. Without loss of generality, we assume X to

be orthogonal to Σ by diffeomorphisms on Σ and Σ_ε [59]. Define a scalar field Φ on Σ by

$$X = \Phi N \tag{8.71}$$

where N is the unit normal vector of Σ. This quantity represents the *distance* between Σ and its infinitesimal deformation. According to the deformation formalism by Capovilla and Guven [59], we have equations which relate Φ with the geometrical quantities on Σ. A tiny fraction of the calculation processes in [59] is incorrect and we recalculate it for our purpose by following their procedure in Appendix C.1.

The deformation of the intrinsic geometry of Σ is related to Φ by

$$(\nabla_N \mathcal{R})\,\Phi = -2\mathcal{R}_{ab}\chi^{ab}\Phi + 2\nabla_a^h\nabla_b^h\left(\chi^{ab}\Phi\right) - 2\Delta^h\left(\theta\Phi\right) \tag{8.72}$$

where $\Delta^h := h^{ab}\nabla_a^h\nabla_b^h$ and $\mathcal{R}_{ab}$ and $\mathcal{R}$ are the Ricci tensor and scalar of Σ_ε, respectively. This is the codimension one version of Eq. (C.10) in Appendix C.1. Note that the indices $a, b, \ldots$ are with respect to the coordinate basis vectors $\{e_a\}$ of Σ. For a tensor T of M, T_{ab} represents $T(e_a, e_b)$ for example. We lower and raise the indices by the induced metric $h_{ab} = g(e_a, e_b)$ and its inverse matrix h^{ab}, respectively. For the deformation of the extrinsic geometry, Φ obeys

$$\nabla_a^h\nabla_b^h\Phi = -\left[\nabla_N\chi_{ab} - \chi_{ac}\chi^c{}_b + R_{aNbN}\right]\Phi \tag{8.73}$$

where the subscripts of N represent the contraction with N, i.e., $R_{aNbN} = R_{\mu\alpha\nu\beta}e_a^\mu N^\alpha e_b^\nu N^\beta$. We obtain the equation from Eq. (4.6) in [59] by setting the codimension one. Note that χ_{ab} and $\mathcal{R}_{ab}$ is now defined on each surface Σ_ε and can be differentiated along N. The equation,

$$2\chi_{ab} = \nabla_N h_{ab}, \tag{8.74}$$

is also useful in the calculations. See Eq. (3.8) in [59] for the derivation.

In the case where each surface Σ_ε obeys the same equations of motion, the deformation $\mathcal{F}_\varepsilon$ should be called *a perturbation*. Then we say Σ *is stable* against the perturbation if Φ is bounded as time evolves along Σ and otherwise *unstable*.

8.4.2 Perturbation of a photon surface

We consider the Z_2-symmetric perturbation of a Z2PTJST $(\mathcal{M}, g, \Sigma)$. The perturbed spacetime $(\widetilde{\mathcal{M}}, g, \widetilde{\Sigma})$ is also Z2PTJST and therefore, from Theorem 8.3.4, the hypersurface $\widetilde{\Sigma}$ is another photon surface of the original spacetime $(M_\pm, g_\pm)$. More precisely, Σ and $\widetilde{\Sigma}$ corresponds to CMC photon surfaces $\Sigma_\pm$ and $\widetilde{\Sigma}_\pm$ of the Λ-vacuum spacetime $(M_\pm, g_\pm)$, respectively, because of Theorem 8.3.4 and Proposition 8.3.3. Then, what we do in the following is to impose the conditions, CMC, totally umbilic (recall Theorem 8.3.2), and Λ-vacuum on the deformation formalism, Eqs. (8.72) and (8.73).

Let Σ be a CMC photon surface of a Λ-vacuum spacetime (M, g). The EOMs of Σ are given by

$$\chi_{ab} = \frac{\theta}{d}h_{ab}, \tag{8.75}$$

$$\theta = \text{const.} \tag{8.76}$$

with the Λ-vacuum condition on the spacetime,

$$G_{\mu\nu} = -\Lambda g_{\mu\nu}, \tag{8.77}$$

where $G_{\mu\nu}$ is the Einstein tensor. We denote the perturbation of Σ to Σ_ε, which also obeys the EOMs, as $\mathcal{F}_\varepsilon^{\rm PS} : \Sigma \to \Sigma_\varepsilon$.

First we calculate Eq. (8.72) for $\mathcal{F}_\varepsilon^{\rm PS}$. The contracted Gauss-Codazzi relation in Λ-vacuum reads

$$\mathcal{R} + \chi^{ab}\chi_{ab} - \theta^2 = -2G_{NN} = 2\Lambda. \tag{8.78}$$

From Eq. (8.75), the equation reduces to

$$\mathcal{R} = \frac{d-1}{d}\theta^2 + 2\Lambda. \tag{8.79}$$

Then the LHS of Eq. (8.72) reduces to

$$\left(\nabla_N \mathcal{R}\right)\Phi = 2\frac{d-1}{d}\left(\theta \nabla_N \theta\right)\Phi. \tag{8.80}$$

The RHS of Eq. (8.72) reduces to

$$\begin{aligned} & -2\chi_{ab}\mathcal{R}^{ab}\Phi + 2\nabla_a^h \nabla_b^h \left(\chi^{ab}\Phi\right) - 2\Delta^h\left(\theta\Phi\right) \\ = \; & -2\frac{\theta}{d}\mathcal{R}\Phi + 2\nabla_a^h\nabla_b^h\left(\frac{\theta}{d}h^{ab}\Phi\right) - 2\Delta^h\left(\theta\Phi\right) \\ = \; & -2\frac{\theta}{d}\mathcal{R}\Phi - 2\frac{d-1}{d}\theta\Delta^h\Phi \end{aligned} \tag{8.81}$$

where we have used Eqs. (8.75) and (8.76) in the first and last equalities, respectively. Equating both sides with the use of Eq. (8.79), we finally obtain

$$\nabla_N\theta = -\frac{\theta^2}{d} - \frac{2}{d-1}\Lambda - \Phi^{-1}\Delta^h\Phi. \tag{8.82}$$

Next we calculate Eq. (8.73) for $\mathcal{F}_\varepsilon^{\rm PS}$. From Eq. (8.75), the first term in the brackets in Eq. (8.73) reduces to

$$\begin{aligned} \nabla_N\chi_{ab} &= \nabla_N\left(\frac{\theta}{d}h_{ab}\right) \\ &= \frac{1}{d}\left[\frac{\theta^2}{d} - \frac{2}{d-1}\Lambda - \Phi^{-1}\Delta^h\Phi\right]h_{ab} \end{aligned} \tag{8.83}$$

where Eqs. (8.74) and (8.82) were used in the last equality. Then the LHS of Eq. (8.73) reduces to

$$\begin{aligned} & -\left[\nabla_N\chi_{ab} - \chi_{ac}\chi^c{}_b + R_{aNbN}\right]\Phi \\ = \; & \frac{1}{d}\Delta^h\Phi h_{ab} + \left[-R_{aNbN} + \frac{2}{d(d-1)}\Lambda h_{ab}\right]\Phi \end{aligned} \tag{8.84}$$

where Eqs. (8.75) and (8.83) were used. Substituting the result into Eq. (8.73), we obtain

$$\nabla^h_a\nabla^h_b\Phi - \frac{1}{d}\Delta^h\Phi h_{ab} = \left[-R_{aNbN} + \frac{2}{d(d-1)}\Lambda h_{ab}\right]\Phi, \tag{8.85}$$

or from the Λ-vacuum condition Eq. (8.77),

$$\nabla^h_a\nabla^h_b\Phi - \frac{1}{d}\Delta^h\Phi h_{ab} = -C_{aNbN}\Phi. \tag{8.86}$$

We have another expression of Eq. (8.86). The contraction of Gauss-Codazzi relation,

$$R_{\alpha\mu\beta\nu}h^\alpha_a h^\mu_c h^\beta_b h^\nu_d = \mathcal{R}_{acbd} - \chi_{ab}\chi_{cd} + \chi_{ad}\chi_{cb},$$

with h^{cd} gives

$$R_{\alpha\beta}h^\alpha_a h^\beta_b - R_{aNbN} = \mathcal{R}_{ab} - \theta\chi_{ab} + \chi_{ac}\chi^c{}_b. \tag{8.87}$$

from $h^{cd}h^\mu_c h^\nu_d = h^{\mu\nu} = g^{\mu\nu} - N^\mu N^\nu$. Using the fact that the spacetime is Λ-vacuum and the hypersurface is totally umbilic, the equation reduces to

$$-C_{aNbN} + \frac{2}{d}\Lambda h_{ab} = \mathcal{R}_{ab} - \frac{d-1}{d^2}\theta^2 h_{ab}. \tag{8.88}$$

From Eq. (8.79), we have

$$-C_{aNbN} = \mathcal{R}_{ab} - \frac{\mathcal{R}}{d}h_{ab}. \tag{8.89}$$

Then Eq. (8.86) is rewritten as

$$\nabla^h_a\nabla^h_b\Phi - \frac{1}{d}\Delta^h\Phi h_{ab} = \left(\mathcal{R}_{ab} - \frac{\mathcal{R}}{d}h_{ab}\right)\Phi. \tag{8.90}$$

The expression tells us that the linear perturbation Φ is governed only by the intrinsic geometry, the Ricci curvature $\mathcal{R}_{ab}$, of (Σ, h).

Note the master equation of the perturbation, Eq. (8.86) or (8.90), does not have its trace part. Therefore, $\Phi^{-1}\Delta^h\Phi$ is unspecified *a priori* and will be determined after we solve the trace-free part of the equation for given initial values of Φ.

8.4.3 Stability of the shell and a photon surface

Let us physically interpret the master equation Eq. (8.86) for the perturbation Φ of the photon surface Σ.

Let $k_p \in T_p\Sigma$ be a null vector at a point $p \in \Sigma$. Since Σ is a photon surface, there always exists a null geodesic $\gamma(\lambda)$ everywhere tangent to Σ such that $k_p = \dot\gamma(0)$. The contraction of Eq. (8.86) with $k = \dot\gamma(\lambda)$ gives

$$\nabla^h_k\nabla^h_k\Phi = -C_{kNkN}\Phi. \tag{8.91}$$

Therefore, we have

$$\frac{d^2}{d\lambda^2}\Phi(\lambda) = -C_{kNkN}\Phi(\lambda) \tag{8.92}$$

along $\gamma(\lambda)$. This implies that given the initial values $\Phi|_{t=t_0}$ and $\partial_a\Phi|_{t=t_0}$ at time $t=t_0$, the value of Φ at the point p in the future is determined by integrating the ordinary differential equation Eq. (8.92) along $\gamma(\lambda)$ from $q=\gamma(\lambda_{t=t_0})$ to p.

The factor $-C_{kNkN}$ in Eq. (8.92) coincides with what determines the *stability of the null geodesic γ on Σ*. That is, an orthogonally perturbed null geodesic $\tilde{\gamma}$ from γ is stable (attracted to Σ) if $-C_{kNkN}<0$ and unstable (repelled from Σ) if $-C_{kNkN}>0$ in our Λ-vacuum case (see Proposition 3.2.2 and 3.2.3). In particular, if Σ is *a strictly stable photon surface*, i.e. all the null geodesics on Σ are stable, the factor in Eq. (8.92) is always negative along any null geodesics. This is suggestive that Φ will be bounded as time evolves. In fact, in the case where $-C_{kNkN}$ varies sufficiently slowly, Φ oscillates with the almost constant amplitude along any null geodesic and will be bounded.

This is quite natural from the physical point of view. Since a photon surface is a hypersurface generated by null geodesics, the photon surface Σ_ε perturbed from Σ is generated by the orthogonally perturbed null geodesics $\tilde{\gamma}$. Therefore, if all the perturbed null geodesics $\tilde{\gamma}$ are attracted to Σ, Σ_ε should also be attracted to Σ. As a consequence, Σ should be stable if the null geodesics along Σ are stable.

Then our conclusion is this: if Σ is a strictly stable photon surface, then Σ is stable against the linear perturbation given by $\mathcal{F}^{\mathrm{PS}}_\varepsilon:\Sigma\to\Sigma_\varepsilon$. For Z2PTJSTs, we also conclude as this: if $\Sigma_\pm$ is a strictly stable photon surface of $(M_\pm,g_\pm)$, then the Z2PTJST $(\mathcal{M},g,\Sigma)$ constructed from $(M_\pm,g_\pm)$ is stable against shell perturbations preserving the Z_2-symmetry.

In Appendix C.2, we explicitly solve the perturbation equation, Eq. (8.86), in the case where the geometry of Σ is static and spherically, planar, and hyperbolically symmetric. The case is frequently seen in, for example, [53, 55, 56]. The induced metric is given by

$$h=a^2(-dt^2+\sigma)$$

where a is constant and σ represents the metric of the $(d-1)$-dimensional space of constant curvature $\alpha=\pm1,0$. The general solution in spherically ($\alpha=1$) and hyperbolically ($\alpha=-1$) symmetric case is given by

$$\Phi=Ce^{\sqrt{\alpha}t}+Fe^{-\sqrt{\alpha}t}\quad(\alpha=\pm1) \tag{8.93}$$

with the arbitrary constants C and F from Eq. (C.51). In the planar case ($\alpha=0$), we have

$$\Phi=D\eta_{ab}x^ax^b+B_ax^a+C\quad(\alpha=0) \tag{8.94}$$

with the arbitrary constants D, B_a, and C from Eq. (C.52). $x^a=(t,x^i)$ is the Cartesian coordinate on Σ. Since the Weyl curvature gives $-C_{kNkN}=\mathcal{R}_{kk}=\alpha$ for any null vector $k\in T\Sigma$ with an appropriate scaling, Σ is a strictly stable photon surface if and only if $\alpha=-1$, i.e. the hyperbolic case, and it is only the case where the solution Φ is bounded for any possible perturbation. Therefore, the result agrees with the above conclusion, indeed. See Appendix C.2 for the derivation and the detailed interpretations of the result.

8.5 Uniqueness of pure-tensional wormholes

A joined spacetime $(\mathcal{M}, g, \Sigma)$ is a wormhole spacetime if both regions $\bar{M}_\pm$ have asymptotically flat domains. If, additionally, $(\mathcal{M}, g, \Sigma)$ is Z_2-symmetric and pure-tensional, the spacetimes $(\bar{M}_\pm, g_\pm)$ constituting $(\mathcal{M}, g, \Sigma)$ are asymptotically flat spacetimes with their inner boundaries $\Sigma_\pm$ being photon surfaces according to Theorem 8.3.4. Cederbaum established the uniqueness theorem of such spacetimes, $(\bar{M}_\pm, g_\pm)$, with some assumptions [11]. Using the theorem, we prove the uniqueness theorem of pure-tensional thin shell wormholes.

In Cederbaum's uniqueness theorem, the spacetime is assumed to be AF-geometrostatic ("AF" stands for "asymptotically flat")(see below) and the lapse function with respect to the static Killing vector is assumed to be constant along the photon surface being the inner boundary. In the following, we call the photon surface under the assumptions *Cederbaum's photon sphere* (Definition 2.6 in [11]).

8.5.1 Pure-tensional wormhole

An *AF-geometrostatic spacetime* (Definition 2.1 in [11]) is a spacetime which is static, asymptotically flat, and a vacuum solution to Einstein equation with the cosmological constant $\Lambda = 0$. We define the following AF-geometrostatic wormhole spacetime:

Definition 8.5.1 (Static pure-tensional wormhole)**.** *Let $(\mathcal{M}, g, \Sigma)$ be a Z2PTJST constructed from $(M_\pm, g_\pm)$. $(\mathcal{M}, g, \Sigma)$ is called a static pure-tensional wormhole if $(\bar{M}_\pm, g_\pm)$ are AF-geometrostatic spacetimes and their inner boundaries $\Sigma_\pm$ are static.*

8.5.2 Proof of the uniqueness

We impose a technical assumption on a static pure-tensional wormhole $(\mathcal{M}, g, \Sigma)$ to prove the uniqueness theorem. Since $(\mathcal{M}, g, \Sigma)$ is Z_2-symmetric and Σ is static, $(\bar{M}_\pm, g_\pm)$ have a common static Killing vector field ∂_t which are tangent to $\Sigma_\pm$ on $\Sigma_\pm$ and satisfies $\psi^* : \partial_t|_{\Sigma_+} \mapsto \partial_t|_{\Sigma_-}$ for the identification of the inner boundaries $\psi : \Sigma_+ \to \Sigma_-$. The lapse functions $\mathcal{N}_\pm$ of $(\bar{M}_\pm, g_\pm)$ and $\mathcal{N}$ of $(\mathcal{M}, g, \Sigma)$ with respect to the Killing vector are given by $\mathcal{N}_\pm^2 = -g_\pm(\partial_t, \partial_t)$ and $\mathcal{N}^2 = -g(\partial_t, \partial_t)$, respectively. Since the first junction condition is satisfied from the Z_2-symmetry, $\mathcal{N}^2 = -g(\partial_t, \partial_t) = -\frac{1}{2}[g_+(\partial_t, \partial_t) + g_-(\partial_t, \partial_t)] = -g_\pm(\partial_t, \partial_t) = \mathcal{N}_\pm^2$. Then we assume that $\mathcal{N}_\pm$ are constant along $\Sigma_\pm$ in $\bar{M}_\pm$ and therefore, $\mathcal{N} =$ const. along Σ in $\mathcal{M}$. This is equivalent to the requirement that the time-time component of the surface stress energy S_{ab} is constant, $S_{tt} = -\epsilon h_{tt} = \epsilon \mathcal{N}|_\Sigma{}^2 =$ const., since $\epsilon =$ const. from Theorem 8.3.4. Although the assumption may restrict the class of solutions, the pure-tensional wormholes which have been investigated satisfy it [55, 56]. We have the following theorem.

Theorem 8.5.2 (Uniqueness of static pure-tensional wormhole spacetimes)**.** *Let $(\mathcal{M}, g, \Sigma)$ be a four-dimensional static pure-tensional wormhole constructed from $(M_\pm, g_\pm)$. Let ϵ and θ be the tension and the mean curvature of Σ, respectively. Assume that the lapse functions $\mathcal{N}_\pm$ of $(\bar{M}_\pm, g_\pm)$ regularly foliate $\bar{M}_\pm$ and are constant along $\Sigma_\pm$. Then, each*

of the regions $\bar{M}_\pm$ *of* $(\mathcal{M}, g, \Sigma)$ *is isometric to the Schwarzschild spacetime with the mass* $m = 1/(\sqrt{3}\theta) = -1/(6\sqrt{3}\pi\epsilon) > 0$.

Proof. From Definition 8.5.1, $\bar{M}_\pm := M_\pm \setminus M_\pm^{\rm in}$, which constitute $\mathcal{M}$ by $\mathcal{M} = \bar{M}_+ \cup_{\psi,\psi_N} \bar{M}_-$, are the manifolds with the asymptotically flat regions and the inner boundaries $\Sigma_\pm$. From Theorem 8.3.4, $\Sigma_\pm$ of $(\bar{M}_\pm, g_\pm)$ are photon surfaces with the constant mean curvatures

$$\theta_\pm = \mp 6\pi\epsilon. \tag{8.95}$$

Therefore, from the assumptions, $(\bar{M}_\pm, g_\pm)$ are AF-geometrostatic spacetimes regularly foliated by $\mathcal{N}_\pm$ and the inner boundaries $\Sigma_\pm$ are Cederbaum's photon spheres, i.e. they are photon surfaces with the constant lapse functions $\mathcal{N}_\pm$ along them in the AF-geometrostatic spacetimes (Definition 2.6 in [11]). Then, from the uniqueness theorem of photon spheres (Theorem 3.1 in [11]), $(\bar{M}_+, g_+)$ is Schwarzschild spacetime with the mass $m = 1/(\sqrt{3}\theta_+) > 0$. From Eq. (8.95), we have

$$m = \frac{1}{\sqrt{3}\theta_+} = -\frac{1}{6\sqrt{3}\pi\epsilon} > 0 \tag{8.96}$$

and $\epsilon < 0$. Since the Z_2-symmetry of $(\mathcal{M}, g, \Sigma)$ implies that $(\bar{M}_\pm, g_\pm)$ are isometric, $(\bar{M}_-, g_-)$ is also Schwarzschild spacetime with the mass

$$m = \frac{1}{\sqrt{3}\theta_+} = -\frac{1}{\sqrt{3}\theta_-} = -\frac{1}{6\sqrt{3}\pi\epsilon} > 0. \tag{8.97}$$

□

Note that the static photon surface in Schwarzschild spacetime is the hypersurface of radius $3m$ [8].

8.6 Summary

We have defined a joined spacetime (JST), which is obtained by truncating and gluing two spacetimes along the boundaries, in Sec. 8.1. Z_2-symmetry of JSTs has been defined in Sec. 8.2. A pure-tensional JST (PTJST) has been defined as a Λ-vacuum JST with a pure tension shell. For a Z_2-symmetric pure-tensional joined spacetime (Z2PTJST), we have proved that its shell must be photon surfaces of the original spacetimes constituting the JST (Theorem 8.3.4) in Sec. 8.3. Conversely, if two isometric Λ-vacuum spacetimes have photon surfaces, we can join them to give a Z2PTJST. Therefore, we have solutions of Z2PTJSTs as many as the photon surfaces of Λ-vacuum spacetimes found in, for example, Chap. 3 and 7 and Refs. [8, 10, 19, 16].

Z2PTJSTs have been widely investigated in the contexts of wormholes [55, 56], baby universes [55], and brane worlds [57, 58]. The shells correspond to the throats in the wormhole cases and the branes we live in in the brane world cases. One can infer that we can extend Theorem 8.3.4 to electrovacuum cases because the coincidence of the shells

and photon spheres holds in the electrovacuum cases in Refs. [55, 56]. It is fascinating since the electric charges enrich the variety of thin shell wormhole solutions.

Theorem 8.3.4 can be used to exclude the possibility to construct a Z2PTJST from a given spacetime. In a stationary axisymmetric spacetime like the Kerr spacetime, there can be null circular geodesics, however, photon surfaces would not exist on the radii. This is because the corotating and counterrotating circular orbits have the different radii in general. Even if the corotating orbits generate a hypersurface on the radius, the counterrotating orbits cannot be tangent to the surface. Then the hypersurface does not satisfy the definition of photon surface. Therefore, we cannot join the two copies of the spacetime along the radii of null circular geodesics to give a Z2PTJST. One needs to violate the Z_2-symmetry, the pure tension equation of state of the shell, or the Λ-vacuum condition to construct shell wormholes from stationary axisymmetric spacetimes.

Since the shell of a Z2PTJST coincides with a photon surface, the stability of the JST against the shell perturbation also coincides with the stability against the surface perturbation of the photon surface in the original spacetime. In Sec. 8.4, after deriving the master equation for the perturbation of photon surfaces, Eq. (8.90), from the surface deformation formalism by Capovilla and Guven [59], we have found its close relationship to the stability of null geodesics on a photon surface introduced in Chap. 3. Namely, if null geodesics on a photon surface are stable (unstable), the photon surface itself, and therefore the Z2PTJST, is stable (unstable) against the surface (shell) perturbation. We have also confirmed it by solving the perturbation equation for photon surfaces explicitly in Appendix C.2 with the specific induced metrics.

It is remarkable that the perturbation equation, Eq. (8.90), is also useful to seek photon surfaces in the vicinity of a given photon surface. Actually, we have found the hyperboloid, Eq. (C.50), by perturbing the plane of $y = 0$ in the 3-Minkowski spacetime $\mathbb{M}^3$. The hyperboloid, as well as the plane, is known to be a timelike photon surface of $\mathbb{M}^3$, indeed [8] (see also Examples 3.1.2–3.1.5 in Chap. 3). In contrast with the planar case, in the spherically and hyperbolically symmetric cases, it is suggested that there would not be photon surfaces violating the spatial symmetries because the perturbation Φ in Eq. (C.51) depends only on the time t.

In the wormhole cases of Z2PTJSTs with the vanishing cosmological constant, we have applied the uniqueness theorem of photon spheres by Cederbaum [11] and established the uniqueness theorem of static pure-tensional wormholes with Z_2-symmetry (Theorem 8.5.2) in Sec. 8.5. The theorem states that both sides of the wormhole are isometric to the Schwarzschild spacetim with the same masses. It is also interesting that the tension of the shell and the mass of the wormhole are inversely proportional to each other and the positive mass implies the negative tension and the negative energy of the shell. This is consistent with the result that wormhole spacetimes have to violate energy conditions in the vicinity of the throats [51, 52].

The static pure-tensional wormhole in our uniqueness theorem has the photon surface (shell) of the geometry (8.93) with $\alpha = +1$. Therefore, from the general solution of the perturbation, Eq. (8.93), in Sec. 8.4, the static pure-tensional wormhole is unstable against general throat (shell) perturbation preserving Z_2-symmetry. Note that the instability of this spacetime was also concluded for the Z_2-symmetric, spherically

symmetric, nonlinear perturbation of the shell in Refs. [55, 56].

Chapter 9

Conclusion

In this thesis, we have studied the basics of a photon sphere and a photon surface and their relevant phenomena.

In Chap. 2, we have overviewed the photon spheres of the Schwarzschild spacetime and the Reissner-Nordström spacetime. They are the spheres along which null geodesics take circular orbits. From the symmetry of the spacetimes, the geodesic equations reduce to the one-dimensional equations of motion with the effective potentials, and therefore, their extrema correspond to the photon spheres. We have found the extrema are local maxima and therefore the corresponding photon spheres are unstable photon spheres excepting the over-extremal case of the Reissner-Nordström spacetime. After deriving the radii of the photon spheres, we have clarified that the edges of the black hole shadows are shaped by the unstable photon spheres. The corresponding smallest incident angles, from which the photons emitted from a light source distant to the black hole can come, have also derived with their relations to the critical impact parameters of the photons.

In Chap. 3, after reviewing the definition, the examples, and the basic theorem of a photon surface, we have defined the stability of null geodesics on a photon surface by reformulating the stability of a photon sphere in a covariant manner. Since such a behavior is subject to the geodesic deviation equation, the stability condition of null geodesics on a photon surface has been given in terms of the Riemann curvature, as in Proposition 3.2.2, or the Weyl and Ricci curvature, as in Proposition 3.2.3. Another expression for the stability condition has also been derived in terms of the trace-free part of the second fundamental form as in Proposition 3.3.1. Several corollaries for the existence of stable and unstable photon surfaces have been shown in Sec. 3.4. Remarkably, it is obvious from Proposition 3.2.3 that the existence of unstable photon surfaces requires the non-zero contribution of the Weyl curvature if the spacetime satisfies the null energy condition. From the physical point of view, it implies that unstable photon surfaces exit only in a strong gravity region, such as the vicinity of a black hole.

In Chap. 4, we have investigated r-photon surfaces in the spacetime given by the metric ansatz (4.1). The ansatz is a general form of a warped spacetime as shown in

Appendix A. The r-photon surfaces indeed exist in the case where the spacetime is the electrovacuum solution to the Einstein equation with the cosmological constant. Since the spacetime is a solution as far as the $(D-2)$-space $\gamma_{ij}dx^i dx^j$ is an Einstein manifold, it implies that static photon surfaces exist in less or non-symmetric electrovacuum spacetimes. Here we conclude that a static photon surface may exist in spacetimes because of the warped structure rather than the high degrees of the Killing symmetry.

In Chap. 5, first we have derived the conditions for photon spheres, the radius and the stability of the corresponding circular orbit of null geodesics in a general D-dimensional static, spherically symmetric spacetime. Next, we have generalized the analysis of accretion problems given by Chaverra and Sarbach [24] to arbitrary dimensions and discussed the relation between sonic points and critical points in general. Then, for ideal photon gas (radiation fluid), it has been shown that radius of a sonic point always coincides with (one of) photon spheres for physical solutions of the accretion problem. The phenomenon has been named sonic point/photon sphere (SP/PS) correspondence. We can expect the significance of the phenomenon from the fact that a black hole shadow is observed by observing light emissions from accreting matter [2]. If radiation fluid are accreting into a black hole, the bright edge of the black hole shadow, corresponding to the radius of the photon sphere (recall Chap. 2), is shaped by the light emissions from the sonic point. We might be able to obtain the characteristic informations of the accreting radiation fluid from the shadow observation or obtain the geometrical informations concerning the photon sphere from a characteristic spectrum of the light emission from the radiation flow.

In Chap. 6, we have formulated the rotational accretion problem of the disk lying on the equatorial plane of the D-dimensional static, spherically symmetric spacetime. We have adopted the simplest accretion disk model similar to the one given by Abraham *et al.* [40]. Then the accretion analysis extended to arbitrary dimensions in Chap. 5 has been further extended to the case of rotational flow. For the disk model, we have found that the SP/PS correspondence holds as far as the fluid is ideal photon gas, or radiation fluid. Since almost all the black holes which have been optically observed are accompanied with accretion disks, the result would be a more realistic extension of the SP/PS correspondence.

In Chap. 7, we have investigated photon surfaces of constant radius in the spherically, planar, and hyperbolically symmetric spacetime, Eq. (7.1). We have formulated the accretion problem of stationary radial fluid flow which is also spatially symmetric depending on the spatial symmetry of the spacetime (7.2). It has been revealed that the master equation (7.25) does not depend on the spatial symmetry explicitly. Then we have applied the dynamical system analysis to the problem and found that the SP/PS correspondence in Chap. 5 holds by replacing *photon sphere (PS)* with *photon surface (PS)* of constant radius. The fact implies that the circularity of photons along a photon sphere is not relevant, but rather the umbilicity of the surface is essential for the correspondence. The further investigation of the correspondence in a general setting is given

in Ref. [44]. In the work, it has been concluded that the correspondence could occur if the system is highly symmetric.

In Chap. 8, we have considered a joined spacetime (JST), which is constructed by the thin shell formalism. For a Z_2-symmetric pure-tensional joined spacetime (Z2PTJST), we have proved that its shell must be photon surfaces of the original spacetimes constituting the JST (Theorem 8.3.4). The result implies that we have solutions of Z2PTJSTs as many as the photon surfaces found in Λ-vacuum spacetimes. We have also shown the stability of Z2PTJSTs coincides with the stability of the photon surfaces along which the original spacetimes are joined. Finally, for asymptotically flat vacuum wormholes of Z2PTJST, we have proved the uniqueness theorem (Theorem 8.5.2) by using the photon sphere uniqueness theorem by Cederbaum [11]. The uniqueness theorem states that a pure-tensional and vacuum thin shell wormhole must be that constructed by joining the two equal-mass Schwarzschild spacetimes along their photon spheres, $r = 3m$. Since such a wormhole has been concluded to be unstable against shell perturbation in this thesis and Refs. [55, 56], it means that there is no stable pure-tensional vacuum thin shell wormhole in general.

The phenomena relevant to a photon surface we have investigated in this thesis appear in quite general situations in the following senses. In Chap. 4, we have shown that the r-photon surfaces may exist on general spacetimes in a class of static warped spacetimes regardless of the symmetry. In Chaps. 5–7, the SP/PS correspondence has been proved, under the symmetry assumed on the fluid and spacetimes, for general spacetimes which need not be solutions to any theories of gravity. In Chap. 8, thin shells of general Z2PTJSTs have been found to correspond to photon surfaces regardless of the symmetry excepting the Z_2-symmetry. These results have shown that a photon surface in a spacetime has more physical significance than its definition. That is, a photon surface is a spacetime structure that is crucial for not only motions of free photons but also accreting matter and pure-tensional matter shells. It is also interesting to investigate the same or similar phenomena for the other generalized notions of a photon sphere that are being extensively investigated recently: the loosely trapped surface [62]; the transversely trapping surface [63, 64]; the wandering set [65]; and the partially umbilic hypersurface [66]. The generalized notions are related to or inspired by the photon surface, and therefore, new phenomena relevant to them other than motions of free photons may be discovered.

Acknowledgement

I am very grateful to my supervisor, Prof. Tomohiro Harada, for the suggestions, discussions, and collaborations. Many of my works were motivated by the discussions. There are many things I have learned through the collaborations; technics of calculations, insights into physics, ways of thinking, and so on. They will be the basics of my researches in the future. I appreciate the examiners T. Kobayashi and S. Kitamoto for their useful suggestions and comments. I also appreciate all of the staffs and my colleagues in Institute of Theoretical Physics in Rikkyo University. Y. K. was supported by JSPS.

Appendix A

Static warped spacetime

The spacetime given by Eq. (4.1),

$$ds^2 = -f(r)dt^2 + g(r)dr^2 + r^2\gamma_{ij}\,(x)\,dx^i dx^j,$$

can be given as a generic static warped product. Consider a warped product of manifolds of the form,

$$M = M_1 \times \mathcal{F} M_2, \tag{A.1}$$

where M_1 is a two-dimensional Lorentzian manifold, M_2 is a $(D-2)$-dimensional Riemannian manifold, and $\mathcal{F} : M_1 \to \mathbb{R}_{>0}$ is a warping function. Letting $\{y^A\}$ and $\{x^i\}$ be the coordinates on M_1 and M_2, respectively, we have

$$ds^2 = g_{AB}(y)dy^A dy^B + \mathcal{F}(y)\gamma_{ij}(x^i)dx^i dx^j. \tag{A.2}$$

Choosing $t \in \{y^A\}$ as the static time and $R \in \{y^A\}$ as the coordinate orthogonal to t, we have

$$ds^2 = g_{tt}(R)dt^2 + g_{RR}(R)dR^2 + \mathcal{F}(R)\gamma_{ij}(x)dx^i dx^j. \tag{A.3}$$

If we additionally assume that $\mathcal{F}'(R) \neq 0$, we can transform the coordinate $R \to r$ by $dr = d(\mathcal{F}^{1/2}) = (1/2)\mathcal{F}^{-1/2}\mathcal{F}'dR$. Then we obtain

$$ds^2 = g_{tt}(R(r))dt^2 + g_{rr}(R(r))dr^2 + r^2\gamma_{ij}(x)dx^i dx^j. \tag{A.4}$$

Defining $-f(r) := g_{tt}(R(r))$ and $g(r) := g_{RR}(R(r))$, we obtain Eq. (4.1).

Appendix B

Gaussian normal coordinates on a Z_2-symmetric joined spacetime

We construct a coordinate system of a Z_2-symmetric joined spacetime $(\mathcal{M}, g, \Sigma)$ which respects the Z_2-symmetry. With the coordinate system, we can verify Definition 8.2.1 explicitly.

Let $(\mathcal{M}, g, \Sigma)$ be Z_2-symmetric joined spacetime of $(M_\pm, g_\pm)$. Consider Gaussian normal coordinates $\mathcal{C}_\pm : p_\pm \in M_\pm \mapsto (l_\pm, x_\pm) \in \mathbb{R}^{d+1}$ with respect to $\Sigma_\pm$ such that

$$g_\pm = dl_\pm^2 + h_{ij}^\pm(\pm l_\pm, x_\pm) dx_\pm^i dx_\pm^j \tag{B.1}$$

with the conditions,

$$\Sigma_\pm = \{l_\pm = 0\}\,, \tag{B.2}$$
$$N_\pm = \partial l_\pm. \tag{B.3}$$

With the isometry $\phi : (M_+, g_+) \to (M_-, g_-)$ in Definition 8.2.1, we can impose that $\mathcal{C}_- \circ \phi \circ \mathcal{C}_+^{-1} : (l_+, x_+) \mapsto (-l_-, x_-)$ on the coordinates. It leads to

$$h_{ij}^+(l, x) = h_{ij}^-(l, x) \tag{B.4}$$

for a variable l. Indeed, the assumption on the coordinates satisfies the requirement for ϕ, Eqs. (8.17) and (8.19):

$$\phi|_{\Sigma_+} : \Sigma_+ = \{l_+ = 0\} \to \{l_- = 0\} = \Sigma_-, \tag{B.5}$$
$$\phi^* : N_+ = \partial l_+ \mapsto -\partial l_- = -N_-. \tag{B.6}$$

Since $\mathcal{C}_- \circ \phi|_{\Sigma_+} \circ \mathcal{C}_+^{-1} : (0, x_+) \mapsto (0, x_-)$, Eq. (8.18) implies that $\mathcal{M} = \bar{M}_+ \cup_{\psi, \psi_N} \bar{M}_-$ is obtained by, after the truncation $M_\pm \to \bar{M}_\pm$, identifying the coordinates on $\Sigma_\pm$ as

$$\mathcal{C}_- \circ \psi \circ \mathcal{C}_+^{-1} : (0, x_+) \mapsto (0, x_-). \tag{B.7}$$

From the identification of the normal vectors $\psi_N : N_+ \mapsto N_-$, Eq. (8.10), we also have

$$\partial l_+|_{l_+=0} = \partial l_-|_{l_-=0}\,. \tag{B.8}$$

Then we introduce the coordinate system $\mathcal{C} : p \in \mathcal{M} \mapsto (l, x)$ into $\mathcal{M}$ by

$$(l, x) = \begin{cases} (l_+, x_+) & (l \geq 0) \\ (l_-, x_-) & (l < 0). \end{cases} \tag{B.9}$$

This choice satisfies the conditions for the gluing, Eqs. (B.7) and (B.8). Finally, we obtain the metric distribution on $\mathcal{M}$,

$$g = dl^2 + h_{ij}(|l|, x)dx^i dx^j, \tag{B.10}$$

where $h_{ij}(l, x) := h^+_{ij}(l, x) = h^-_{ij}(l, x)$ for $l \geq 0$.

Obviously, the transformation $l \to -l$ leaves g and Σ invariant and exchanges the regions of $\mathcal{M}$ as $M^{\rm ex}_+ \leftrightarrow M^{\rm ex}_-$. Definition 8.2.1 gives a Z_2-symmetric joined spacetime, indeed.

The quantities appearing in the junction conditions are given as follows. From $h_\pm(X, Y) = g_\pm(X, Y)\ \forall X, Y \in T\Sigma_\pm$, the induced metric is

$$h_+ = h_{ij}(0, x)dx^i dx^j = h_-. \tag{B.11}$$

From $\chi_\pm = (1/2)\mathcal{L}_{N_\pm} h_\pm$ [21], the second fundamental form is

$$\chi_+ = \frac{1}{2} h_{ij,l}(0, x)dx^i dx^j = -\chi_-. \tag{B.12}$$

We can easily see that Proposition 8.2.2 holds from the expressions.

Appendix C

Deformation of hypersurfaces

The derivation of the results for surface deformation obtained in Chap. 8 is supported by the following calculations. In Appendix C.1, we make the corrections to a part of the surface deformation formalism given in [59]. In Appendix C.2, we explicitly solve the perturbation equation of a photon surface in specific cases.

C.1 Calculations in deformation of hypersurfaces

We recalculate a part of the calculation in [59] following their procedure. The notations in [59] are converted to those used in Chap. 8 in the following.

We consider an embedded surface Σ of a spacetime (M, g) and its deformation. The dimension $d := \dim(\Sigma) \geq 1$ is arbitrary here and therefore we have $(D-d)$ unit normal vectors N^i and the deviation scalars Φ_i where $i = 1, ..., D-d$. From Eq. (3.9) in [59], the deformation of the Christoffel symbol $\Gamma_{ab}{}^c$ with respect to the induced metric h_{ab} of the surface Σ is given by

$$\begin{aligned} \nabla_\delta \Gamma_{ab}{}^c &= \frac{1}{2} h^{cd} \left[\nabla^h_a \left(\nabla_\delta h_{bd} \right) + \nabla^h_b \left(\nabla_\delta h_{ad} \right) - \nabla^h_d \left(\nabla_\delta h_{ab} \right) \right] \\ &= h^{cd} \left[\nabla^h_a \left(\chi_{bd}{}^i \Phi_i \right) + \nabla^h_b \left(\chi_{ad}{}^i \Phi_i \right) - \nabla^h_d \left(\chi_{ab}{}^i \Phi_i \right) \right] \end{aligned} \tag{C.1}$$

where $\delta := \Phi_i N^i$, ∇ is the covariant derivative associated with g, ∇^h is the covariant derivative associated with h_{ab}, $\chi_{ab}{}^i$ is the i-th extrinsic curvature of Σ with respect to N^i, and $\nabla_\delta := \delta^\mu \nabla_\mu$. In general, a variation of a metric $g_{\mu\nu} \to g_{\mu\nu} + \Delta g_{\mu\nu}$ gives the variations Δ of the connection coefficients $\Gamma^\alpha{}_{\mu\nu}$ and the curvatures $R^\alpha{}_{\mu\beta\nu}$, $R_{\mu\nu}$, and R of a spacetime as [25, 67]

$$\Delta R^\alpha{}_{\mu\beta\nu} = \nabla_\beta \Delta\Gamma^\alpha{}_{\mu\nu} - \nabla_\nu \Delta\Gamma^\alpha{}_{\mu\beta}, \tag{C.2}$$

$$\Delta R_{\mu\nu} = \nabla_\alpha \Delta\Gamma^\alpha{}_{\mu\nu} - \nabla_\nu \Delta\Gamma^\alpha{}_{\mu\alpha}, \tag{C.3}$$

$$\Delta R = -R^{\mu\nu} \Delta g_{\mu\nu} + g^{\mu\nu} \left(\nabla_\alpha \Delta\Gamma^\alpha{}_{\mu\nu} - \nabla_\nu \Delta\Gamma^\alpha{}_{\mu\alpha} \right), \tag{C.4}$$

$$\Delta \left(\sqrt{-g} R \right) = \frac{1}{2} g^{\mu\nu} \Delta g_{\mu\nu} \sqrt{-g} R + \sqrt{-g} \Delta R. \tag{C.5}$$

Applying the equations to our case and replacing Δ by ∇_δ, we have

$$\begin{aligned}
\nabla_\delta \mathcal{R}^a_{cbd} &= \nabla^h_b \left(\nabla_\delta \Gamma_{cd}{}^a\right) - \nabla^h_c \left(\nabla_\delta \Gamma_{bd}{}^a\right), && \text{(C.6)}\\
\nabla_\delta \mathcal{R}_{cd} &= \nabla^h_a \left(\nabla_\delta \Gamma_{cd}{}^a\right) - \nabla^h_d \left(\nabla_\delta \Gamma_{ca}{}^a\right) && \text{(C.7)}\\
\nabla_\delta \mathcal{R} &= -\mathcal{R}^{cd} \nabla_\delta h_{cd} + h^{cd} \left(\nabla^h_a \nabla_\delta \Gamma_{cd}{}^a - \nabla^h_d \nabla_\delta \Gamma_{ca}{}^a\right), && \text{(C.8)}\\
\nabla_\delta \left(\sqrt{-\gamma}\mathcal{R}\right) &= \sqrt{-h}\left(\frac{1}{2} h^{ab} \nabla_\delta h_{ab} \mathcal{R} + \nabla_\delta \mathcal{R}\right) && \text{(C.9)}
\end{aligned}$$

for the curvatures of (Σ, h). In particular, substituting Eq. (C.1) into the identities and using Eq. (3.8) in [59], $\nabla_\delta h_{ab} = 2\chi_{ab}{}^i \Phi_i$, we obtain

$$\begin{aligned}
\nabla_\delta \mathcal{R} &= -2\mathcal{R}^{cd} \chi_{cd}{}^i \Phi_i + 2\nabla^h_a \nabla^h_c \left(\chi^{aci} \Phi_i\right) - 2\Delta^h \left(\theta^i \Phi_i\right), && \text{(C.10)}\\
\nabla_\delta \left(\sqrt{-h}\mathcal{R}\right) &= -2\sqrt{-h}\mathcal{G}^{ab} \chi_{ab}{}^i \Phi_i + \partial_a \left(\sqrt{-h} J^a\right), && \text{(C.11)}
\end{aligned}$$

where $J^a := 2\left(\nabla^h_c \left(\chi^{aci}\Phi_i\right) - \nabla^{ha}\left(\theta^i \Phi_i\right)\right)$ and $\mathcal{G}_{ab}$ is the Einstein tensor of (Σ, h). Note that, modulo a divergence, Eqs. (C.10) and (C.11) coincide with Eqs. (3.11) and (3.12) of [59], respectively.

C.2 Generic solutions to the photon surface perturbation equation

The perturbation equation Eq.(8.90),

$$\nabla^h_a \nabla^h_b \Phi - \frac{1}{d} \Delta^h \Phi h_{ab} = \left(\mathcal{R}_{ab} - \frac{\mathcal{R}}{d} h_{ab}\right) \Phi,$$

for constant mean curvature (CMC) photon surfaces was derived in Sec. 8.4. Here we solve the equation explicitly and derive the general solutions in specific cases.

Consider the case where the induced metric h on the photon surface Σ is given by

$$h = a^2(-dt^2 + \sigma) \tag{C.12}$$

where a is a constant and σ is the metric of the $(d-1)$-dimensional space of constant curvature $\alpha = 0, \pm 1$. This corresponds to the static cases of [55, 56] with an appropriate scaling of time t. We express the space part as

$$\sigma = d\chi^2 + s^2(\chi)\Omega_{d-2} \tag{C.13}$$

with $s(\chi) = \chi, \sin(\chi), \sinh(\chi)$ for $\alpha = 0, +1, -1$, respectively, and the metric of the unit $(d-2)$-sphere Ω_{d-2}. Hereafter we omit the subscript $d-2$ of Ω_{d-2}. For simplicity, we scale h by a constant so that

$$h = -dt^2 + \sigma \tag{C.14}$$

and solve the perturbation equation, Eq. (8.90), with this induced metric in the following. Note that it is sufficient to specify only the intrinsic geometry (Σ, h) to solve the equation.

C.2.1 $\alpha = \pm 1$

Consider $\alpha = \pm 1$ cases. The Ricci curvatures of (Σ, h) are given by

$$\mathcal{R}_{tt} = 0, \quad \mathcal{R}_{ti} = 0 \quad \mathcal{R}_{ij} = \alpha\sigma_{ij}, \quad \mathcal{R} = (d-1)\alpha \tag{C.15}$$

where $i, j = \chi, x^A$ and x^A $(A = 1, ..., d-2)$ are the spherical coordinates of Ω. The double null coordinates $\{\lambda_\pm := t \pm \chi, x^A\}$ give null geodesics of (Σ, h) with the tangents

$$k_\pm = \partial_{\lambda_\pm}. \tag{C.16}$$

From the fact that $\mathcal{R}_{k_\pm k_\pm} = \alpha$ and the contraction of Eq. (8.90) with $k_\pm$, we have

$$\partial^2_{\lambda_\pm}\Phi(\lambda_+, \lambda_-, x^A) = \frac{1}{4}\alpha\Phi(\lambda_+, \lambda_-, x^A). \tag{C.17}$$

The integration of the "plus" one of the equation gives

$$\Phi(\lambda_+, \lambda_-, x^A) = A(\lambda_-, x^A)e^{\sqrt{\alpha}\lambda_+/2} + B(\lambda_-, x^A)e^{-\sqrt{\alpha}\lambda_+/2} \tag{C.18}$$

for the arbitrary functions $A(\lambda_-, x^A)$ and $B(\lambda_-, x^A)$. Substituting this into the "minus" one, we have

$$\partial^2_{\lambda_-}A(\lambda_-, x^A) = \frac{1}{4}\alpha A(\lambda_-, x^A), \tag{C.19}$$

$$\partial^2_{\lambda_-}B(\lambda_-, x^A) = \frac{1}{4}\alpha B(\lambda_-, x^A) \tag{C.20}$$

leading to

$$A(\lambda_-, x^A) = C(x^A)e^{\sqrt{\alpha}\lambda_-/2} + D(x^A)e^{-\sqrt{\alpha}\lambda_-/2}, \tag{C.21}$$

$$B(\lambda_-, x^A) = E(x^A)e^{\sqrt{\alpha}\lambda_-/2} + F(x^A)e^{-\sqrt{\alpha}\lambda_-/2}. \tag{C.22}$$

Therefore, we obtain

$$\begin{aligned}\Phi &= C(x^A)e^{\sqrt{\alpha}(\lambda_+ + \lambda_-)/2} + D(x^A)e^{\sqrt{\alpha}(\lambda_+ - \lambda_-)/2} \\ &\quad + E(x^A)e^{-\sqrt{\alpha}(\lambda_+ - \lambda_-)/2} + F(x^A)e^{-\sqrt{\alpha}(\lambda_+ + \lambda_-)/2} \\ &= C(x^A)e^{\sqrt{\alpha}t} + D(x^A)e^{\sqrt{\alpha}\chi} + E(x^A)e^{-\sqrt{\alpha}\chi} + F(x^A)e^{-\sqrt{\alpha}t}\end{aligned} \tag{C.23}$$

for the arbitrary functions $C(x^A)$, $D(x^A)$, $E(x^A)$, and $F(x^A)$.

The Christoffel symbols ${\Gamma^a}_{bc}$ with respect to h_{ab} are calculated as

$$\begin{aligned}&{\Gamma^t}_{ab} = {\Gamma^a}_{tb} = {\Gamma^\chi}_{\chi\chi} = {\Gamma^\chi}_{\chi A} = 0 \\ &{\Gamma^\chi}_{AB} = -ss'\Omega_{AB}, \quad {\Gamma^A}_{\chi\chi} = 0, \quad {\Gamma^A}_{\chi B} = \frac{s'}{s}\delta^A_B, \quad {\Gamma^A}_{BC} = {}^\Omega{\Gamma^A}_{BC}\end{aligned} \tag{C.24}$$

where ${}^\Omega{\Gamma^A}_{BC}$ is the Christoffel symbol with respect to Ω_{AB}. The nondiagonal components of Eq. (8.90) reduce to

$$\partial_a\partial_b\Phi - {\Gamma^i}_{ab}\partial_i\Phi = 0 \quad (a \neq b). \tag{C.25}$$

For $(a,b)=(t,\chi)$, Eq. (C.25) gives

$$\partial_t\partial_\chi\Phi=0 \tag{C.26}$$

and this is consistent with Eq. (C.23). For $(a,b)=(t,A)$, we have

$$\partial_t\partial_A\Phi=\sqrt{\alpha}\left[C(x^A)_{,A}e^{\sqrt{\alpha}t}-F(x^A)_{,A}e^{-\sqrt{\alpha}t}\right]=0 \tag{C.27}$$

by using Eq. (C.23). This implies $C(x^A)_{,A}=F(x^A)_{,A}=0$ and thus they are constant,

$$C(x^A)=C,\quad F(x^A)=F. \tag{C.28}$$

For $(a,b)=(\chi,A)$, we have

$$\partial_\chi\partial_A\Phi-\frac{s'}{s}\partial_A\Phi=D(x^A)_{,A}\left[\sqrt{\alpha}-\frac{s'}{s}\right]e^{\sqrt{\alpha}\chi}-E(x^A)_{,A}\left[\sqrt{\alpha}+\frac{s'}{s}\right]e^{-\sqrt{\alpha}\chi}=0. \tag{C.29}$$

This implies $D(x^A)_{,A}=E(x^A)_{,A}=0$ and thus they are constant,

$$D(x^A)=D,\quad E(x^A)=E. \tag{C.30}$$

Now we have

$$\Phi=Ce^{\sqrt{\alpha}t}+De^{\sqrt{\alpha}\chi}+Ee^{-\sqrt{\alpha}\chi}+Fe^{-\sqrt{\alpha}t} \tag{C.31}$$

from Eqs. (C.23), (C.28), and (C.30).

From Eq. (C.31), we have $\partial_A\Phi=0$ and thus,

$$\nabla^h_a\nabla^h_b\Phi=\partial_a\partial_b\Phi-\Gamma^\chi{}_{ab}\partial_\chi\Phi. \tag{C.32}$$

Together with Eq. (C.24), we have

$$\Delta^h\Phi=-\partial_t^2\Phi+\partial_\chi^2\Phi+(d-2)\frac{s'}{s}\partial_\chi\Phi. \tag{C.33}$$

Then the tt-, $\chi\chi$-, and AB-component of Eq. (8.90) give

$$\begin{aligned}
\partial_t^2\Phi+\frac{1}{d}\left[-\partial_t^2\Phi+\partial_\chi^2\Phi+(d-2)\frac{s'}{s}\partial_\chi\Phi\right] &= \frac{d-1}{d}\alpha\Phi,\\
\partial_\chi^2\Phi-\frac{1}{d}\left[-\partial_t^2\Phi+\partial_\chi^2\Phi+(d-2)\frac{s'}{s}\partial_\chi\Phi\right] &= \frac{1}{d}\alpha\Phi,\\
\frac{s'}{s}\partial_\chi\Phi-\frac{1}{d}\left[-\partial_t^2\Phi+\partial_\chi^2\Phi+(d-2)\frac{s'}{s}\partial_\chi\Phi\right] &= \frac{1}{d}\alpha\Phi,
\end{aligned} \tag{C.34}$$

respectively. The sum of the first and second equations gives

$$\partial_t^2\Phi+\partial_\chi^2\Phi=\alpha\Phi \tag{C.35}$$

and this is already satisfied by Eq. (C.31). The subtraction of the second equation times $(d-1)$ from the first equation gives

$$D\left[\sqrt{\alpha}s - s'\right]e^{\sqrt{\alpha}\chi} + E\left[\sqrt{\alpha}s + s'\right]e^{-\sqrt{\alpha}\chi} = 0 \tag{C.36}$$

with the substitution of Eq. (C.31). This requires

$$D = E = 0 \tag{C.37}$$

and therefore $\partial_\chi \Phi = 0$. The third equation in Eq. (C.34) then reduces to

$$\partial_t^2 \Phi = \alpha \Phi \tag{C.38}$$

and this is already satisfied by Eq. (C.34) with the vanishing of D and E.

As a consequence, the general solution of Eq. (8.90) with the geometry Eq. (C.14) for $\alpha = \pm 1$ is given by

$$\Phi = Ce^{\sqrt{\alpha}t} + Fe^{-\sqrt{\alpha}t} \tag{C.39}$$

with the arbitrary constants C and F.

C.2.2 $\alpha = 0$

Consider the $\alpha = 0$ case of the geometry of Eq. (C.14). Since the geometry (Σ, h) is the d-dimensional Minkowski spacetime, we adopt Cartesian coordinates $\{t, x^i\}$ on it and the curvatures and the Christoffel symbols identically vanish. Then the master equation Eq. (8.90) for the perturbation Φ reduces to

$$\partial_a \partial_b \Phi - \frac{1}{d}\eta^{cd}\partial_c \partial_d \Phi \eta_{ab} = 0. \tag{C.40}$$

From the nondiagonal components, Φ must be the sum of one-variable functions of t and x^i. We express it as

$$\Phi = f_t(t) + \sum_{j=1}^{d-1} f_j(x^j) \tag{C.41}$$

with the arbitrary functions $f_t(t)$ and $f_i(x^i)$. The tt- and ii-component give

$$(d-1)\partial_t^2 \Phi + \sum_{j=1}^{d-1} \partial_j^2 \Phi = 0, \tag{C.42}$$

$$\partial_t^2 \Phi + d\partial_i^2 \Phi - \sum_{j=1}^{d-1} \partial_j^2 \Phi = 0, \tag{C.43}$$

respectively. The equations give

$$\partial_t^2 \Phi + \partial_i^2 \Phi = 0 \tag{C.44}$$

by the summation of them. From Eq. (C.41), this leads to

$$-\partial_t^2 f_t(t) = \partial_i^2 f_i(x^i) = 2D \tag{C.45}$$

with the arbitrary constant D. Integrating the equations, we have the general solution of Φ for $\alpha = 0$,

$$\Phi = D\left[-t^2 + \sum_{j=1}^{d-1}(x^j)^2\right] + C_t t + \sum_{j=1}^{d-1} C_j x^j + C, \tag{C.46}$$

with the arbitrary constants D, C_t, C_i, and C. The solution satisfies Eq. (C.40), indeed.

The solution can be rewritten as

$$\Phi = D\eta_{ab}x^a x^b + B_a x^a + C \tag{C.47}$$

with $x^a = (t, x^i)$ and $B_a = (C_t, C_i)$. C represents the perturbation parallel to Σ, or the shift of Σ. It displaces $\Sigma \to \Sigma_\varepsilon$ by a constant distance $C\varepsilon$ at each point $p \in \Sigma$. B_a rotates Σ with the fixed axes A^a given by $B_a A^a = 0$. Points satisfying $x^a \propto A^a$ are fixed by the perturbation and the set of A^a spans $(d-1)$-dimensional surface, actually. If the surface is timelike, the perturbation is a spatial rotation of Σ while if spacelike, it is a Lorentz boost of Σ. D provides the perturbation which depends only on the length of x^a and fixes the origin $x^a = 0$ and the null rays $\eta_{ab}x^a x^b = 0$ passing the origin. We can understand D as follows.

To imagine the effect of D, let us consider that Σ is embedded into the $(d+1)$-dimensional Minkowski spacetime $\mathbb{M}^{d+1}$ by the embedding $x^a \in \Sigma \mapsto x^\mu = (x^a, y = 0) \in M^{d+1}$, for example. Suppose $B_a = C = 0$ for simplicity. The photon surface Σ is given by $y = 0$ with the normal vector $N^\mu = (0, 1)$. The perturbed photon surface Σ_ε is given by

$$x_\varepsilon^\mu = x^\mu + \Phi N^\mu \varepsilon = \left(x^a, D\varepsilon\eta_{ab}x^a x^b\right) \tag{C.48}$$

from Eqs. (8.70) and (8.71). In the case of $d = 2$ and $x^a = (t, x)$ for simplicity, it is $x_\varepsilon^\mu = (t, x, D\varepsilon(-t^2 + x^2))$, or expressed as the quadratic equation,

$$-t^2 + x^2 - \frac{1}{D\varepsilon}y = 0. \tag{C.49}$$

This coincides with the expansion about y of the one-sheeted hyperboloid given by

$$-t^2 + x^2 + (y - a)^2 = a^2 \tag{C.50}$$

in $\mathbb{M}^3$ around $y = 0$ in linear order, where the "radius" a is specified by $a = (2D\varepsilon)^{-1}$. In fact, timelike planes and one-sheeted hyperboloids are known to be timelike photon surfaces of the Minkowski spacetime [8]. Furthermore, by the large radius limit, or equivalently the zero-curvature limit, $a \to \infty$, the local geometry of the hyperboloid approaches to that of planes. The limit corresponds to $\varepsilon \to 0$ in our case. Therefore, the parameter D gives the perturbation of the plane Σ to a hyperboloid Σ_ε of infinitely large radius $a = (2D\varepsilon)^{-1}$. Note that although the local geometries coincide with each other in the limit, their global topologies, which would be subject to the nonlinear order, in the Minkowski spacetime are different. It is also worth noting that the hyperboloid in the Minkowski spacetime has the geometry of de Sitter spacetime [8].

C.2.3 Stability

The scaling of Eq. (C.14) to Eq. (C.12) gives $\alpha \to a^{-2}\alpha$ and $t \to at$. As a result, the most general solutions of the linear perturbation Φ of the photon surface which has the surface geometry of Eq. (C.12) are

$$\Phi = Ce^{\sqrt{\alpha}t} + Fe^{-\sqrt{\alpha}t} \quad (\alpha = \pm 1) \tag{C.51}$$

with the arbitrary constants C, F and

$$\Phi = D\eta_{ab}x^a x^b + B_a x^a + C \quad (\alpha = 0) \tag{C.52}$$

with the arbitrary constants D, B_a, and C. The photon surface is stable, i.e. Φ is bounded, against all the possible perturbations if and only if the spatial geometry is hyperbolically symmetric, $\mathcal{R} = (d-1)\alpha < 0$. The case is where $-C_{kNkN} = \mathcal{R}_{kk} < 0$ for any null vector $k \in T_p\Sigma$ at any point $p \in \Sigma$, i.e. Σ is a strictly stable photon surface as we expected. The $\alpha = 0$ case corresponds to a marginally stable case where $-C_{kNkN} = \mathcal{R}_{kk} = 0$. If one perturbs Σ with the initial condition $\partial_a\Phi|_{t=t_0} = 0$, it leads to $D = B_a = 0$ and the deviation remains constant, $\Phi = C$, and is bounded. It is worth noting that any perturbation violating the spatial symmetry of the surface is not allowed for $\alpha = \pm 1$. The relatively high degrees of freedom of the perturbation for $\alpha = 0$ come from that the geometry (Σ, h) restores the maximal symmetry on it.

If we apply the results to the perturbation of a Z_2-symmetric pure-tensional joined spacetime in Sec. 8.4, it is consistent with the Λ-vacuum case of [55, 56] and implies that the perturbations the authors investigated for the spherically and hyperbolical symmetric cases are the most general under the Z_2-symmetry of the joined spacetime in the sense of Eq. (C.51).

Eq. (8.86) or (8.90) can shed light on seeking photon surfaces around a given photon surface. This is because the existence of the possible linear perturbations of a photon surface should imply the existence of nearby photon surfaces. The result, Eq. (C.51), in the example tells us that, in the vicinity of the spherically and hyperbolically symmetric photon surface of a Λ-vacuum spacetime, there would be no photon surface which does not have the same spatial symmetry. Eq. (C.52) indicates that there exist photon surfaces around a given planar photon surface. They are obtained by the shift, the rotation, the boost, and the transformation to hyperboloids.

Bibliography

[1] B. P. Abbott *et al.* [LIGO Scientific Collaboration and Virgo Collaboration], *Observation of Gravitational Waves from a Binary Black Hole Merger*, *Phys. Rev. Lett.* **116** (2016) 061102.

[2] K. Akiyama et al., *First M87 Event Horizon Telescope Results. I. The Shadow of the Supermassive Black Hole*, *Astrophys. J. Lett.* **875** (2019) L1 [1906.11238].

[3] J.L. Synge, *The escape of photons from gravitationally intense stars*, *Monthly Notices Roy Astron. Soc.* **131** (1966) 463.

[4] V. Cardoso, A.S. Miranda, E. Berti, H. Witek and V.T. Zanchin, *Geodesic stability, Lyapunov exponents, and quasinormal modes*, *Phys. Rev. D* **79** (2009) 064016 [0812.1806].

[5] S. Hod, *Black-hole quasinormal resonances: Wave analysis versus a geometric-optics approximation*, *Phys. Rev. D* **80** (2009) 064004 [0909.0314].

[6] P.V.P. Cunha, E. Berti and C.A.R. Herdeiro, *Light ring stability in ultra-compact objects*, *Phys. Rev. Lett.* **119** (2017) 251102 [1708.04211].

[7] V. Cardoso, L.C.B. Crispino, C.F.B. Macedo, H. Okawa and P. Pani, *Light rings as observational evidence for event horizons: long-lived modes, ergoregions and nonlinear instabilities of ultracompact objects*, *Phys. Rev. D* **90** (2014) 044069 [1406.5510].

[8] C.-M. Claudel, K. Virbhadra and G. Ellis, *The Geometry of photon surfaces*, *J. Math. Phys.* **42** (2001) 818 [gr-qc/0005050].

[9] V. Perlick, *On totally umbilic submanifolds of semi-riemannian manifolds*, *Nonlinear Analysis* **63** (2005) e511 [gr-qc/0512066].

[10] G.W. Gibbons and C.M. Warnick, *Aspherical Photon and Anti-Photon Surfaces*, *Phys. Lett. B* **763** (2016) 169 [1609.01673].

[11] C. Cederbaum, *Uniqueness of photon spheres in static vacuum asymptotically flat spacetimes*, *Contemp. Math* **653** (2015) 86 [1406.5475].

[12] C. Cederbaum and G.J. Galloway, *Uniqueness of photon spheres in electro-vacuum spacetimes*, *Class. Quant. Grav.* **33** (2016) 075006 [1508.00355].

[13] M. Rogatko, *Uniqueness of photon sphere for Einstein-Maxwell-dilaton black holes with arbitrary coupling constant*, *Phys. Rev. D* **93** (2016) 064003 [1602.03270].

[14] S. Yazadjiev, *Uniqueness of the static spacetimes with a photon sphere in Einstein-scalar field theory*, *Phys. Rev. D* **91** (2015) 123013 [1501.06837].

[15] Y. Koga and T. Harada, *Stability of null orbits on photon spheres and photon surfaces*, *Phys. Rev. D* **100** (2019) 064040 [1907.07336].

[16] Y. Koga, T. Igata and K. Nakashi, *Photon surfaces in less symmetric spacetimes*, 2011.10234.

[17] Y. Koga and T. Harada, *Correspondence between sonic points of ideal photon gas accretion and photon spheres*, *Phys. Rev. D* **94** (2016) 044053 [1601.07290].

[18] Y. Koga and T. Harada, *Rotating accretion flows in D dimensions: sonic points, critical points and photon spheres*, *Phys. Rev. D* **98** (2018) 024018 [1803.06486].

[19] Y. Koga, *Photon surfaces in spherically, planar and hyperbolically symmetric spacetimes of D-dimensions: Sonic point/photon sphere correspondence*, *Phys. Rev. D* **99** (2019) 064034 [1901.02592].

[20] Y. Koga, *Photon surfaces as pure tension shells: Uniqueness of thin shell wormholes*, *Phys. Rev. D* **101** (2020) 104022 [2003.10859].

[21] R.M. Wald, *General Relativity*, The University of Chicago Press, Chicago (1984).

[22] J. Keir, *Slowly decaying waves on spherically symmetric spacetimes and ultracompact neutron stars*, *Classical Quantum Gravity* **33** (2016) 135009 [1404.7036].

[23] V. Cardoso, L.C.B. Crispino, C.F.B. Macedo, H. Okawa and P. Pani, *Light rings as observational evidence for event horizons: long-lived modes, ergoregions and nonlinear instabilities of ultracompact objects*, *Phys. Rev. D* **90** (2014) 044069 [1406.5510].

[24] E. Chaverra and O. Sarbach, *Radial accretion flows on static spherically symmetric black holes*, *Class. Quantum Grav.* **32** (2015) 155006 [1501.01641].

[25] E. Poisson, *A Relativist's Toolkit*, Cambridge University Press, Cambridge, England (2004).

[26] M. Bañados, C. Teitelboim and J. Zanelli, *Black Hole in Three-Dimensional Spacetime*, *Phys. Rev. Lett.* **69** (1992) 1840 [1009.3749].

[27] H. Kodama and A. Ishibashi, *Master equations for perturbations of generalized static black holes with charge in higher dimensions*, *Prog. Theor. Phys. Suppl.* **111** (2004) 29 [0308128].

[28] G.R. Jensen, *Homogeneous einstein spaces of dimension four*, *J. Differ. Geom.* **3** (1969) 309.

[29] J. Fine and B. Premoselli, *Examples of compact einstein four-manifolds with negative curvature*, *J. Amer. Math. Soc.* **33** (2020) 991 [1802.00608].

[30] D. Alekseevsky, I. Dotti and C. Ferraris, *Homogeneous ricci positive 5-manifolds*, *Pac. J. Math.* **175** (1996) 1.

[31] B. Grajales and L. Grama, *NON-DIAGONAL INVARIANT EINSTEIN METRICS ON REAL FLAG MANIFOLDS*, 1907.02626.

[32] A.L. Besse, *Einstein Manifolds (Classics in Mathematics)*, Springer-Verlag, Berlin (1986).

[33] H. Bondi, *On spherically symmetrical accretion*, *Monthly Notices Roy Astron. Soc.* **112** (1952) 195.

[34] F. Michel, *Accretion of matter by condensed objects*, *Astrophysics and Space Science* **15** (1972) 153.

[35] P. Mach, E. Malec and J. Karkowski, *Dependence on the cosmological constant, exact isothermal solutions, and applications to cosmology*, *Phys. Rev. D* **88** (2013) 084056 [1309.1252].

[36] J. Karkowski and E. Malec, *Bondi accretion onto cosmological black holes*, *Phys. Rev. D* **87** (2013) 044007 [1211.3618].

[37] F.S. Guzman and F.D. Lora-Clavijo, *Exploring the effects of pressure on the radial accretion of dark matter by a Schwarzschild supermassive black hole*, *Mon. Not. R. Astron. Soc.* **415** (2011) 225 [1103.5497].

[38] B. Carter, G.W. Gibbons, D.N.C. Lin and M.J. Perry, *Black Hole Emission Process in the High Energy Limit*, *Astronomy and Astrophysics* **52** (1976) 427.

[39] S. Chandrasekhar, *The Mathematical Theory of Black Holes*, Oxford University Press, New York (1983).

[40] H. Abraham, N. Bilic and T.K. Das, *Acoustic horizons in axially symmetric relativistic accretion*, *Classical and Quantum Gravity* **23** (2006) 2371 [gr-qc/0509057].

[41] T.K. Das, N. Bilic and S. Dasgupta, *Black-Hole Accretion Disc as an Analogue Gravity Model*, *JCAP* **0706** (2007) 009 [astro-ph/0604477].

[42] P. Barai, T.K. Das and P.J. Wiita, *Dependence of general relativistic accretion on black hole spin*, *Astrophys. J.* **613** (2004) L49.

[43] M.A. Abramowicz, A. Lanza and M.J. Percival, *Accretion disks around Kerr black holes: vertical equilibrium revisited*, *Astrophys. J.* **479** (1997) 179.

[44] M. Tsuchiya, C.-M. Yoo, Y. Koga and T. Harada, *Sonic Point and Photon Surface*, *Phys. Rev. D* **102** (2020) 044057 [2003.10125].

[45] P. Kanti, B. Kleinhaus and J. Kunz, *Wormholes in Dilatonic Einstein-Gauss-Bonnet Theory*, *Phys. Rev. Lett.* **107** (2011) 271101 [1108.3003].

[46] P. Kanti, B. Kleinhaus and J. Kunz, *Stable Lorentzian wormholes in dilatonic Einstein-Gauss-Bonnet theory*, *Phys. Rev. D* **85** (2012) 044007 [1111.4049].

[47] T. Harko, F.S.N. Lobo, M.K. Mak and S.V. Sushkov, *Modified-gravity wormholes without exotic matter*, *Phys. Rev. D* **87** (2013) 067504 [1301.6878].

[48] M. Rogatko, *Uniqueness of higher-dimensional phantom field wormholes*, *Phys. Rev. D* **97** (2018) 024001 [1801.01987].

[49] S. Yazadjiev, *Uniqueness theorem for static wormholes in Einstein-phantom scalar field theory*, *Phys. Rev. D* **96** (2017) 044045 [1707.03654].

[50] M. Rogatko, *Uniqueness of higher-dimensional Einstein-Maxwell-phantom dilaton wormholes*, *Phys. Rev. D* **97** (2018) 064023 [1803.08296].

[51] M.S. Morris and K.S. Thorne, *Wormholes in spacetime and their use for interstellar travel: A tool for teaching general relativity*, *Am. J. Phys.* **56** (1988) 395.

[52] D. Hochberg and M. Visser, *Null Energy Condition in Dynamic Wormholes*, *Phys. Rev. Lett.* **81** (1998) 746 [gr-qc/9802048].

[53] M. Visser, *Traversable wormholes from surgically modified Schwarzschild spacetimes*, *Nucl.Phys.* **B328** (1989) 203 [0809.0927].

[54] W. Israel, *Singular hypersurfaces and thin shells in general relativity*, *Nuovo Cimento* **44B** (1966) 1.

[55] C. Barcelo and M. Visser, *Brane surgery: energy conditions, traversable wormholes, and voids*, *Nucl. Phys.* **B584** (2000) 415 [0004022].

[56] T. Kokubu and T. Harada, *Negative tension branes as stable thin shell wormholes*, *Class. Quant. Grav.* **32** (2015) 205001 [1411.5454].

[57] L. Randall and R. Sundrum, *An alternative to Compactification*, *Phys. Rev. Lett.* **83** (1999) 4690 [hep-th/9906064].

[58] L. Randall and R. Sundrum, *Large mass Hierarchy from a Small Extra Dimension*, *Phys. Rev. Lett.* **83** (1999) 3370 [hep-ph/9905221].

[59] R. Capovilla and J. Guven, *GEOMETRY OF DEFORMATIONS OF RELATIVISTIC MEMBRANES*, *Phys. Rev. D* **51** (1995) 6736 [9411060].

[60] W. Kinnersley and M. Walker, *Uniformly Accelerating Charged Mass in General Relativity*, *Phys. Rev. D* **2** (1970) 1359.

[61] W. Smith and R. Mann, *Formation of Topological Black holes from Gravitational Collapse*, *Phys. Rev. D* **56** (1997) 4942 [gr-qc/9703007].

[62] T. Shiromizu, Y. Tomikawa, K. Izumi and H. Yoshino, *Area bound for a surface in a strong gravity region*, *Prog. Theor. Exp. Phys.* **2017** (2017) 033E01 [1701.00564].

[63] H. Yoshino, K. Izumi, T. Shiromizu and Y. Tomikawa, *Extension of photon surfaces and their area: Static and stationary spacetimes*, *Prog. Theor. Exp. Phys.* **2017** (2017) 063E01 [1704.04637].

[64] H. Yoshino, K. Izumi, T. Shiromizu and Y. Tomikawa, *Transversely trapping surfaces: Dynamical version*, *Prog. Theor. Exp. Phys.* **2020** (2020) 023E02 [1909.08420].

[65] M. Siino, *Causal concept for black hole shadows*, *Class. Quant. Grav.* **38** (2020) 025005 [1908.02921].

[66] K.V. Kobialko and D.V. Gal'tsov, *Photon regions and umbilic conditions in stationary axisymmetric spacetimes*, *Eur. Phys. J. C* **80** (2020) 527 [2002.04280].

[67] S.W. Hawking and G.F.R. Ellis, *The Large Scale Structure of Space-Time*, Cambridge University Press, Cambridge, England (1973).